

Quantum State Transfer with Spin Chains

Daniel Klaus Burgarth

A thesis submitted to the University of London
for the degree of Doctor of Philosophy

Department of Physics and Astronomy
University College London

December 2006

Declaration

I, Daniel Klaus Burgarth, confirm that the work presented in this thesis is my own. Where information has been derived from other sources, I confirm that this has been indicated in the thesis.

Abstract

In the last few decades the idea came up that by making use of the superposition principle from Quantum Mechanics, one can process information in a new and much faster way. Hence a new field of information technology, QIT (Quantum Information Technology), has emerged. From a physics point of view it is important to find ways of implementing these new methods in real systems. One of the most basic tasks required for QIT is the ability to connect different components of a Quantum Computer by *quantum wires* that obey the superposition principle. Since superpositions can be very sensitive to noise this turns out to be already quite difficult. Recently, it was suggested to use chains of permanently coupled spin-1/2 particles (*quantum chains*) for this purpose. They have the advantage that no external control along the wire is required during the transport of information, which makes it possible to isolate the wire from sources of noise. The purpose of this thesis is to develop and investigate advanced schemes for using quantum chains as wires. We first give an introduction to basic quantum state transfer and review existing advanced schemes by other authors. We then introduce two new methods which were created as a part of this thesis. First, we show how the fidelity of transfer can be made perfect by performing measurements at the receiving end of the chain. Then we introduce a scheme which is based on performing unitary operations at the end of the chain. We generalise both methods and discuss them from the more fundamental point of view of mixing properties of a quantum channel. Finally, we study the effects of a non-Markovian environment on quantum state transfer.

Acknowledgements

Most of all, I would like to thank my supervisor Sougato Bose for much inspiration and advice. I am very grateful for many inspiring and fruitful discussions and collaborations with Vittorio Giovannetti, and with Floor Paauw, Christoph Bruder, Jason Twamley, Andreas Buchleitner and Vladimir Korepin. Furthermore I would like to thank all my teachers and those who have guided and motivated me along my journey through physics, including Heinz-Peter Breuer, Francesco Petruccione, Lewis Ryder, John Strange, Werner Riegler, Carsten Schuldt and Rolf Bussmann. I acknowledge financial support by the UK Engineering and Physical Sciences Research Council through the grant GR/S62796/01. Finally I would like to thank my parents for their loving support.

Notation

X, Y, Z	Pauli matrices
X_n, Y_n, Z_n	Pauli matrices acting on the Hilbert-space of qubit n
$ 0\rangle, 1\rangle$	Single qubit state in the canonical basis
$ \mathbf{0}\rangle$	Quantum chain in the product state $ 0\rangle \otimes \dots \otimes 0\rangle$
$ \mathbf{n}\rangle$	"Single excitation" state $X_n \mathbf{0}\rangle$
Tr_X	Partial trace over subsystem X
$\ \dots\ $	Euclidean vector norm
$\ \dots\ _1$	Trace norm
$\ \dots\ _2$	Euclidean matrix norm

We also use the following graphical representation:

$$|0\rangle \equiv \bigcirc$$

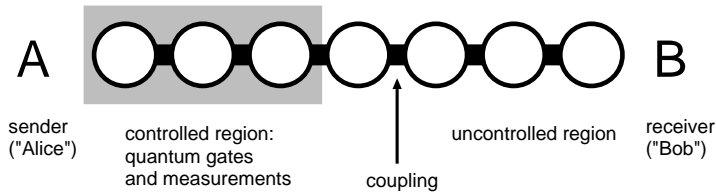
$$|1\rangle \equiv \bullet$$

$$|\psi\rangle = \alpha|0\rangle + \beta|1\rangle \equiv \bigcirc$$

$$|\mathbf{0}\rangle \equiv \bigcirc - \bigcirc - \bigcirc - \bigcirc - \bigcirc - \bigcirc - \bigcirc$$

$$|\mathbf{n}\rangle \equiv \bigcirc - \bigcirc - \bigcirc - \bullet - \bigcirc - \bigcirc - \bigcirc$$

n th qubit



Contents

1	Introduction	9
1.1	Quantum Computation and Quantum Information	10
1.2	Quantum state transfer along short distances	11
1.3	Implementations and experiments	15
1.4	Basic communication protocol	15
1.4.1	Initialisation and end-gates	17
1.4.2	Symmetries	18
1.4.3	Transfer functions	18
1.4.4	Heisenberg Hamiltonian	20
1.4.5	Dynamic and Dispersion	21
1.4.6	How high should $p(t)$ be?	27
1.5	Advanced communication protocols	29
1.5.1	Engineered Hamiltonians	29
1.5.2	Weakly coupled sender and receiver	29
1.5.3	Encoding	31
1.5.4	Time-dependent control	31
1.6	Motivation and outline of this work	31
2	Dual Rail encoding	34
2.1	Introduction	34
2.2	Scheme for conclusive transfer	35
2.3	Arbitrarily perfect state transfer	38
2.4	Estimation of the time-scale the transfer	40
2.5	Decoherence and imperfections	42
2.6	Disordered chains	44
2.7	Conclusive transfer in the presence of disorder	45
2.8	Arbitrarily perfect transfer in the presence of disorder	48
2.9	Tomography	50
2.10	Numerical Examples	51

2.11	Coupled chains	54
2.12	Conclusion	57
3	Multi Rail encoding	58
3.1	Introduction	58
3.2	The model	58
3.3	Efficient encoding	62
3.4	Perfect transfer	62
3.5	Convergence theorem	66
3.6	Quantum chains with nearest-neighbour interactions	69
3.7	Comparison with Dual Rail	70
3.8	Conclusion	71
4	Ergodicity and mixing	72
4.1	Introduction	72
4.2	Topological background	74
4.3	Generalised Lyapunov Theorem	76
4.3.1	Topological spaces	76
4.3.2	Metric spaces	81
4.4	Quantum Channels	84
4.4.1	Mixing criteria for Quantum Channels	84
4.4.2	Beyond the density matrix operator space: spectral properties	86
4.4.3	Ergodic channels with pure fixed points	88
4.5	Conclusion	92
5	Read and write access by local control	93
5.1	Introduction	93
5.2	Protocol	94
5.3	Decomposition equations	96
5.4	Coding transformation	97
5.5	Fidelities for reading and writing	99
5.6	Application to spin chain communication	101
5.7	Conclusion	103
6	A valve for probability amplitude	104
6.1	Introduction	104
6.2	Arbitrarily Perfect State Transfer	104
6.3	Practical Considerations	107

6.4	Conclusion	109
7	External noise	110
7.1	Introduction	110
7.2	Model	112
7.3	Results	114
7.4	Conclusion	119
8	Conclusion and outlook	120
	List of Figures	121
	List of Tables	126
	Bibliography	127
	Index	141

1 Introduction

The Hilbert space that contains the states of quantum mechanical objects is huge, scaling exponentially with the number of particles described. In 1982, Richard Feynman suggested to make use of this as a resource for *simulating* quantum mechanics in a *quantum computer*, i.e. a device where the physical interaction could be “programmed” to yield a specific Hamiltonian. This has led to the new fields of Quantum Computation and Quantum Information. A quantum computer can solve questions one could never imagine to solve using an ordinary computer. For example, it can factorise large numbers into primes efficiently, a task of greatest importance for cryptography. It may thus be a surprise that more than twenty years after the initial ideas, these devices still haven’t been built or only in ridiculously small size. The largest quantum computer so far can only solve problems that any child could solve within seconds. A closer look reveals that the main problem in the realisation of quantum computers is the “programming”, i.e. the design of a specific (time-dependent) Hamiltonian, usually described as a set of discrete unitary gates. This turns out to be extremely difficult because we need to connect microscopic objects (those behaving quantum mechanically) with macroscopic devices that *control* the microscopic behaviour. Even if one manages to find a link between the micro- and the macroscopic world, such as laser pulses and electric or magnetic fields, then the connection introduces not only control but also noise (dissipation and decoherence) to the microscopic system, and its quantum behaviour is diminished.

The vision of this thesis is to develop theoretical methods narrowing the gap between what is imagined theoretically and what can be done experimentally. As a method we consider chains (or more general graphs) of *permanently coupled* quantum systems. This idea has been originally put forward by S. Bose for the specific task of quantum communication [1]. Due to the permanent coupling, these devices can in principle be built in such a way that they don’t require external control to perform their tasks, just like a mechanical clockwork. This also overcomes the problem of decoherence as they can be separated from any source of noise. Unfortunately, most schemes that have been developed so far still require external control, though much less than an “ordinary” quantum computer. Furthermore, internal dispersion in these devices is

leading to a decrease of their fidelity. A third problem is, that for building these devices the permanent couplings still need to be realised, although only once, and experimental constraints such as resolution and errors need to be considered. We are thus left with the following questions: which is the best way to perform quantum state transfer using a permanently coupled graph? How much control do we need, and how difficult will it be to implement the couplings? How do errors and noise affect the scheme? All these points are highly related and it cannot be expected to find an *absolute*, i.e. system independent answer. The purpose of this research is to develop advanced schemes for the transfer of quantum information, to improve and generalise existing ideas, to relate them to each other and to investigate their stability and efficiency.

1.1 Quantum Computation and Quantum Information

In this Section we review some of the basic concepts of Quantum Computation. We will be very brief and only focus on those aspects that we require later on in the thesis. A more detailed introduction can be found in [2].

In information science, an algorithm is a list of instructions that a computer performs on a given input to achieve a specific task. For instance, a *factoring algorithm* has an arbitrary integer as its input, and gives its prime factors as an output. A *quantum factoring algorithm* can be thought of in a similar way, i.e. it has an integer as input, and its prime factors as an output. *In-between* however it encodes information in a quantum mechanical system. Due to the superposition principle, the information of a quantum system cannot be represented as *bits*. The valid generalisation of the bit to the quantum case is called *qubit*. The possible states of a qubit are written as

$$\alpha|0\rangle + \beta|1\rangle, \tag{1.1}$$

where α, β are normalised complex coefficients, and $|0\rangle$ and $|1\rangle$ are vectors of a two-dimensional complex vector space. Peter W. Shor has shown in a famous paper [3] that the *detour* of representing the intermediate part of a factoring algorithm in a quantum system (as well as using quantum gates, see below) can be very beneficial: it runs *much* faster. This is important, because many cryptographic methods rely on factoring algorithms being slow. Shor's algorithm is definitely not the only reason why it would be very nice to have a *quantum computer*, i.e. a machine that represents information in a quantum way and can perform instructions on it, and many more details can be found in the textbook mentioned above.

Algorithms on a computer can be represented as list of logical operations on bits. Likewise, a (standard) quantum algorithm can be represented as a list of *quantum logical operations*, or *quantum gates*, acting on qubits. The most general quantum algorithm is given by an arbitrary unitary operator. A *universal set of gates* is a set such that any quantum algorithm (i.e. unitary operator) can be decomposed into a sequence of gates belonging to this set. In the *standard model* of quantum computation, one assumes that such a set is available on the machine [4]. Also the ability to perform measurements is assumed. We refer to this as the *full control* case.

From a information theoretic point of view, qubits are not only *useful* objects to perform algorithms with, but also very interesting from a fundamental point of view. To give a (too simple) analogy consider the following. If you read the word "chocolate", you can associate a positive/negative or neutral feeling of whether you would like to eat some chocolate now. However, what was the state of your mind concerning chocolate *before you read* the word? Unless you were already craving for chocolate beforehand, or you have just eaten a lot, your mind was probably *undecided*. Moreover, it would have been very difficult - if not impossible - to describe to someone in plain language which opinion you had about the chocolate before you read the word.

In a similar manner, the quantum information contained in a single *arbitrary and unknown* qubit cannot be described by classical information. When it is measured, it behaves like a normal bit in the sense that the outcome is only 0 or 1, but when it is not measured, it behaves in some way as if it was undecided between 0 and 1. Of course one has to be very careful with these analogies. But for the purpose of this thesis it is important to stress that quantum information cannot be transported by any classical methods [5]. This is why it is so important and also so difficult to develop new wires, dubbed *quantum wires*, that are capable of doing this.

1.2 Quantum state transfer along short distances

In theory, additional devices for the transfer of unknown quantum states are not required for building a quantum computer, unless it is being used for typical quantum communication purposes, such as secret key distribution [4]. This is because the *universal set of gates* on the quantum computer can be used to transfer quantum states by applying sequences of two-qubit swap gates (Fig. 1.1).

However in practice it is crucial to minimise the required number of quantum gates, as each gate typically introduces *errors*. In this light it appears costly to perform $N-1$ swap gates between nearest neighbours to just move a qubit state over a distance of N sites. For example, Shor's algorithm on N qubits can be implemented by only

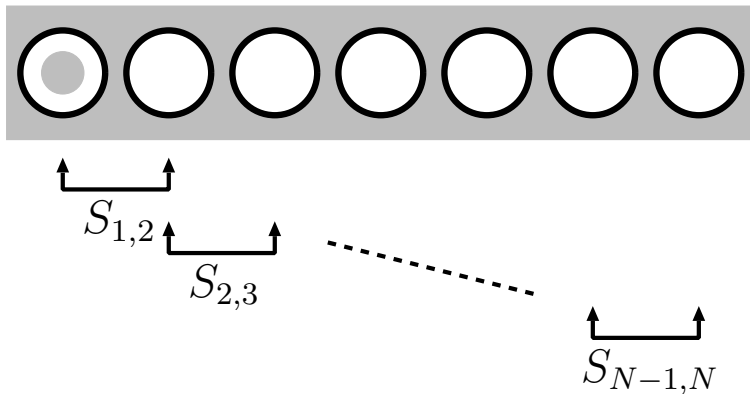


Figure 1.1: In areas of universal control, quantum states can easily be transferred by sequences of unitary swap gates $S_{j,k}$ between nearest neighbours.

$\log N$ quantum gating operations [6] if long distant qubit gates are available. These long distant gates could consist of local gates followed by a quantum state transfer. If however the quantum state transfer is implemented as a sequence of local gates, then the number of operations blows up to the order of N gates. The quantum state transfer can even be thought of as the source of the *power of quantum computation*, as any quantum circuit with $\log N$ gates and *local gates only* can be efficiently simulated on a classical computer [7,8].

A second reason to consider devices for quantum state transfer is related to *scalability*. While small quantum computers have already been built [9], it is very difficult to build large arrays of fully controllable qubits. A *black box* that transports unknown quantum states could be used to build larger quantum computers out of small components by connecting them. Likewise, quantum state transfer can be used to connect *different* components of a quantum computer, such as the processor and the memory (see also Fig. 1.2). On larger distances, flying qubits such as photons, ballistic electrons and guided atoms/ions are considered for this purpose [10,11]. However, converting back and forth between stationary qubits and mobile carriers of quantum information and interfacing between different physical implementations of qubits is very difficult and worthwhile only for short communication distances. This is the typical situation one has to face in solid state systems, where quantum information is usually contained in the states of *fixed objects* such as quantum dots or Josephson junctions. In this case permanently coupled *quantum chains* have recently been proposed as prototypes of reliable quantum communication lines [1,12]. A quantum chain (also referred to as *spin chain*) is a one-dimensional array of qubits which are coupled by some Hamiltonian (cf. Fig. 1.3). These couplings can transfer states *without external classical control*.

In many cases, such permanent couplings are easy to build in solid state devices (in fact a lot of effort usually goes into *suppressing* them). The qubits can be of the *same type* as the other qubits in the device, so no interfacing is required.

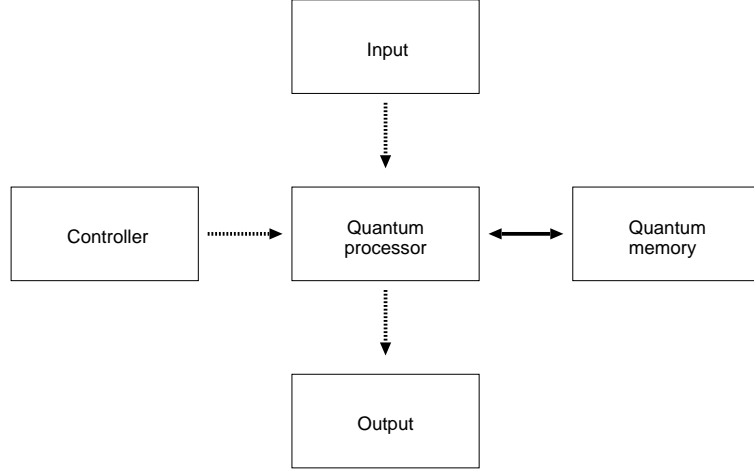


Figure 1.2: Schematic layout of a quantum computer. The solid arrows represent the flow of quantum information, and the dashed arrows the flow of classical information.

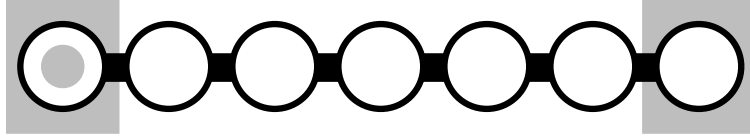


Figure 1.3: Permanently coupled quantum chains can transfer quantum states without control along the line. Note that the ends still need to be controllable to initialise and read out quantum states.

Another related motivation to consider quantum chains is that they can simplify the *layout* of quantum devices on wafers. A typical chip can contain millions of qubits, and the fabrication of many qubits is in principle no more difficult than the fabrication of a single one. In the last couple of years, remarkable progress was made in experiments with quantum dots [13, 14] and super-conducting qubits [15, 16]. It should however be emphasised that for initialisation, control and readout, those qubits have to be connected to the macroscopic world (see Fig. 1.2). For example, in a typical flux qubit gate, microwave pulses are applied onto specific qubits of the sample. This requires many (classical) wires on the chip, which is thus a *compound* of quantum and classical components. The macroscopic size of the classical control is likely to be the bottleneck of the scalability as a whole. In this situation, quantum chains are useful in order to keep some distance between the controlled quantum parts. A possible layout for such

a quantum computer is shown in Fig. 1.4. It is built out of blocks of qubits, some of which are dedicated to communication and therefore connected to another block through a quantum chain. Within each block, arbitrary unitary operations can be performed in a fast and reliable way (they may be decomposed into single and two-qubit operations). Such blocks do not currently exist, but they are the focus of much work in solid state quantum computer architecture. The distance between the blocks is determined by the length of the quantum chains between them. It should be large enough to allow for classical control wiring of each block, but short enough so that the time-scale of the quantum chain communication is well below the time-scale of decoherence in the system.

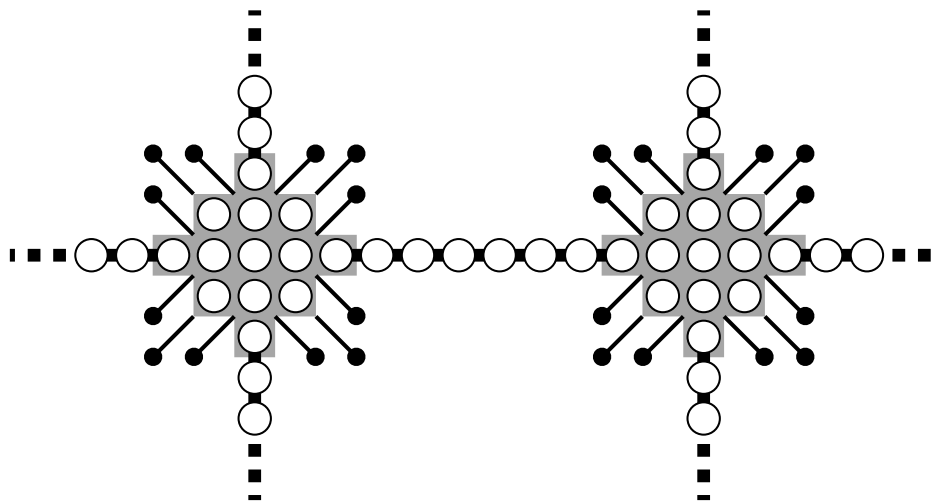


Figure 1.4: Small blocks (grey) of qubits (white circles) connected by quantum chains. Each block consists of (say) 13 qubits, 4 of which are connected to outgoing quantum chains (the thick black lines denote their nearest-neighbour couplings). The blocks are connected to the macroscopic world through classical wires (thin black lines with black circles at their ends) through which arbitrary unitary operations can be triggered on the block qubits. The quantum chains require no external control.

Finally, an important reason to study quantum state transfer in quantum chains stems from a more fundamental point of view. Such systems in principle allow tests of Bell-inequalities and non-locality in solid-state experiments well before the realisation of a quantum computer. Although quantum transport is quite an established field, the quantum information point of view offers many new perspectives. Here, one looks at the transport of information rather than excitations, and at entanglement [17–20] rather than correlation functions. It has recently been shown that this sheds new light on well-known physical phenomena such as quantum phase transitions [21–24],

quantum chaos [25–28] and localisation [29, 30]. Furthermore, quantum information takes on a more *active* attitude. The correlations of the system are not just calculated, but one also looks at how they may be *changed*.

1.3 Implementations and experiments

As we have seen above, the main advantage of state transfer with quantum chains is that the qubits can be of the same type as those used for the quantum computation. Therefore, most systems that are thought of as possible realisations of a quantum computer can also be used to build quantum chains. Of course there has to be some coupling between the qubits. This is typically easy to achieve in solid state systems, such as Josephson junctions with charge qubits [31, 32], flux qubits [33, 34] (see also Fig. 1.5) or quantum dots using the electrons [35, 36] or excitons [37, 38]. Other systems where quantum chain Hamiltonians can at least be *simulated* are NMR qubits [39–41] and optical lattices [42]. Such a simulation is particularly useful in the latter case, where local control is extremely difficult. Finally, qubits in cavities [43, 44] and coupled arrays of cavities were considered [45, 46].

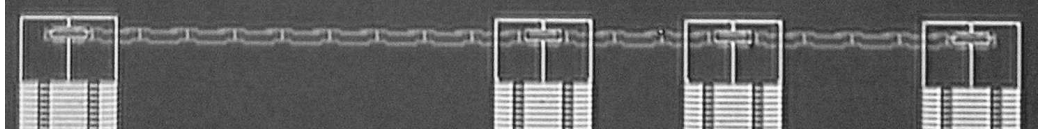


Figure 1.5: A quantum chain consisting of $N = 20$ flux qubits [34] (picture and experiment by Floor Paauw, TU Delft). The chain is connected to four larger SQUIDS for readout and gating.

For the more fundamental questions, such as studies of entanglement transfer, non-locality and coherent transport, the quantum chains could also be realised by systems which are not typically thought of as qubits, but which are *natural spin chains*. These can be molecular systems [47] or quasi-1D solid state materials [48, 49].

1.4 Basic communication protocol

We now review the most basic transport protocol for quantum state transfer, initially suggested in [1]. For the sake of simplicity, we concentrate on the linear chain setting, though more general graphs of qubits can be considered in the same way. The protocol consists of the following steps:

1. Initialise the quantum chain in the ground state

$$|G\rangle. \quad (1.2)$$

2. Put an arbitrary and unknown qubit with (possibly mixed) state ρ at the sending end of the chain

$$\rho \otimes \text{Tr}_1 \{|G\rangle\langle G|\}. \quad (1.3)$$

3. Let the system evolve under its Hamiltonian H for a time t

$$\exp\{-iHt\} \rho \otimes \text{Tr}_1 \{|G\rangle\langle G|\} \exp\{iHt\}. \quad (1.4)$$

4. Pick up the quantum state at the end of the chain

$$\sigma \equiv \text{Tr}_{1,\dots,N-1} [\exp\{-iHt\} \rho \otimes \text{Tr}_1 \{|G\rangle\langle G|\} \exp\{iHt\}]. \quad (1.5)$$

Some practical aspects how to realise these steps are discussed in the next section. For the moment, we will concentrate on the *quality* of quantum state transfer given that the above steps can be performed. From a quantum information perspective, the above equations describe a *quantum channel* [5] τ that maps input states ρ at one end of the chain to output states $\tau(\rho) = \sigma$ on the other end. A very simple measure of the quality of such a quantum channel is the *fidelity* [2, 50, 51]

$$F(\rho, \sigma) \equiv \left(\text{Tr} \sqrt{\rho^{1/2} \sigma \rho^{1/2}} \right)^2. \quad (1.6)$$

More advanced measures of the quality of transfer will be discussed in Chapter 3. Note also that some authors define the fidelity without taking the square of the trace. It is a real-valued, symmetric function with range between 0 and 1, assuming unity if and only if $\rho = \sigma$. Since the transported state that is an unknown result of some quantum computation, we are interested in the *minimal fidelity*

$$F_0 \equiv \min_{\rho} F(\rho, \tau(\rho)). \quad (1.7)$$

We remark that some authors also assume an equal distribution of input states and compute the *average fidelity* [1]. Using the strong concavity of the fidelity [2] and the linearity of τ we find that the minimum must be assumed on pure input states,

$$F_0 = \min_{\psi} \langle \psi | \tau(\psi) | \psi \rangle. \quad (1.8)$$

In the present context, $F_0 = F_0(H, t)$ is a function of the Hamiltonian H of the quantum chain (through the specific role of the ground state in the protocol and through the time evolution), and of the time interval t that the system is evolving in the third step of the protocol.

1.4.1 Initialisation and end-gates

There are two strong assumptions in the protocol from the last section. The first one is that the chain can be initialised in the ground state $|G\rangle$. How can that be achieved if there is no local control along the chain? The answer appears to be quite easy: one just applies a strong global magnetic field and strong cooling (such as laser cooling or dilution refrigeration) and lets the system reach its ground state by relaxation. The cooling needs to be done for the remaining parts of the quantum computer anyway, so no extra devices are required. However there is a problem with the time-scale of the relaxation. If the system is brought to the ground state by cooling, it must be coupled to some environment. But during the quantum computation, one clearly does not want such an environment. This is usually solved by having the time-scale of the computation much smaller (say microseconds) than the time-scale of the cooling (say seconds or minutes). But if the quantum chain should be used multiple times during one computation, then how is it reset between each usage? This is important to avoid memory effects [52], and there are two solutions to this problem. Either the protocol is such that at the end the chain is automatically in the ground state. Such a protocol usually corresponds to *perfect state transfer*. The other way is to use the control at the ends of the chain to bring it back to the ground state. A simple *cooling protocol* is given by the following: one measures the state of the last qubit of the chain. If it is in $|0\rangle$, then one just lets the chain evolve again and repeats. If however it is found to be in $|1\rangle$, one applies the Pauli operator X to flip it before evolving and repeating. It will become clear later on in the thesis that such a protocol typically converges exponentially fast to the ground state of the chain.

The second assumption in the last section is that the sender and receiver are capable of swapping in and out the state much quicker than the time-scale of the interaction of the chain. Alternatively, it is assumed that they can switch on and off the interaction between the chain and their memory in such time-scale. It has recently been shown [33] that this is not a fundamental problem, and that finite switching times can even slightly improve the fidelity if they are carefully included in the protocol. But this requires to solve the full time-dependent Schrödinger equation, and introduces further parameters to the model (i.e. the raise and fall time of the couplings). For the sake of simplicity,

we will therefore assume that the end gates are much faster than the time evolution of the chain (see also Section 6.3).

1.4.2 Symmetries

The dimensionality of the Hilbert space \mathcal{H} of a quantum chain of N qubits is 2^N . This makes it quite hopeless in general to determine the minimal fidelity Eq. (1.8) for long quantum chains. Most investigations on quantum state transfer with quantum chains up to date are therefore concentrating on Hamiltonians with additional symmetries. With few exceptions [21,22,34,53] Hamiltonians that conserve the number of excitations are considered. In this case the Hilbert space is a direct sum of subspaces invariant under the time evolution,

$$\mathcal{H} = \bigoplus_{\ell=0}^N \mathcal{H}_{\ell}, \quad (1.9)$$

with $\dim \mathcal{H}_{\ell} = \binom{N}{\ell}$, and where ℓ is the number of excitations. These Hamiltonians are *much* easier to handle both analytically and numerically, and it is also easier to get an intuition of the dynamics. Furthermore, they occur quite naturally as a coupling between qubits in the relevant systems. We stress though that there is *no fundamental* reason to restrict quantum chain communication to this case.

1.4.3 Transfer functions

The space \mathcal{H}_0 only contains the state $|\mathbf{0}\rangle$ which is thus always an eigenstate of H . We will assume here that it is also the ground state,

$$|G\rangle = |\mathbf{0}\rangle. \quad (1.10)$$

This can be achieved by applying a strong global magnetic field (or equivalent) to the system. The space \mathcal{H}_1 is spanned by the vectors $\{|\mathbf{k}\rangle, k = 1, \dots, N\}$ having exactly one excitation. The above protocol becomes:

1. Initialise the quantum chain in the ground state

$$|\mathbf{0}\rangle \quad (1.11)$$

2. Put an arbitrary and unknown qubit in the pure state $|\psi\rangle = \alpha|0\rangle + \beta|1\rangle$ at the

sending end of the chain

$$\alpha|\mathbf{0}\rangle + \beta|\mathbf{1}\rangle \quad (1.12)$$

3. Let the system evolve for a time t

$$\alpha|\mathbf{0}\rangle + \beta \exp\{-iHt\}|\mathbf{1}\rangle \quad (1.13)$$

4. Pick up the quantum state at the end of the chain (see [1])

$$\tau(\psi) = (1 - p(t))|0\rangle\langle 0| + p(t)|\psi\rangle\langle\psi|, \quad (1.14)$$

with the minimal fidelity given by

$$F_0 = \min_{\psi} \langle\psi|\tau(\psi)|\psi\rangle \quad (1.15)$$

$$= p(t) + (1 - p(t))\min_{\psi} |\langle 0|\psi\rangle|^2 = p(t). \quad (1.16)$$

The function $p(t)$ is the transition probability from the state $|\mathbf{1}\rangle$ to $|\mathbf{N}\rangle$ given by

$$p(t) = |\langle \mathbf{N} | \exp\{-iHt\} | \mathbf{1} \rangle|^2. \quad (1.17)$$

We see that in the context of quantum state transfer, a *single* parameter suffices to characterise the properties of an excitation conserving chain. The averaged fidelity [1] is also easily computed as

$$\bar{F} = \frac{\sqrt{p(t)}}{3} + \frac{p(t)}{6} + \frac{1}{2}. \quad (1.18)$$

Even more complex measures of transfer such as the quantum capacity only depend on $p(t)$ [54]. It is also a physically intuitive quantity, namely a particular matrix element of the time evolution operator,

$$f_{n,m}(t) \equiv \langle \mathbf{n} | \exp\{-iHt\} | \mathbf{m} \rangle \quad (1.19)$$

$$= \sum_k e^{-iE_k t} \langle \mathbf{n} | E_k \rangle \langle E_k | \mathbf{m} \rangle, \quad (1.20)$$

where $|E_k\rangle$ and E_k are the eigenstates and energy levels of the Hamiltonian in \mathcal{H}_1 .

1.4.4 Heisenberg Hamiltonian

The Hamiltonian chosen in [1] is a Heisenberg Hamiltonian

$$H = -\frac{J}{2} \sum_{n=1}^{N-1} (X_n X_{n+1} + Y_n Y_{n+1} + Z_n Z_{n+1}) - B \sum_{n=1}^N Z_n + c, \quad (1.21)$$

with a constant term

$$c = \frac{J(N-1)}{2} + NB \quad (1.22)$$

added to set the ground state energy to 0. For $J > 0$ it fulfils all the assumptions discussed above, namely its ground state is given by $|\mathbf{0}\rangle$ and it conserves the number of excitations in the chain. The Heisenberg interaction is very common and serves here as a typical and analytically solvable model for quantum state transfer.

In the first excitation subspace \mathcal{H}_1 , the Heisenberg Hamiltonian Eq. (1.21) is expressed in the basis $\{|\mathbf{n}\rangle\}$ as

$$\begin{pmatrix} 1 & -1 & & & \\ -1 & 2 & -1 & & \\ & -1 & 2 & \ddots & \\ & & \ddots & \ddots & -1 \\ & & & -1 & 2 & -1 \\ & & & & -1 & 1 \end{pmatrix}. \quad (1.23)$$

A more general study of such *tridiagonal* matrices can be found in a series of articles on coherent dynamics [55–58]. Some interesting analytically solvable models have also been identified [56, 57, 59] (we shall come back to that point later).

For the present case, the eigenstates of Eq (1.23) are [1]

$$|E_k\rangle = \sqrt{\frac{1+\delta_{k0}}{N}} \sum_{n=1}^N \cos\left[\frac{\pi k}{2N}(2n-1)\right] |\mathbf{n}\rangle \quad (k = 0, \dots, N-1), \quad (1.24)$$

with the corresponding energies given by

$$E_k = 2B + 2J \left[1 - \cos \frac{\pi k}{N}\right]. \quad (1.25)$$

The parameter B has no relevance for the fidelity but determines the stability of the ground state (the energy of the first excited state is given by $2B$). The minimal fidelity

for a Heisenberg chain is given by

$$p(t) = N^{-2} \left| 1 + \sum_{k=1}^{N-1} \exp \left\{ -2iJt \left(1 - \cos \frac{\pi k}{N} \right) \right\} (-1)^k \left(1 + \cos \frac{\pi k}{N} \right) \right|^2. \quad (1.26)$$

As an example, Fig 1.6 shows $p(t)$ for $N = 50$.

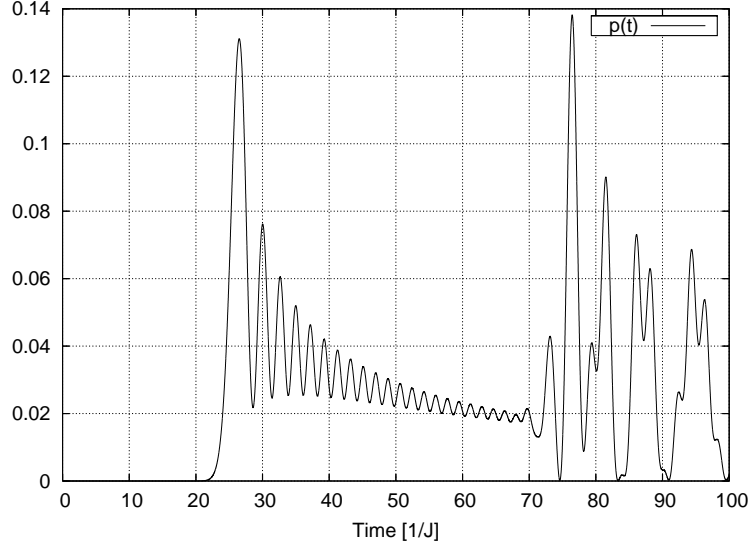


Figure 1.6: Minimal fidelity $p(t)$ for a Heisenberg chain of length $N = 50$.

1.4.5 Dynamic and Dispersion

Already in [1] has been realised that the fidelity for quantum state transfer along spin chains will in general not be perfect. The reason for the imperfect transfer is the *dispersion* [60] of the information along the chain. Initially the quantum information is localised at the sender, but as it travels through the chain it also spreads (see Fig. 1.7 and Fig. 1.8). This is not limited to the Heisenberg coupling considered here, but a very common quantum effect. Due to the dispersion, the probability amplitude peak that reaches Bob is typically small, and becomes even smaller as the chains get longer.

The fidelity given Eq. (1.26) is shown in Fig. 1.6. We can see that a wave of quantum information is travelling across the chain. It reaches the other end at a time of approximately

$$t_{\text{peak}} \approx \frac{N}{2J} \quad (1.27)$$

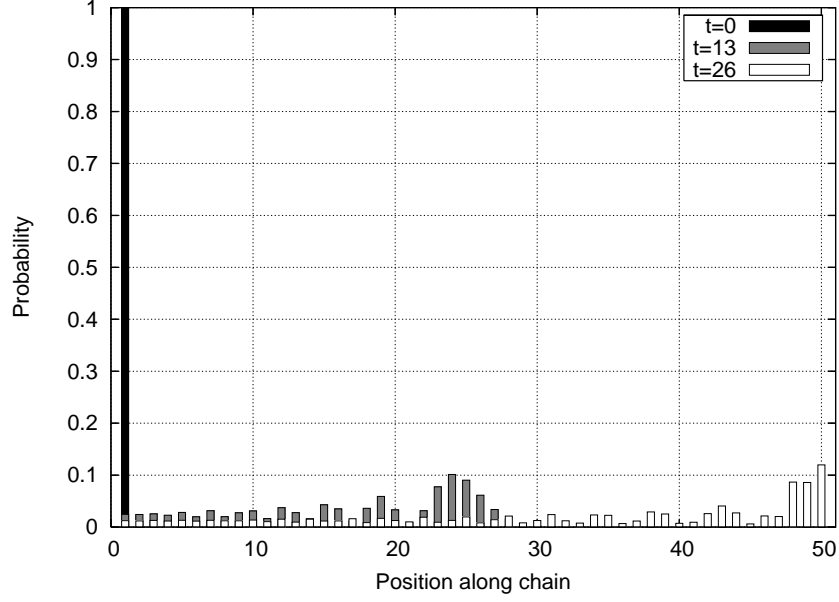


Figure 1.7: Snapshots of the time evolution of a Heisenberg chain with $N = 50$. Shown is the distribution $|f_{n,1}(t)|^2$ of the wave-function in space at different times if initially localised at the first qubit.

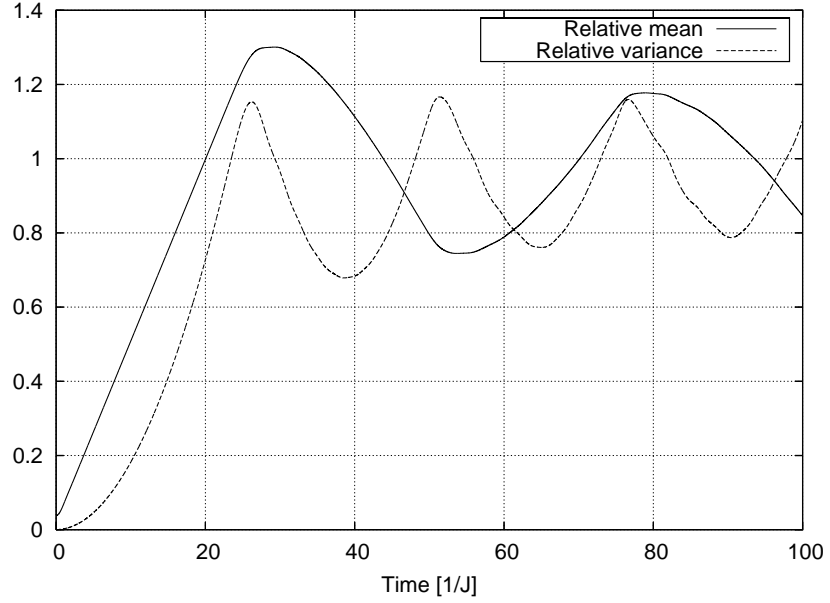


Figure 1.8: Mean and variance of the state $|\mathbf{1}\rangle$ as a function of time. Shown is the case $N = 50$ with the y-axis giving the value *relative* to the mean $N/2 + 1$ and variance $(N^2 - 1)/12$ of an equal distribution $\frac{1}{\sqrt{N}} \sum |\mathbf{n}\rangle$.

As a rough estimate of the scaling of the fidelity with respect to the chain length around this peak we can use [1,61] (see also Fig. 1.9)

$$|f_{N,1}(t)|^2 \approx |2J_N(\frac{2t}{J})|^2 \approx \left| \left(\frac{16}{N} \right)^{1/3} \text{ai} \left[\left(\frac{2}{N} \right)^{1/3} \left(N - \frac{2t}{J} \right) \right] \right|^2, \quad (1.28)$$

where $J_N(x)$ is a Bessel function of first kind and $\text{ai}(x)$ is the Airy function. The airy function $\text{ai}(x)$ has a maximum of 0.54 at $x = -1.02$. Hence we have

$$p(t_{\text{peak}}) = |f_{N,1}(\frac{N}{2J})|^2 \approx 1.82N^{-2/3}. \quad (1.29)$$

It is however possible to find times where the fidelity of the chain is much higher. The reason for this is that the wave-packet is reflected at the ends of the chain and starts interfering with itself (Fig 1.6). As the time goes on, the probability distribution becomes more and more random. Sometimes high peaks at the receiving end occur. From a theoretical point of view, it is interesting to determine the *maximal peak* occurring, i.e.

$$p_M(T) \equiv \max_{0 < t < T} p(t). \quad (1.30)$$

As we can see in Fig. 1.10 there is quite a potential to improve from the estimate Eq. (1.29).

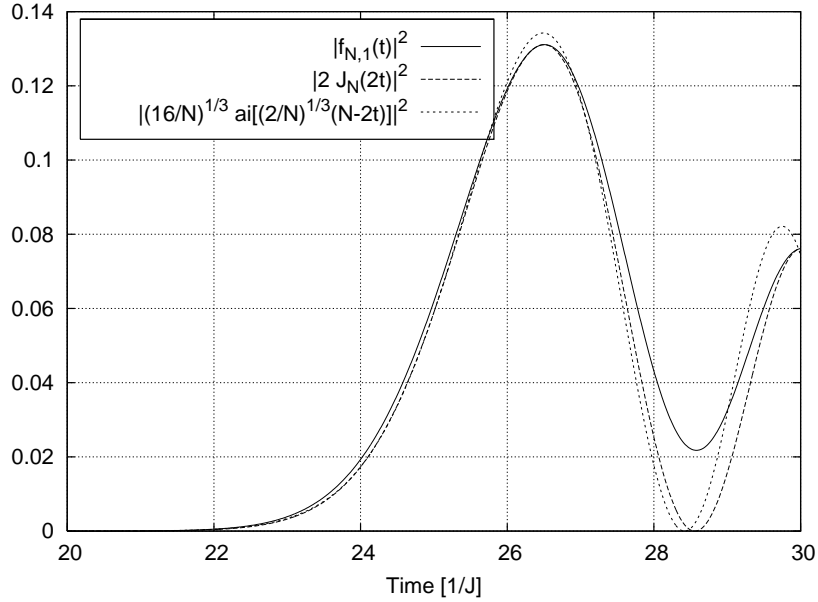


Figure 1.9: Approximation of the transfer amplitude for $N = 50$ around the first maximum by Bessel and Airy functions [1,61].

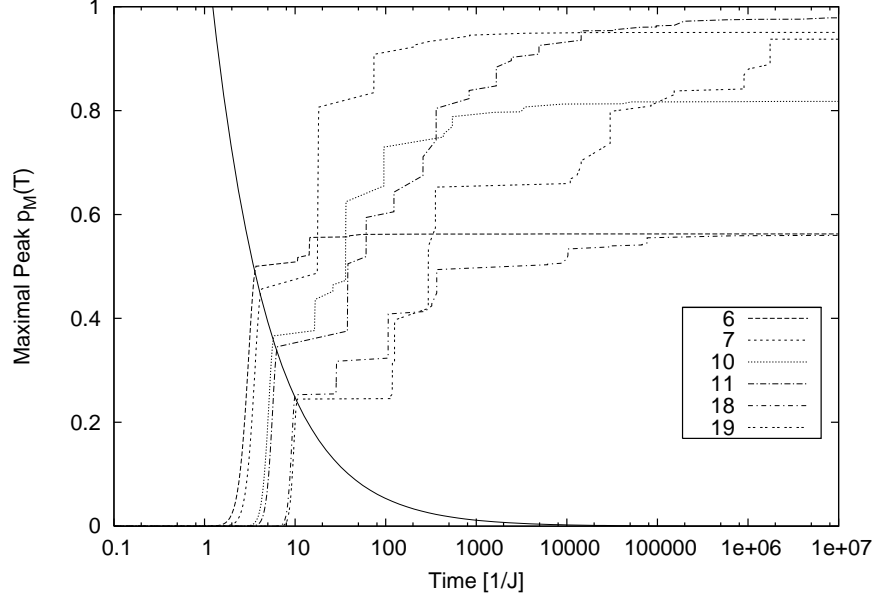


Figure 1.10: $p_M(T)$ as a function of T for different chain lengths. The solid curve is given by $1.82(2T)^{-2/3}$ and corresponds to the first peak of the probability amplitude (Eq. 1.29)

We will now show a perhaps surprising connection of the function $p_M(T)$ to number theory. Some speculations on the dependence of the fidelity on the chain length being divisible by 3 were already made in [1], but not rigorously studied. As it turns out, for chains with *prime number length* the maximum of the fidelity is actually converging to unity (see Fig. 1.10). To show this, we first prove the following

Lemma 1.1 *Let N be an odd prime. Then the set*

$$\left\{ \cos \frac{k\pi}{N} \quad (k = 0, 1, \dots, \frac{N-1}{2}) \right\} \quad (1.31)$$

is linear independent over the rationals \mathbb{Q} .

PROOF Assume that

$$\sum_{k=0}^{\frac{N-1}{2}} \lambda_k \cos \frac{k\pi}{N} = 0 \quad (1.32)$$

with $\lambda_k \in \mathbb{Q}$. It follows that

$$\sum_{k=0}^{\frac{N-1}{2}} \lambda_k \left\{ \exp \frac{ik\pi}{N} + \exp \frac{-ik\pi}{N} \right\} = 0 \quad (1.33)$$

and hence

$$\sum_{k=0}^{\frac{N-1}{2}} \lambda_k \exp \frac{ik\pi}{N} - \sum_{k=0}^{\frac{N-1}{2}} \lambda_k \exp \frac{i(N-k)\pi}{N} = 0. \quad (1.34)$$

Changing indexes on the second sum we get

$$\sum_{k=0}^{\frac{N-1}{2}} \lambda_k \exp \frac{ik\pi}{N} - \sum_{k=\frac{N+1}{2}}^N \lambda_{N-k} \exp \frac{ik\pi}{N} = 0. \quad (1.35)$$

and finally

$$\sum_{k=0}^{N-1} \tilde{\lambda}_k \exp \frac{ik\pi}{N} = 0, \quad (1.36)$$

where

$$\tilde{\lambda}_0 = 2\lambda_0 \quad (1.37)$$

$$\tilde{\lambda}_k = \lambda_k \quad (k = 1, \dots, \frac{N-1}{2}) \quad (1.38)$$

$$\tilde{\lambda}_k = -\lambda_{N-k} \quad (k = \frac{N+1}{2}, \dots, N-1). \quad (1.39)$$

Since N is prime, the roots of unity in Eq. (1.36) are all primitive and therefore linearly independent over \mathbb{Q} [62, Theorem 3.1, p. 313]. Hence $\lambda_k = 0$ for all k . \blacksquare

Theorem 1.1 (Half recurrence) *Let N be an odd prime. For a Heisenberg chain of length N we have*

$$\lim_{T \rightarrow \infty} p_M(T) = \lim_{T \rightarrow \infty} \left[\max_{0 < t < T} p(t) \right] = 1. \quad (1.40)$$

PROOF The eigenfrequencies of the Hamiltonian in the first excitation sector \mathcal{H}_1 are given by

$$E_k = 2B + 2J \left[1 - \cos \frac{\pi k}{N} \right] \quad (k = 0, 1, \dots, N-1). \quad (1.41)$$

Using Kronecker's theorem [63] and Lemma 1.1, the equalities

$$\exp \{itE_k\} = (-1)^k e^{2(B+J)t} \quad (k = 0, 1, \dots, \frac{N-1}{2}) \quad (1.42)$$

can be fulfilled *arbitrarily well* by choosing an appropriate t . Since

$$\cos \frac{k\pi}{N} = -\cos \frac{(N-k)\pi}{N}, \quad (1.43)$$

the equalities (1.42) are then also fulfilled arbitrarily well for $k = 0, \dots, N-1$. This is known as a sufficient condition for perfect state transfer in mirror symmetric chains [64], where the eigenstates can be chosen such that they are alternately symmetric and antisymmetric. Roughly speaking, Eq. (1.42) introduces the correct phases (a sign change for the antisymmetric eigenstates) to move the state $|1\rangle$ to $|N\rangle$ and hence the theorem. ■

Remark 1.1 The time-scale for finding high valued peaks is however *exponential* in the chain length [63]. Therefore the above theorem has little practical use. For non-prime chain lengths, the eigenfrequencies are not sufficiently independent to guarantee a perfect state transfer, with the algebraic dimensionality of the roots of unity for non-prime N given by the Euler totient function $\phi(N)$ [62, Theorem 3.1, p. 313]. We also remark that due to its asymptotic character, the above result is not contradicting [65], where it was shown that chains longer than $N \geq 4$ never have perfect fidelity.

Having proved that there are many chains that can in principle perform arbitrarily well, it is important to find a cut-off time for the optimisation Eq. (1.30). Faster transfer than linear in N using local Hamiltonians is impossible due to the Lieb-Robinson bound [66, 67], which is a "speed limit" in non-relativistic quantum mechanics giving rise to a well defined group velocity. Transport faster than this group velocity is exponentially suppressed. Going back to the motivation of quantum state transfer, a natural comparison [37] for the time-scale of quantum state transfer is given by the time it would take to perform a sequence of swap gates (cf. Fig 1.1) that are realised by a pairwise switchable coupling Hamiltonian

$$\frac{J}{2}(X_n X_{n+1} + Y_n Y_{n+1}). \quad (1.44)$$

This time is linear in the chain length:

$$t_{\text{swap}} = \frac{(N-1)\pi}{2J}. \quad (1.45)$$

Ideally one could say that the time for quantum state transfer should not take much longer than this. However one may argue that there is a trade-off between quick transfer on one hand, and minimising control on the other hand. A second cut-off

time may be given by the *decoherence time* of the specific implementation. But short decoherence times could always be counteracted by increasing the chain coupling J . A more general and implementation independent limit is given by the requirement that the *peak width* Δt_{peak} should not be too small with respect to the total time. Otherwise it is difficult to pick up the state at the correct time. For the first peak, we can estimate the width by using the full width at half height of the airy function. From Eq. (1.28) we get an absolute peak width of $\Delta t_{\text{peak}} \approx 0.72N^{1/3}/J$ and a relative width of

$$\frac{\Delta t_{\text{peak}}}{t_{\text{peak}}} \approx 1.44N^{-2/3}. \quad (1.46)$$

This is already quite demanding from an experimental perspective and we conclude that the transfer time should not be chosen much longer than those of the first peak.

1.4.6 How high should $p(t)$ be?

We have not discussed yet what the actual value of $p(t)$ should be to make such a spin chain useful as a device for quantum state transfer. $p(t) = 0$ corresponds to no state transfer, $p(t) = 1$ to a perfect state transfer. But what are the relevant scales for intermediate $p(t)$? In practice, the quantum transfer will suffer from additional external noise (Chapter 7) and also the quantum computer itself is likely to be very noisy. From this point of view, requiring $p(t) = 1$ seems a bit too demanding.

From a theoretical perspective, it is interesting that for any $p(t) > 0$, one can already do things which are impossible using classical channels, namely entanglement transfer and distillation [2]. The entanglement of formation between the sender (*Alice*) and the receiver (*Bob*) is simply given by $\sqrt{p(t)}$ [1]. This entanglement can be partially distilled [68] into singlets, which could be used for state transfer using teleportation [2]. It is however not known *how much*, i.e. at which rate, entanglement can be distilled (we will develop lower bounds for the entanglement of distillation in Section 2.2 and Section 3.4). Also, entanglement distillation is a quite complex procedure that requires local unitary operations and measurements, additional classical communication, and multiple chain usages; and few explicit protocols are known. This is likely to preponderate the benefits of using a quantum chain.

When the chain is used without encoding and further operation, the averaged fidelity Eq. (1.18) becomes better than the classical¹ averaged fidelity [1] when $p(t) > 3 -$

¹By "classical fidelity", we mean the fidelity that can be achieved by optimising the following protocol: Alice performs measurements on her state and sends Bob the outcome through a classical communication line. Bob then tries to rebuild the state that Alice had before the measurement based on the information she sent. For qubits, the classical fidelity is given by $2/3$ [69].

$2\sqrt{2}$. Following the conclusion from the last subsection that the first peak is the most relevant one, this would mean that only chains with length until $N = 33$ perform better than the classical fidelity.

Finally, the *quantum capacity* [54, 70] of the channel becomes non-zero only when $p(t) > 1/2$, corresponding to chain lengths up to $N = 6$. Roughly speaking, it is a measure of the number of perfectly transmitted qubits per chain usage that can be achieved asymptotically using encoding and decoding operations on multiple channel usages. The quantum capacity considered here is not assumed to be assisted by a classical communication, and the threshold of $p(t) > 0.5$ to have a non-zero quantum capacity is a result of the non-cloning theorem [2]. This is not contradicting the fact that entanglement distillation is possible for *any* $p(t) > 0$, as the entanglement distillation protocols require additional classical communication.

All the above points are summarised in Fig. 1.11. We can see that only very short chains reach reasonable values (say > 0.6) for the minimal fidelity.

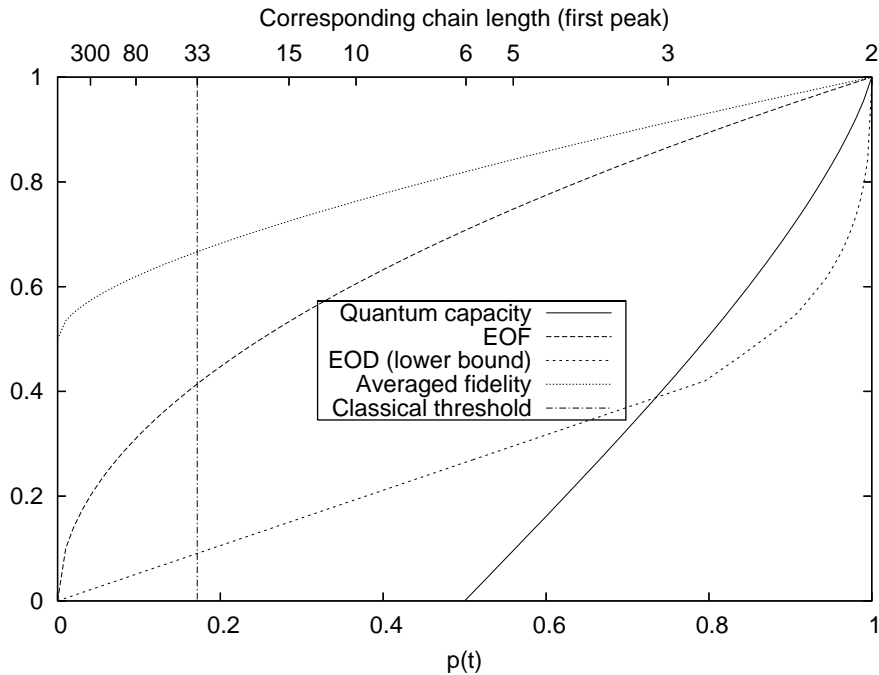


Figure 1.11: Quantum capacity, entanglement of formation (EOF), a lower bound for the entanglement of distillation (EOD) and the averaged fidelity as a function of $p(t)$. We also show the corresponding chain length which reaches this value as a first peak and the classical threshold $3 - 2\sqrt{2}$. The explicit expression for the quantum capacity plotted here is given in [54], and the lower bound of the entanglement of distillation will be derived in Section 3.4.

1.5 Advanced communication protocols

We have seen in the last section that without much further effort, i.e. entanglement distillation, unmodulated Heisenberg chains are useful only when they are very short. Shortly after the initial proposal [1] it has been shown that there are ways to achieve even *perfect state transfer* with arbitrarily long chains. These advanced proposals can roughly be grouped into four categories, which we will now briefly describe.

1.5.1 Engineered Hamiltonians

The Heisenberg model chosen by Bose features many typical aspects of coherent transport, i.e. the wave-like behaviour, the dispersion, and the almost-periodicity of the fidelity. These features do not depend so much on the specific choices of the parameters of the chain, such as the couplings strengths. There are however *specific couplings* for quantum chains that show a quite different time evolution, and it was suggested in [71] and independently in [72] to use these to achieve a *perfect* state transfer:

$$H = -J \sum_{n=1}^{N-1} \sqrt{n(N-n)} (X_n X_{n+1} + Y_n Y_{n+1}) \quad (1.47)$$

These values for engineered couplings also appear in a different context in [57,73]. The time evolution under the Hamiltonian (1.47) features an additional *mirror symmetry*: the wave-packet disperses initially, but the dispersion is reversed after its centre has passed the middle of the chain (Fig. 1.12). This approach has been extended by various authors [19,53,59,64,65,74–84], and many other choices of parameters for perfect or near perfect state transfer in various settings were found [59,81,83].

1.5.2 Weakly coupled sender and receiver

A different approach of tuning the Hamiltonian was suggested in [85]. There, only the first and the last couplings j of the chain are engineered to be *much weaker* than the remaining couplings J of the chain, which can be quite arbitrary. The fidelity can be made arbitrarily high by making the edge coupling strengths smaller. It was shown [86,87] that to achieve a fidelity of $1 - \delta$ in a chain of odd length, it takes approximately a time of

$$2N\pi/\sqrt{\delta} \quad (1.48)$$

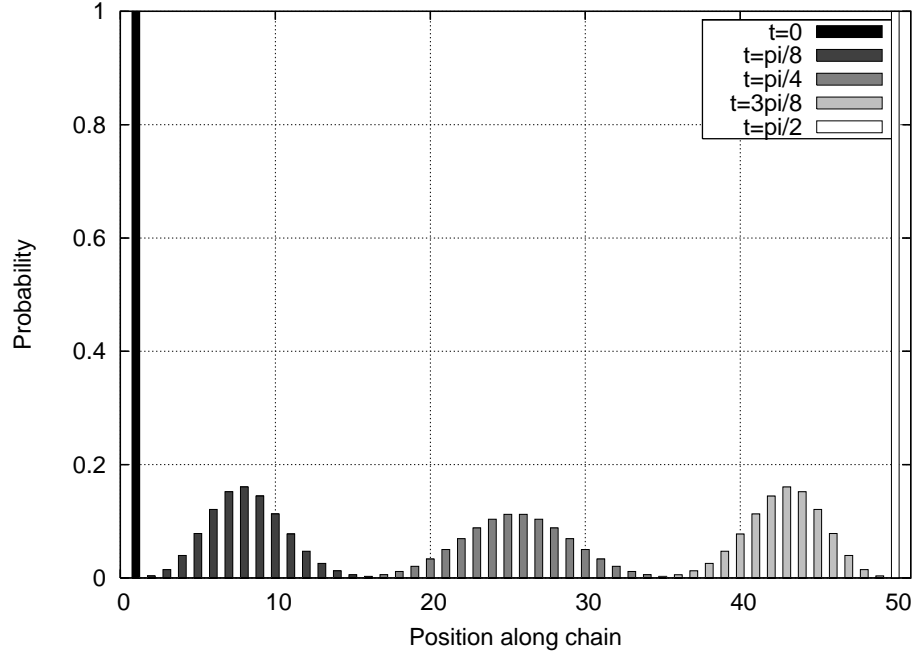


Figure 1.12: Snapshots of the time evolution of a quantum chain with engineered couplings (1.47) for $N = 50$. Shown is the distribution of the wave-function in space at different times if initially localised at the first qubit (compare Fig. 1.7).

and the coupling ratio has to be approximately $j/J \approx \sqrt{\delta/N}$. Some specific types of quantum chains which show high fidelity for similar reasons were also investigated [88–91].

1.5.3 Encoding

We have seen in Subsec. 1.4.6 that if $p(t) < 1/2$, the fidelity cannot be improved by using any encoding/decoding strategy (because the quantum capacity is zero). However it is possible to *change the protocol* described in Sec. 1.4 slightly such that the fidelity is much higher. This can be thought of as a “hardware encoding”, and was suggested first in [60]. There, it was assumed that the chain consists of three sections: one part of length $\approx 2N^{1/3}$ controlled by the sending party, one “free” part of length N and one part of length $\approx 2.8N^{1/3}$ controlled by the receiving party. The sender encodes the qubit not only in a single qubit of the chain, but in a *Gaussian-modulated superposition* of his qubits. These Gaussian packets are known to have minimal dispersion. Likewise, the receiver performs a decoding operation on all qubits he controls. Near-perfect fidelity can be reached.

1.5.4 Time-dependent control

Finally, a number of authors found ways of improving the fidelity by time-dependent control of some parameters of the Hamiltonian. In [92] it is shown that if the end couplings can be controlled as arbitrary (in general complex valued) smooth functions of time the encoding scheme [60] could be *simulated* without the requirement of additional operations and qubits. Another possibility to achieve perfect state transfer is to have an Ising interaction with additionally pulsed global rotations [40, 93, 94]. Further related methods of manipulating the transfer by global fields were reported in [25, 28, 95–98].

1.6 Motivation and outline of this work

While the advanced transfer protocols have shown that in principle high fidelity can be achieved with arbitrarily long chains, they have all come at a cost. Engineering each coupling of the Hamiltonian puts extra demands on the experimental realisation, which is often already at its very limits just to ensure the *coherence* of the system. Furthermore, the more a scheme relies on particular properties of the Hamiltonian, the more it will be affected by imperfections in its implementation [84, 99]. For example, simulating an engineered chain of length $N = 50$ with a (relative) disorder of 5%, we

get a fidelity peak of 0.95 ± 0.02 . For a disorder of 10% we get 0.85 ± 0.05 . The weakly coupled system is very stable for off-site disorder [85], but suffers strongly from on-site disorder (i.e. magnetic fields in z -direction) at the ends of the chain. For example, for a chain of $N = 50$ with edge couplings $j = 0.01$ and the remaining couplings being $J = 1$, we find that already a magnetic field of the order of 0.00001 lowers the fidelity to 0.87 ± 0.12 . For fields of the order of 0.00005 we find 0.45 ± 0.32 . This is because these fluctuations must be small with respect to the *small* coupling, so there is a double scaling. Also, the time-scale of the transfer is longer than in other schemes (note though that this may sometimes even be useful for having enough time to pick up the received state). On the other hand, encoding and time-dependent control require additional resources and gating operations. It is not possible to judge independently of the realisation which of the above schemes is the "most practical" one. We summarise the different aspects that are important in the following five criteria for quantum state transfer:

1. *High efficiency*: How does the fidelity depend on the length of the chain? Which rate [74,81,100] can be achieved?
2. *Minimal control*: How many operations are required to achieve a certain fidelity? *Where*² is control required?
3. *Minimal resources*: What additional resources are required?
4. *Minimal design*: How general is the coupling type³? What values of the coupling strengths are allowed?
5. *Robustness*: How is the fidelity affected by static disorder, by time-dependent disorder, by gate and timing errors, and by external noise such as decoherence and dissipation?

At the start of this research, only the engineering and encoding schemes were available. The engineering schemes are strong in the points 2 and 3, but quite weak in the points 4 and 5. The encoding scheme on the other hand has its weakness in points 2 and 3. It was hence desirable to develop more balanced schemes. Since most experiments in Quantum Information are extremely sensitive and at the cutting edge of their parameters (i.e. requiring extremely low temperatures, well tuned lasers, and so forth,

²For example, gates at the ends of the chain are always needed for write-in and read-out, and thus "cheaper" than gates along the chain. Global control along the whole chain is often easier than local control.

³Often the coupling type is already fixed by the experiment

to maintain their quantum behaviour), we particularly wanted to find schemes which are strong in the points 4 and 5. Also, from a more fundamental point of view, we were interested in seeing how much information on the state of a quantum chain could be obtained by the receiver in principle, and how the receiver might even be able to *prepare* states on the whole chain.

The main achievements of this thesis are two schemes for the transfer of quantum information using measurements (Chapter 2 and 3) or unitary operations (Chapter 5 and 6) at the receiving end of the chain. Since both schemes use convergence properties of quantum operations, it seemed natural to investigate these properties in a more abstract way (Chapter 4). There, we found a new way of characterising mixing maps, which has applications beyond quantum state transfer, and may well be relevant for other fields such as chaos theory or statistical physics. Finally, in Chapter 7 we discuss problems quantum state transfer in the presence of external noise. The results in Chapters 3-6 were developed in collaboration with Vittorio Giovannetti from Scuola Normale, Pisa. Much of the material discussed in this thesis has been published or submitted for publication [101–110].

2 Dual Rail encoding

2.1 Introduction

The role of measurement in quantum information theory has become more active recently. Measurements are not only useful to obtain information about some state or for preparation, but also, instead of gates, for quantum computation [111]. In the context of quantum state transfer, it seems first that measurements would spoil the coherence and destroy the state. The first indication that measurements can actually be used to transfer quantum information along anti-ferromagnetic chains was given in [24]. However there the measurements had to be performed along the whole chain. This may in some cases be easier than to perform swap gates, but still requires high local accessibility. We take a "hybrid" approach here: along the chain, we let the system evolve coherently, but at the receiving end, we try to *help* the transfer by measuring. The main disadvantage of the encoding used in the protocols above is that once the information dispersed, there is no way of finding out where it is without destroying it. A dual rail encoding [112] as used in quantum optics on the other hand allows us to perform parity type measurements that do *not* spoil the coherence of the state that is sent. The outcome of the measurement tells us if the state has arrived at the end (corresponding to a perfect state transfer) or not. We call this *conclusively perfect state transfer*. Moreover, by performing repetitive measurements, the probability of success can be made arbitrarily close to unity. As an example of such an *amplitude delaying channel*, we show how two parallel Heisenberg spin chains can be used as quantum wires. Perfect state transfer with a probability of failure lower than P in a Heisenberg chain of N qubits can be achieved in a time-scale of the order of $0.33J^{-1}N^{1.7}|\ln P|$. We demonstrate that our scheme is more robust to decoherence and non-optimal timing than any scheme using single spin chains.

We then generalise the dual rail encoding to disordered quantum chains. The scheme performs well for both spatially correlated and uncorrelated fluctuations if they are relatively weak (say 5%). Furthermore, we show that given a quite arbitrary pair of quantum chains, one can check whether it is capable of perfect transfer by only local operations at the ends of the chains, and the system in the middle being a *black box*.

We argue that unless some specific symmetries are present in the system, it *will* be capable of perfect transfer when used with dual rail encoding. Therefore our scheme puts minimal demand not only on the control of the chains when using them, but also on the design when building them.

This Chapter is organised as follows. In Section 2.2, we suggest a scheme for quantum communication using two parallel spin chains of the most natural type (namely those with constant couplings). We require modest encodings (or gates) and measurements only at the ends of the chains. The state transfer is *conclusive*, which means that it is possible to tell by the outcome of a quantum measurement, without destroying the state, if the transfer took place or not. If it did, then the transfer was *perfect*. The transmission time for conclusive transfer is not longer than for single spin chains. In Section 2.3, we demonstrate that our scheme offers even more: if the transfer was not successful, then we can wait for some time and just repeat the measurement, without having to resend the state. By performing sufficiently many measurements, the probability for perfect transfer approaches unity. Hence the transfer is *arbitrarily perfect*. We will show in Section 2.4 that the time needed to transfer a state with a given probability scales in a reasonable way with the length of the chain. In Section 2.5 we show that encoding to parallel chains and the conclusiveness also makes our protocol more robust to decoherence (a hitherto unaddressed issue in the field of quantum communication through spin chains). In the last part of this chapter, we show how this scheme can be generalised to disordered chains (Sections 2.6-2.10) and even coupled chains (Section 2.11).

2.2 Scheme for conclusive transfer

We intend to propose our scheme in a system-independent way with occasional references to systems where conditions required by our scheme are achieved. We assume that our system consists of two identical uncoupled spin-1/2-chains (1) and (2) of length N , described by the Hamiltonian

$$H = H^{(1)} \otimes I^{(2)} + I^{(1)} \otimes H^{(2)} - E_g I^{(1)} \otimes I^{(2)}. \quad (2.1)$$

The term identical states that $H^{(1)}$ and $H^{(2)}$ are the same apart from the label of the Hilbert space they act on. The requirement of parallel chains instead of just one is not a real problem, since in many experimental realisations of spin chains, it is much easier to produce a whole bunch of parallel uncoupled [48, 49] chains than just a single one.

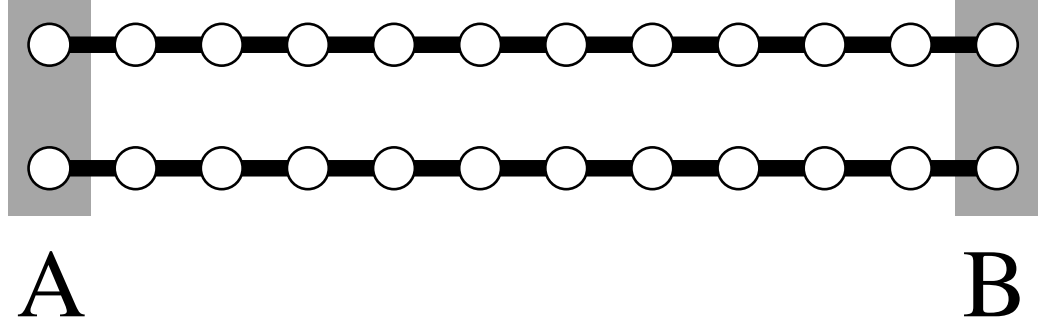


Figure 2.1: Two quantum chains interconnecting A and B . Control of the systems is only possible at the two qubits of either end.

We assume that the ground state of each chain is $|\mathbf{0}\rangle_i$, i.e. a ferromagnetic ground state, with $H^{(i)}|\mathbf{0}\rangle_i = E_g|\mathbf{0}\rangle_i$, and that the subspace consisting of the single spin excitations $|\mathbf{n}\rangle_i$ is invariant under $H^{(i)}$. Let us assume that the state that Alice wants to send is at the first qubit of the first chain, i.e.

$$|\psi_A\rangle_1 \equiv \alpha|\mathbf{0}\rangle_1 + \beta|\mathbf{1}\rangle_1, \quad (2.2)$$

and that the second chain is in the ground state $|\mathbf{0}\rangle_2$. The aim of our protocol is to transfer quantum information from the 1st (“Alice”) to the N th (“Bob”) qubit of the first chain:

$$|\psi_A\rangle_1 \rightarrow |\psi_B\rangle_1 \equiv \alpha|\mathbf{0}\rangle_1 + \beta|\mathbf{N}\rangle_1. \quad (2.3)$$

The first step (see also Fig. 2.2) is to encode the input qubit in a *dual rail* [112] by applying a NOT gate on the first qubit of system (2) controlled by the first qubit of system (1) being zero, resulting in a superposition of excitations in both systems,

$$|s(0)\rangle = \alpha|\mathbf{0}, \mathbf{1}\rangle + \beta|\mathbf{1}, \mathbf{0}\rangle, \quad (2.4)$$

where we have introduced the short notation $|\mathbf{n}, \mathbf{m}\rangle \equiv |\mathbf{n}\rangle_1 \otimes |\mathbf{m}\rangle_2$. This is assumed to take place in a much shorter time-scale than the system dynamics. Even though a 2-qubit gate in solid state systems is difficult, such a gate for charge qubits has been reported [15]. For the same qubits, Josephson arrays have been proposed as single spin chains for quantum communication [31]. For this system, both requisites of our scheme are thus available. In fact, the demand that Alice and Bob can do measurements and apply gates to their local qubits (i.e. the ends of the chains) will be naturally fulfilled in practice since we are suggesting a scheme to transfer information between quantum computers (as described in Section 1.2).

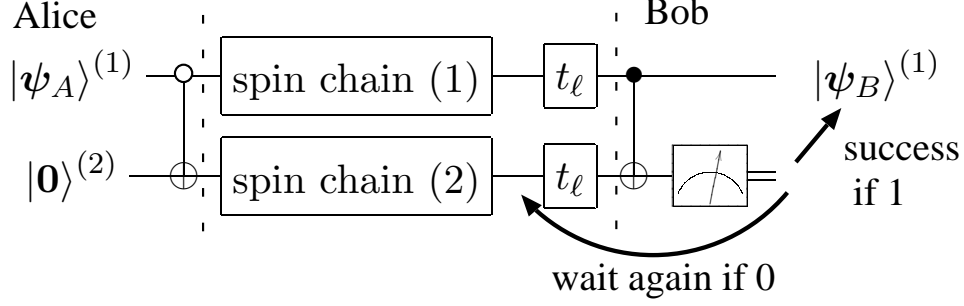


Figure 2.2: Quantum circuit representation of conclusive and arbitrarily perfect state transfer. The first gate at Alice's qubits represents a NOT gate applied to the second qubit controlled by the first qubit being zero. The qubit $|\psi_A\rangle_1$ on the left hand side represents an arbitrary input state at Alice's site, and the qubit $|\psi_B\rangle_1$ represents the same state, successfully transferred to Bob's site. The t_ℓ -gate represents the unitary evolution of the spin chains for a time interval of t_ℓ .

Under the system Hamiltonian, the excitation in Eq. (2.4) will travel along the two systems. The state after the time t_1 can be written as

$$|\phi(t_1)\rangle = \sum_{n=1}^N f_{n,1}(t_1) |\mathbf{s}(n)\rangle, \quad (2.5)$$

where $|\mathbf{s}(n)\rangle = \alpha |\mathbf{0}, \mathbf{n}\rangle + \beta |\mathbf{n}, \mathbf{0}\rangle$ and the complex amplitudes $f_{n,1}(t_1)$ are given by Eq. (1.19). We can *decode* the qubit by applying a CNOT gate at Bob's site. Assuming that this happens on a time-scale much shorter than the evolution of the chain, the resulting state is given by

$$\sum_{n=1}^{N-1} f_{n,1}(t_1) |\mathbf{s}(n)\rangle + f_{N,1}(t_1) |\psi_B\rangle_1 \otimes |\mathbf{N}\rangle_2. \quad (2.6)$$

Bob can now perform a measurement on his qubit of system (2). If the outcome of this measurement is 1, he can conclude that the state $|\psi\rangle_1^{(1)}$ has been successfully transferred to him. This happens with the probability $|f_{N,1}(t_1)|^2$. If the outcome is 0, the system is in the state

$$\frac{1}{\sqrt{P(1)}} \sum_{n=1}^{N-1} f_{n,1}(t_1) |\mathbf{s}(n)\rangle, \quad (2.7)$$

where $P(1) = 1 - |f_{N,1}(t_1)|^2$ is the probability of *failure* for the first measurement. If the protocol stopped here, and Bob would just assume his state as the transferred one,

the channel could be described as an *amplitude damping channel* [54], with exactly the same fidelity as the single chain scheme discussed in [1]. Note that here the encoding is symmetric with respect to α and β , so the minimal fidelity is the same as the averaged one.

But success probability is more valuable than fidelity: Bob has gained knowledge about his state, and may reject it and ask Alice to retransmit (this is known as a *quantum erasure channel* [113]). Of course in general the state that Alice sends is the unknown result of some quantum computation and cannot be sent again easily. This can be overcome in the following way: Alice sends one e-bit on the dual rail first. If Bob measures a success, he tells Alice, and they both start to teleport the unknown state. If he measures a failure, they reset the chains and start again. Since the joint probability of failure converges exponentially fast to zero this is quite efficient. In fact the conclusive transfer of entanglement is possible even on a *single chain* by using the same chain again instead of a second one [114]. This can be seen as a very simple entanglement distillation procedure, achieving a rate of $|f_{N,1}(t)|^2/2$. However the chain needs to be reset between each transmission (see Section 1.4.1 for problems related to this), and Alice and Bob require classical communication. We will show in the next section, that the reuse of the chain(s) is not necessary, as arbitrarily perfect state transfer can already be achieved in the first transmission.

2.3 Arbitrarily perfect state transfer

Because Bob's measurement has not revealed anything about the input state (the success probability is independent of the input state), the information is still residing in the chain. By letting the state (2.7) evolve for another time t_2 and applying the CNOT gate again, Bob has another chance of receiving the input state. The state before performing the second measurement is easily seen to be

$$\frac{1}{\sqrt{P(1)}} \sum_{n=1}^N \{f_{n,1}(t_2 + t_1) - f_{n,N}(t_2)f_{N,1}(t_1)\} |\mathbf{s}(n)\rangle. \quad (2.8)$$

Hence the probability to receive the qubit at Bob's site at the second measurement is

$$\frac{1}{P(1)} |f_{N,1}(t_2 + t_1) - f_{N,N}(t_2)f_{N,1}(t_1)|^2. \quad (2.9)$$

If the transfer was still unsuccessful, this strategy can be repeated over and over. Each time Bob has a probability of failed state transfer that can be obtained from the

generalisation of Eq. (2.8) to an arbitrary number of iterations. The joint probability that Bob fails to receive the state all the time is just the product of these probabilities. We denote the joint probability of failure for having done l unsuccessful measurements as $P(\ell)$. This probability depends on the time intervals t_ℓ between the $(\ell - 1)$ th and ℓ th measurement, and we are interested in the case where the t_ℓ are chosen such that the transfer is fast. It is possible to write a simple algorithm that computes $P(\ell)$ for any transition amplitude $f_{r,s}(t)$. Figure 2.3 shows some results for the Heisenberg Hamiltonian given by Eq. (1.21).

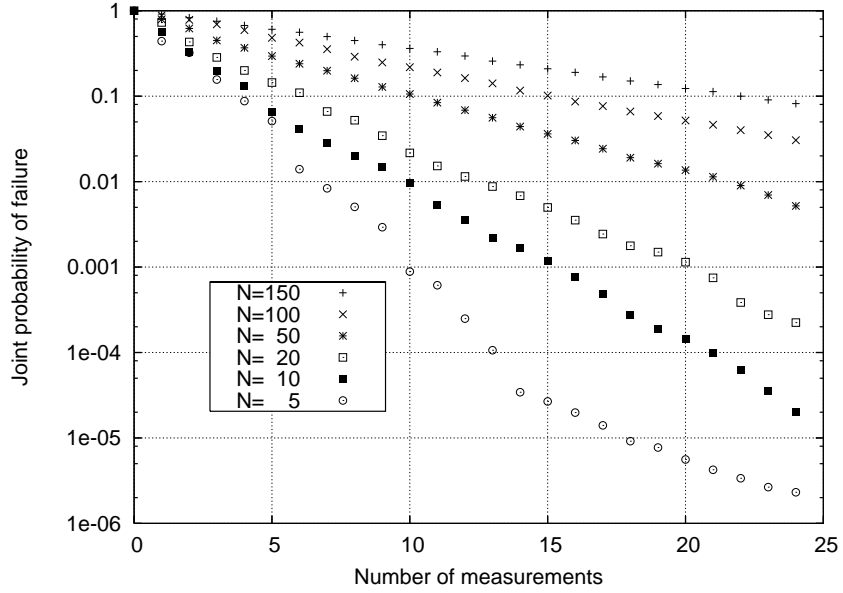


Figure 2.3: Semilogarithmic plot of the joint probability of failure $P(\ell)$ as a function of the number of measurements ℓ . Shown are Heisenberg spin-1/2-chains with different lengths N . The times between measurements t_ℓ have been optimised numerically.

An interesting question is whether the joint probability of failure can be made arbitrarily small with a large number of measurements. In fact, the times t_ℓ can be chosen such that the transfer becomes arbitrarily perfect. We will prove this in the next Chapter, where a generalisation of the dual rail scheme and a much wider class of Hamiltonians is considered. In the limit of large number of measurements, the spin channel will not damp the initial amplitude, but only *delay* it.

2.4 Estimation of the time-scale the transfer

The achievable fidelity is an important, but not the only criterion of a state transfer protocol. In this Section, we give an heuristic approach to estimate the time that it needs to achieve a certain fidelity in a Heisenberg spin chain. The comparison with numeric examples is confirming this approach.

Let us first describe the dynamic of the chain in a very qualitative way. Once Alice has initialised the system, an excitation wave packet will travel along the chain. As shown in Subsection 1.4.5, it will reach Bob at a time of the order of

$$t_{\text{peak}} \approx \frac{N}{2J}, \quad (2.10)$$

with an amplitude of

$$\left| f_{N,1}(t_{\text{peak}}) \right|^2 \approx 1.82N^{-2/3}. \quad (2.11)$$

It is then reflected and travels back and forth along the chain. Since the wave packet is also dispersing, it starts interfering with its tail, and after a couple of reflections the dynamic is becoming quite randomly. This effect becomes even stronger due to Bobs measurements, which change the dynamics by projecting away parts of the wave packet. We now assume that $2t_{\text{peak}}$ (the time it takes for a wave packet to travel twice along the chain) remains a good estimate of the time-scale in which significant probability amplitude peaks at Bobs site occur, and that Eq. (2.11) remains a good estimate of the amplitude of these peaks¹. Therefore, the joint probability of failure is expected to scale as

$$P(\ell) \approx \left(1 - 1.82N^{-2/3} \right)^\ell \quad (2.12)$$

in a time of the order of

$$t(\ell) \approx 2t_{\text{max}}\ell = J^{-1}N\ell. \quad (2.13)$$

If we combine Eq. (2.12) and (2.13) and solve for the time $t(P)$ needed to reach a certain probability of failure P , we get for $N \gg 1$

$$t(P) \approx 0.55J^{-1}N^{5/3} |\ln P|. \quad (2.14)$$

We compare this rough estimate with exact numerical results in Fig. 2.4. The best fit

¹This is not a strong assumption. If the excitation was fully randomly distributed, the probability would scale as N^{-1} . By searching for good arrival times, this can be slightly increased to $N^{-2/3}$.

for the range shown in the figure is given by

$$t(P) = 0.33J^{-1}N^{5/3}|\ln P|. \quad (2.15)$$

We can conclude that the transmission time for arbitrarily perfect transfer is scaling not much worse with the length N of the chains than the single spin chain schemes. Despite of the logarithmic dependence on P , the time it takes to achieve high fidelity is still reasonable. For example, a system with $N = 100$ and $J = 20K * k_B$ will take approximately $1.3ns$ to achieve a fidelity of 99%. In many systems, decoherence is completely negligible within this time-scale. For example, some Josephson junction systems [115] have a decoherence time of $T_\phi \approx 500ns$, while trapped ions have even larger decoherence times.

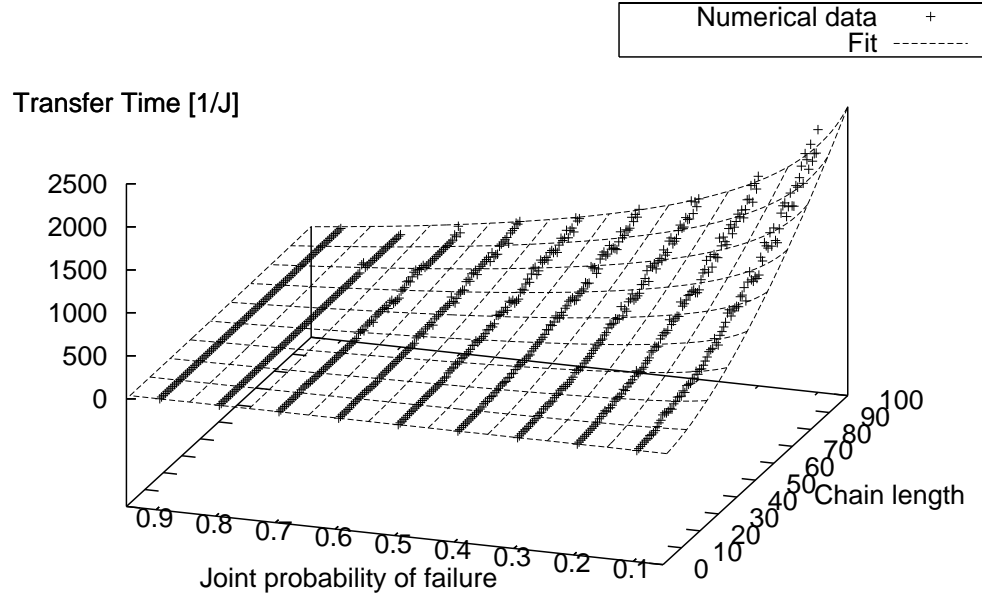


Figure 2.4: Time t needed to transfer a state with a given joint probability of failure P across a chain of length N . The points denote exact numerical data, and the fit is given by Eq. (2.15).

2.5 Decoherence and imperfections

If the coupling between the spins J is very small, or the chains are very long, the transmission time may no longer be negligible with respect to the decoherence time. It is interesting to note that the dual rail encoding then offers some significant general advantages over single chain schemes. Since we are suggesting a system-independent scheme, we will not study the effects of specific environments on our protocol, but just qualitatively point out its general advantages.

At least theoretically, it is always possible to cool the system down or to apply a strong magnetic field so that the environment is not causing further excitations. For example in flux qubit systems, the system is cooled to $\approx 25mK$ to ensure that the energy splitting $\Delta \gg k_B T$ [116]. Then, there are two remaining types of quantum noise that will occur: phase noise and amplitude damping. Phase noise is a serious problem and arises here *only* when an environment can distinguish between spin flips on the first chain and spin flips on the second chain. It is therefore important that the environment cannot resolve their difference. In this case, the environment will only couple with the total z -component

$$Z_n^{(1)} + Z_n^{(2)} \tag{2.16}$$

of the spins of both chains at each position n . This has been discussed for spin-boson models in [117,118] but also holds for spin environments as long as the chains are close enough. The qubit is encoded in a decoherence-free subspace [119] and the scheme is fully robust to phase noise. Even though this may not be true for all implementations of dual rail encoding, it is worthwhile noticing it because such an opportunity does not exist *at all* for single chain schemes, where the coherence between two states with different total z -component of the spin has to be preserved. Having shown one way of avoiding phase noise, at least in some systems, we now proceed to amplitude damping.

The evolution of the system in presence of amplitude damping of a rate Γ can be easily derived using a quantum-jump approach [120]. This is based on a quantum master equation approach, which is valid in the Born-Markov approximation [121] (i.e. it holds for weakly coupled environments without memory effects). Similarly to phase noise, it is necessary that the environment acts symmetrically on the chains. The dynamics is then given by an effective non-Hermitian Hamiltonian

$$H_{eff} = H + i\Gamma \sum_n \left(Z_n^{(1)} + Z_n^{(2)} + 2 \right) / 2 \tag{2.17}$$

if no jump occurs. If a jump occurs, the system is back in the ground state $|\mathbf{0}\rangle$. The state of the system before the first measurement conditioned on no jump is given by

$$e^{-\Gamma t} \sum_{n=1}^N f_{n,1}(t) |\mathbf{s}(n)\rangle, \quad (2.18)$$

and this happens with the probability of $e^{-2\Gamma t}$ (the norm of the above state). If a jump occurs, the system will be in the ground state

$$\sqrt{1 - e^{-2\Gamma t}} |\mathbf{0}, \mathbf{0}\rangle. \quad (2.19)$$

The density matrix at the time t is given by a mixture of (2.18) and (2.19). In case of (2.19), the quantum information is completely lost and Bob will always measure an unsuccessful state transfer. If Bob however measures a success, it is clear that no jump has occurred and he has the perfectly transferred state. Therefore the protocol *remains conclusive*, but the success probability is lowered by $e^{-2\Gamma t}$. This result is still valid for multiple measurements, which leave the state (2.19) unaltered. The probability of a successful transfer at each particular measurement ℓ will decrease by $e^{-2\Gamma t(\ell)}$, where $t(\ell)$ is the time at which the measurement takes place. After a certain number of measurements, the *joint* probability of failure will no longer decrease. Thus the transfer will no longer be *arbitrarily* perfect, but can still reach a very high fidelity. Some numerical examples of the minimal joint probability of failure that can be achieved,

$$\lim_{\ell \rightarrow \infty} P(\ell) \approx \prod_{\ell=1}^{\infty} \left(1 - 1.35 N^{-2/3} e^{-\frac{2\Gamma N}{J} \ell} \right) \quad (2.20)$$

are given in Fig. 2.5. For $J/\Gamma = 50K \text{ ns}$ nearly perfect transfer is still possible for chains up to a length of $N \approx 40$.

Even if the amplitude damping is not symmetric, its effect is weaker than in single spin schemes. This is because it can be split in a symmetric and asymmetric part. The symmetric part can be overcome with the above strategies. For example, if the amplitude damping on the chains is Γ_1 and Γ_2 with $\Gamma_1 > \Gamma_2$, the state (2.18) will be

$$\sum_{n=1}^N f_{n,1}(t) \{ \alpha e^{-\Gamma_2 t} |\mathbf{0}, \mathbf{n}\rangle + \beta e^{-\Gamma_1 t} |\mathbf{n}, \mathbf{0}\rangle \} \quad (2.21)$$

$$\approx e^{-\Gamma_2 t} \sum_{n=1}^N f_{n,1}(t) |\mathbf{s}(n)\rangle \quad (2.22)$$

provided that $t \ll (\Gamma_1 - \Gamma_2)^{-1}$. Using a chain of length $N = 20$ with $J = 20K * k_B$ and $\Gamma_1^{-1} = 4ns$, $\Gamma_2^{-1} = 4.2ns$ we would have to fulfil $t \ll 164ns$. We could perform approximately 10 measurements (cf. Eq. (2.13)) without deviating too much from the state (2.22). In this time, we can use our protocol in the normal way. The resulting success probability given by the finite version of Eq. (2.20) would be 75%. A similar reasoning is valid for phase noise, where the environment can be split into common and separate parts. If the chains are close, the common part will dominate and the separate parts can be neglected for short times.

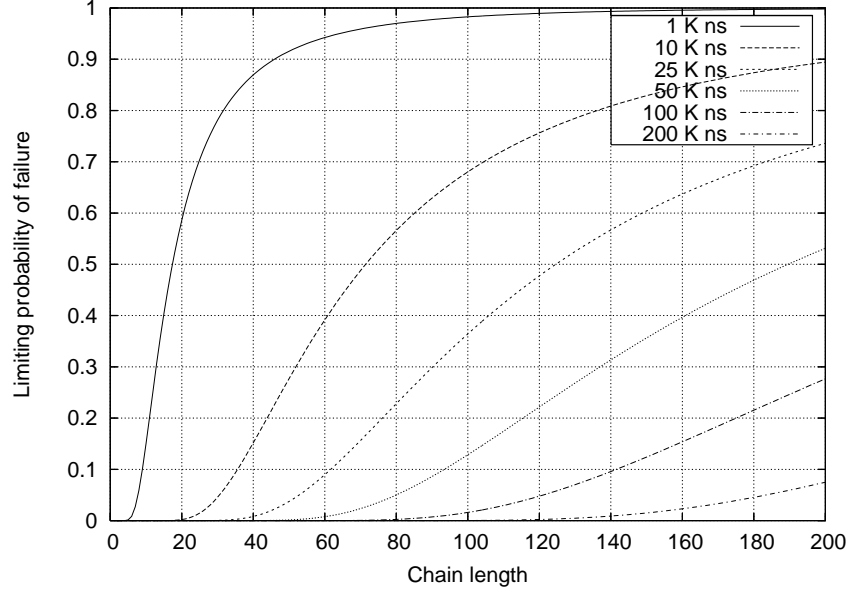


Figure 2.5: The minimal joint probability of failure $P(\ell)$ for chains with length N in the presence of amplitude damping. The parameter J/Γ of the curves is the coupling of the chain (in Kelvin) divided by the decay rate (ns^{-1}).

2.6 Disordered chains

The main requirement for perfect transfer with dual rail encoding in the above is that two *identical* quantum chains have to be designed. While this is not so much a theoretical problem, for possible experimental realizations of the scheme [31] the question arises naturally how to cope with slight asymmetries of the channels. We are now going to demonstrate that in many cases, perfect state transfer with dual rail encoding is possible for quantum chains with differing Hamiltonians.

By doing so, we also offer a solution to another and perhaps more *general* problem:

if one implements *any* of the schemes for quantum state transfer, the Hamiltonians will always be different from the theoretical ones by some random perturbation. This will lead to a decrease of fidelity in particular where specific energy levels were assumed (see [84,99] for an analysis of fluctuations affecting the engineered chains described in Subsection 1.5.1). This problem can be avoided using the scheme described below. In general, disorder can lead to an Anderson localisation [29,30,122] of the eigenstates (and therefore to low fidelity transport of quantum information). In this section however this is not relevant, as we consider only short chains ($N < 100$) and small disorder ($\approx 10\%$ of the coupling strength), and the localisation length is much longer than the length of the chain. We will show numerically that the dual rail scheme can still achieve arbitrarily perfect transfer for a uniformly coupled Heisenberg Hamiltonian with disordered coupling strengths (both for the case of spatially correlated and uncorrelated disorder). Moreover, for any two quantum chains, we show that Bob and Alice can check whether their system is capable of dual rail transfer without directly measuring their Hamiltonians or local properties of the system along the chains but by only measuring *their* part of the system.

2.7 Conclusive transfer in the presence of disorder

We consider two uncoupled quantum chains (1) and (2), as shown in Fig. 2.6. The chains are described by the two Hamiltonians $H^{(1)}$ and $H^{(2)}$ with total Hamiltonian given by

$$H = H^{(1)} \otimes I^{(2)} + I^{(1)} \otimes H^{(2)}, \quad (2.23)$$

and the time evolution operator factorising as

$$U(t) = \exp(-iH^{(1)}t) \otimes \exp(-iH^{(2)}t). \quad (2.24)$$

For the moment, we assume that both chains have equal length N , but it will become clear in Section 2.9 that this is not a requirement of our scheme. All other assumptions remain as in the first part of the chapter.

Initially, Alice encodes the state as

$$\alpha |\mathbf{0}, \mathbf{1}\rangle + \beta |\mathbf{1}, \mathbf{0}\rangle. \quad (2.25)$$

This is a superposition of an excitation in the first qubit of the first chain and an

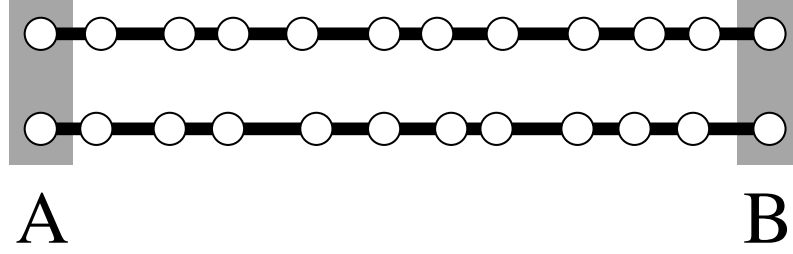


Figure 2.6: Two *disordered* quantum chains interconnecting A and B . Control of the systems is only possible at the two qubits of either end.

excitation in the first qubit of the second chain. The state will evolve into

$$\sum_{n=1}^N \{ \alpha g_{n,1}(t) |\mathbf{0}, \mathbf{n}\rangle + \beta f_{n,1}(t) |\mathbf{n}, \mathbf{0}\rangle \}, \quad (2.26)$$

with

$$f_{n,1}(t) \equiv \langle \mathbf{n}, \mathbf{0} | U(t) | \mathbf{1}, \mathbf{0} \rangle \quad (2.27)$$

$$g_{n,1}(t) \equiv \langle \mathbf{0}, \mathbf{n} | U(t) | \mathbf{0}, \mathbf{1} \rangle. \quad (2.28)$$

In Section 2.2, these functions were identical. For differing chains this is no longer the case. We may, however, find a time t_1 such that the modulus of their amplitudes at the last spins are the same (see Fig. 2.7),

$$g_{N,1}(t_1) = e^{i\phi_1} f_{N,1}(t_1). \quad (2.29)$$

At this time, the state (2.26) can be written as

$$\begin{aligned} & \sum_{n=1}^{N-1} \{ \alpha g_{n,1}(t_1) |\mathbf{0}, \mathbf{n}\rangle + \beta f_{n,1}(t_1) |\mathbf{n}, \mathbf{0}\rangle \} + \\ & f_{N,1}(t_1) \left\{ e^{i\phi_1} \alpha |\mathbf{0}, \mathbf{N}\rangle + \beta |\mathbf{N}, \mathbf{0}\rangle \right\}. \end{aligned} \quad (2.30)$$

Bob decodes the state by applying a CNOT gate on his two qubits, with the first qubit

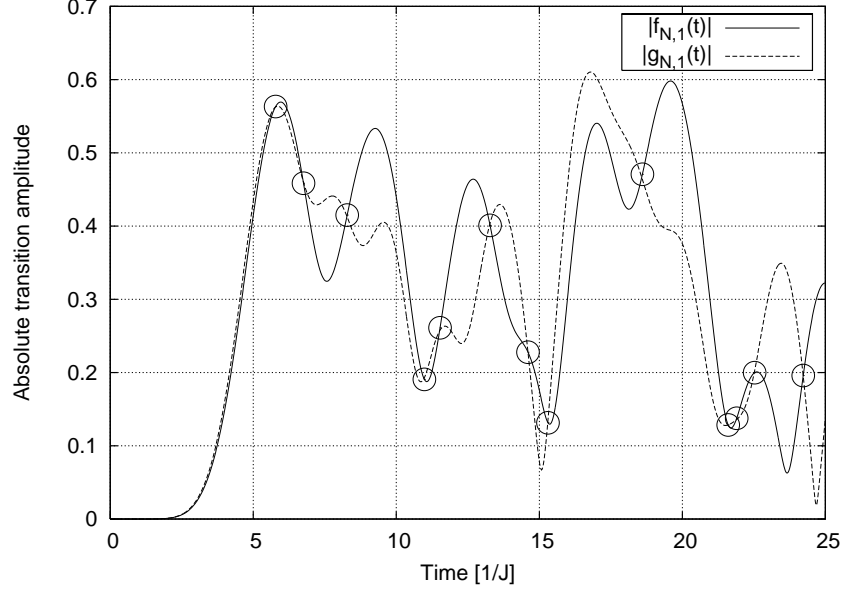


Figure 2.7: The absolute values of the transition amplitudes $f_{N,1}(t)$ and $g_{N,1}(t)$ for two Heisenberg chains of length $N = 10$. The couplings strengths of both chains were chosen randomly from the interval $[0.8J, 1.2J]$. The circles show times where Bob can perform measurements without gaining information on α and β .

as the control bit. The state thereafter is

$$\begin{aligned} & \sum_{n=1}^{N-1} \{ \alpha g_{n,1}(t_1) |\mathbf{0}, \mathbf{n}\rangle + \beta f_{n,1}(t_1) |\mathbf{n}, \mathbf{0}\rangle \} + \\ & f_{N,1}(t_1) \left\{ e^{i\phi_1} \alpha |\mathbf{0}\rangle^{(1)} + \beta |\mathbf{N}\rangle^{(1)} \right\} \otimes |\mathbf{N}\rangle^{(2)}. \end{aligned} \quad (2.31)$$

Bob then measures his second qubit. Depending on the outcome of this measurement, the systems will either be in the state

$$\frac{1}{\sqrt{p_1}} \sum_{n=1}^{N-1} \{ \alpha g_{n,1}(t_1) |\mathbf{0}, \mathbf{n}\rangle + \beta f_{n,1}(t_1) |\mathbf{n}, \mathbf{0}\rangle \} \quad (2.32)$$

or in

$$\left\{ e^{i\phi_1} \alpha |\mathbf{0}\rangle^{(1)} + \beta |\mathbf{N}\rangle^{(1)} \right\} \otimes |\mathbf{N}\rangle^{(2)}, \quad (2.33)$$

where $p_1 = 1 - |f_{N,1}(t_1)|^2 = 1 - |g_{N,1}(t_1)|^2$ is the probability that Bob has *not* received the state. The state (2.33) corresponds to the correctly transferred state with a *known* phase error (which can be corrected by Bob using a simple phase gate). If Bob finds the system in the state (2.32), the transfer has been unsuccessful, but the information is

still in the chain. We thus see that conclusive transfer is still possible with randomly coupled chains as long as the requirement (2.29) is met. This requirement will be further discussed and generalised in the next section.

2.8 Arbitrarily perfect transfer in the presence of disorder

If the transfer was unsuccessful, the state (2.32) will evolve further, offering Bob further opportunities to receive Alice's message. For identical quantum chains, leads to a success for any reasonable Hamiltonian (Section 3.6). For differing chains, this is not necessarily the case, because measurements are only allowed at times where the probability amplitude at the end of the chains is equal, and there may be systems where this is never the case. In this section, we will develop a criterion that generalises Eq. (2.29) and allows to check numerically whether a given system is capable of arbitrarily perfect state transfer.

The quantity of interest for conclusive state transfer is the joint probability $P(\ell)$ that after having checked l times, Bob still has not received the proper state at his end of the chains. Optimally, this should approach zero if ℓ tends to infinity. In order to derive an expression for $P(\ell)$, let us assume that the transfer has been unsuccessful for $\ell - 1$ times with time intervals t_ℓ between the ℓ th and the $(\ell - 1)$ th measurement, and calculate the probability of failure at the ℓ th measurement. In a similar manner, we assume that all the $\ell - 1$ measurements have met the requirement of conclusive transfer (that is, Bob's measurements are unbiased with respect to α and β) and derive the requirement for the ℓ th measurement.

To calculate the probability of failure for the ℓ th measurement, we need to take into account that Bob's measurements disturb the unitary dynamics of the chain. If the state before a measurement with the outcome "failure" is $|\psi\rangle$, the state after the measurement will be

$$\frac{1}{\sqrt{p_\ell}} Q |\psi\rangle, \quad (2.34)$$

where Q is the projector

$$Q = I - |\mathbf{0}, \mathbf{N}\rangle \langle \mathbf{0}, \mathbf{N}| - |\mathbf{N}, \mathbf{0}\rangle \langle \mathbf{N}, \mathbf{0}|, \quad (2.35)$$

and p_ℓ is the probability of failure at the l th measurement. The dynamics of the chain is alternating between unitary and projective, such that the state before the ℓ th

measurement is given by

$$\frac{1}{\sqrt{P(\ell-1)}} \prod_{k=1}^{\ell} \{U(t_k)Q\} \{\alpha |\mathbf{1}, \mathbf{0}\rangle + \beta |\mathbf{0}, \mathbf{1}\rangle\}, \quad (2.36)$$

where

$$P(\ell-1) = \prod_{k=1}^{\ell-1} p_k. \quad (2.37)$$

Note that the operators in (2.36) do not commute and that the time ordering of the product (the index k increases from right to left) is important. The probability that there is an excitation at the N th site of either chain is given by

$$\frac{1}{P(\ell-1)} \left\{ |\alpha|^2 |F(\ell)|^2 + |\beta|^2 |G(\ell)|^2 \right\}, \quad (2.38)$$

with

$$F(\ell) \equiv \langle \mathbf{N}, \mathbf{0} | \prod_{k=1}^{\ell} \{U(t_k)Q\} | \mathbf{1}, \mathbf{0} \rangle, \quad (2.39)$$

and

$$G(\ell) \equiv \langle \mathbf{0}, \mathbf{N} | \prod_{k=1}^{\ell} \{U(t_k)Q\} | \mathbf{0}, \mathbf{1} \rangle. \quad (2.40)$$

Bob's measurements are therefore unbiased with respect to α and β if and only if

$$|F(\ell)| = |G(\ell)| \quad \forall \ell. \quad (2.41)$$

In this case, the state can still be transferred conclusively (up to a known phase). The probability of failure at the ℓ th measurement is given by

$$p_{\ell} = 1 - \frac{|F(\ell)|^2}{P(\ell-1)}. \quad (2.42)$$

It is easy (but not very enlightening) to show [103] that the condition (2.41) is equivalent to

$$\left\| \prod_{k=1}^{\ell} \{U(t_k)Q\} | \mathbf{1}, \mathbf{0} \rangle \right\| = \left\| \prod_{k=1}^{\ell} \{U(t_k)Q\} | \mathbf{0}, \mathbf{1} \rangle \right\| \quad \forall \ell, \quad (2.43)$$

and that the joint probability of failure - if at each measurement the above condition

is fulfilled - is simply given by

$$P(\ell) = \left\| \prod_{k=1}^{\ell+1} \{U(t_k)Q\} |\mathbf{1}, \mathbf{0}\rangle \right\|^2. \quad (2.44)$$

It may look as if Eq. (2.43) was a complicated multi-time condition for the measuring times t_ℓ , that becomes increasingly difficult to fulfil with a growing number of measurements. This is not the case. If proper measuring times have been found for the first $\ell - 1$ measurements, a trivial time t_ℓ that fulfils Eq. (2.43) is $t_\ell = 0$. In this case, Bob measures immediately after the $(\ell - 1)$ th measurement and the probability amplitudes on his ends of the chains will be equal - and zero (a useless measurement). But since the left and right hand side of Eq. (2.43) when seen as functions of t_ℓ are both almost-periodic functions with initial value zero, it is likely that they intersect many times, unless the system has some specific symmetry or the systems are completely different. Note that we do not claim at this point that any pair of chains will be capable of arbitrary perfect transfer. We will discuss in the next system how one can check this for a given system by performing some simple experimental tests.

2.9 Tomography

Suppose someone gives you two different experimentally designed spin chains. It may seem from the above that knowledge of the full Hamiltonian of both chains is necessary to check how well the system can be used for state transfer. This would be a very difficult task, because we would need access to all the spins along the channel to measure all the parameters of the Hamiltonian. In fact by expanding the projectors in Eq. (2.43) one can easily see that the only matrix elements of the evolution operator which are relevant for conclusive transfer are

$$f_{N,1}(t) = \langle \mathbf{N}, \mathbf{0} | U(t) | \mathbf{1}, \mathbf{0} \rangle \quad (2.45)$$

$$f_{N,N}(t) = \langle \mathbf{N}, \mathbf{0} | U(t) | \mathbf{N}, \mathbf{0} \rangle \quad (2.46)$$

$$g_{N,1}(t) = \langle \mathbf{0}, \mathbf{N} | U(t) | \mathbf{0}, \mathbf{1} \rangle \quad (2.47)$$

$$g_{N,N}(t) = \langle \mathbf{0}, \mathbf{N} | U(t) | \mathbf{0}, \mathbf{N} \rangle. \quad (2.48)$$

Physically, this means that the only relevant properties of the system are the transition amplitudes to *arrive* at Bob's ends and to *stay* there. The modulus of $f_{N,1}(t)$ and $f_{N,N}(t)$ can be measured by initialising the system in the states $|\mathbf{1}, \mathbf{0}\rangle$ and $|\mathbf{N}, \mathbf{0}\rangle$ and then performing a reduced density matrix tomography at Bob's site at different times

t , and the complex phase of these functions is obtained by initialising the system in $(|0, 0\rangle + |1, 0\rangle)/\sqrt{2}$ and $(|0, 0\rangle + |N, 0\rangle)/\sqrt{2}$ instead. In the same way, $g_{N,1}(t)$ and $g_{N,N}(t)$ are obtained. All this can be done in the spirit of *minimal control* at the sending and receiving ends of the chain only, and needs to be done only once. It is interesting to note that the dynamics in the middle part of the chain is not relevant at all. It is a *black box* (see Fig. 2.8) that may involve even completely different interactions, number of spins, etc., as long as the total number of excitations is conserved. Once the transition amplitudes [Equations (2.45)-(2.48)] are known, one

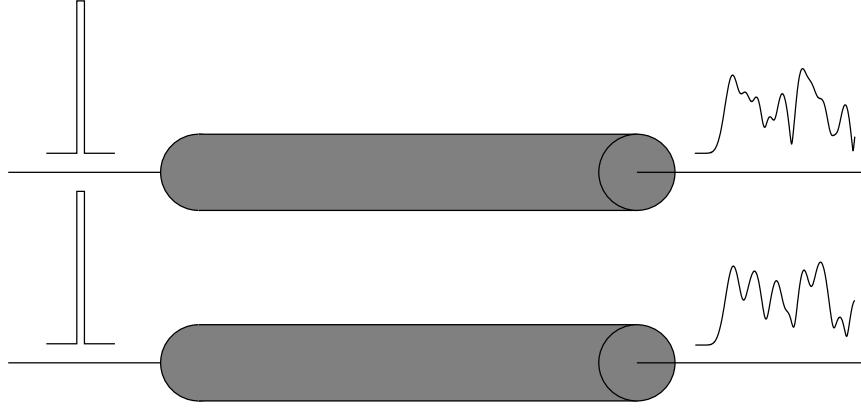


Figure 2.8: The relevant properties for conclusive transfer can be determined by measuring the response of the two systems at their ends only.

can search numerically for optimised measurement times t_ℓ using Eq. (2.44) and the condition from Eq. (2.43).

One weakness of the scheme described here is that the times at which Bob measures have to be very precise, because otherwise the measurements will not be unbiased with respect to α and β . This demand can be relaxed by measuring at times where not only the probability amplitudes are similar, but also their *slope* (see Fig. 2.7). The computation of these optimal timings for a given system may be complicated, but they only need to be done once.

2.10 Numerical Examples

In this section, we show some numerical examples for two chains with Heisenberg couplings J which are fluctuating. The Hamiltonians of the chains $i = 1, 2$ are given

by

$$H^{(i)} = \sum_{n=1}^{N-1} J(1 + \delta_n^{(i)}) \left(X_n^{(i)} X_{n+1}^{(i)} + Y_n^{(i)} Y_{n+1}^{(i)} + Z_n^{(i)} Z_{n+1}^{(i)} \right), \quad (2.49)$$

where $\delta_n^{(i)}$ are uniformly distributed random numbers from the interval $[-\Delta, \Delta]$. We have considered two different cases: in the first case, the $\delta_n^{(i)}$ are completely uncorrelated (i.e. independent for both chains and all sites along the chain). In the second case, we have taken into account a spacial correlation of the signs of the $\delta_n^{(i)}$ along each of the chains, while still keeping the two chains uncorrelated. For both cases, we find that arbitrarily perfect transfer remains possible except for some very rare realisations of the $\delta_n^{(i)}$.

Because measurements must only be taken at times which fulfil the condition (2.43), and these times usually do not coincide with the optimal probability of finding an excitation at the ends of the chains, it is clear that the probability of failure at each measurement will in average be higher than for chains without fluctuations. Therefore, more measurements have to be performed in order to achieve the same probability of success. The price for noisy couplings is thus a longer transmission time and a higher number of gating operations at the receiving end of the chains. Some averaged values are given in Table 2.1 for the Heisenberg chain with uncorrelated coupling fluctuations.

	$\Delta = 0$	$\Delta = 0.01$	$\Delta = 0.03$	$\Delta = 0.05$	$\Delta = 0.1$
$t \left[\frac{1}{J} \right]$	377	524 ± 27	694 ± 32	775 ± 40	1106 ± 248
M	28	43 ± 3	58 ± 3	65 ± 4	110 ± 25

Table 2.1: The total time t and the number of measurements M needed to achieve a probability of success of 99% for different fluctuation strengths Δ (uncorrelated case). Given is the statistical mean and the standard deviation. The length of the chain is $N = 20$ and the number of random samples is 10. For strong fluctuations $\Delta = 0.1$, we also found particular samples where the success probability could not be achieved within the time range searched by the algorithm.

For the case where the signs of the $\delta_n^{(i)}$ are correlated, we have used the same model as in [99], introducing the parameter c such that

$$\delta_n^{(i)} \delta_{n-1}^{(i)} > 0 \quad \text{with propability } c, \quad (2.50)$$

and

$$\delta_n^{(i)} \delta_{n-1}^{(i)} < 0 \quad \text{with propability } 1 - c. \quad (2.51)$$

For $c = 1$ ($c = 0$) this corresponds to the case where the signs of the couplings are completely correlated (anti-correlated). For $c = 0.5$ one recovers the case of uncorrelated couplings. We can see from the numerical results in Table 2.2 that arbitrarily perfect transfer is possible for the whole range of c .

	$c = 0$	$c = 0.1$	$c = 0.3$	$c = 0.7$	$c = 0.9$	$c = 1$
$t \left[\frac{1}{J} \right]$	666 ± 20	725 ± 32	755 ± 41	797 ± 35	882 ± 83	714 ± 41
M	256 ± 2	62 ± 3	65 ± 4	67 ± 4	77 ± 7	60 ± 4

Table 2.2: The total time t and the number of measurements M needed to achieve a probability of success of 99% for different correlations c between the couplings [see Eq. (2.50) and Eq. (2.51)]. Given is the statistical mean and the standard deviation for a fluctuation strength of $\Delta = 0.05$. The length of the chain is $N = 20$ and the number of random samples is 20.

For $\Delta = 0$, we know from Section 2.4 that the time to transfer a state with probability of failure P scales as

$$t(P) = 0.33J^{-1}N^{1.6}|\ln P|. \quad (2.52)$$

If we want to obtain a similar formula in the presence of noise, we can perform a fit to the exact numerical data. For uncorrelated fluctuations of $\Delta = 0.05$, this is shown in Fig. 2.9. The best fit is given by

$$t(P) = 0.2J^{-1}N^{1.9}|\ln P|. \quad (2.53)$$

We conclude that weak fluctuations (say up to 5%) in the coupling strengths do not deteriorate the performance of our scheme much for the chain lengths considered. Both the transmission time and the number of measurements raise, but still in a reasonable way [cf. Table 2.1 and Fig. 2.9]. For larger fluctuations, the scheme is still applicable in principle, but the amount of junk (i.e. chains not capable of arbitrary perfect transfer) may get too large.

Note that we have considered the case where the fluctuations δ_n^i are constant in time. This is a reasonable assumption if the dynamic fluctuations (e.g. those arising from thermal noise) can be neglected with respect to the constant fluctuations (e.g. those arising from manufacturing errors). If the fluctuations were varying with time, the tomography measurements in Sec. 2.9 would involve a time-average, and Bob would not measure exactly at the correct times. The transferred state (2.33) would then be affected by both phase and amplitude noise.

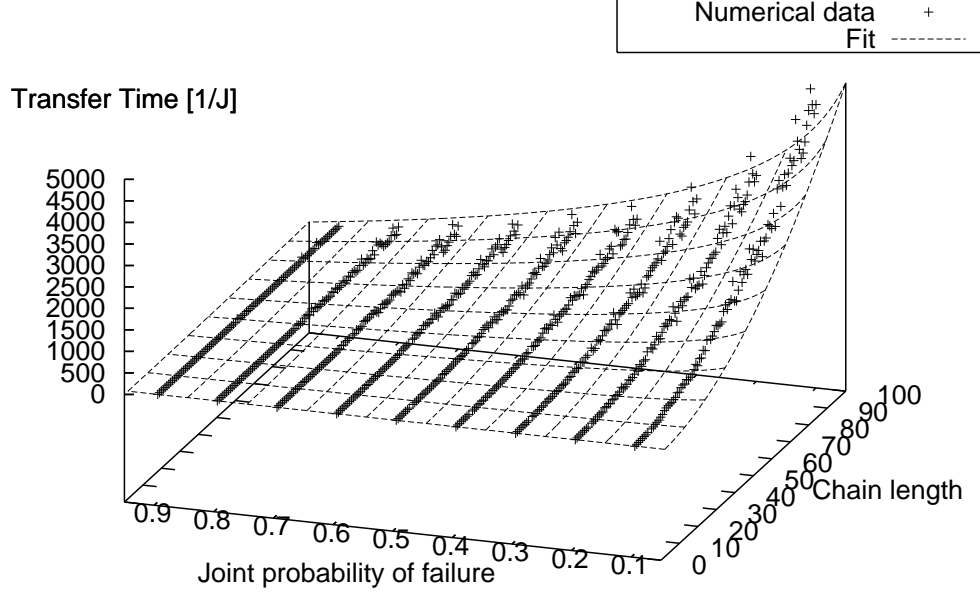


Figure 2.9: Time t needed to transfer a state with a given joint probability of failure P across a chain of length N with uncorrelated fluctuations of $\Delta = 0.05$. The points denote numerical data averaged over 100 realisations, and the fit is given by Eq. (2.53). This figure should be compared with Fig. 2.4 where $\Delta = 0$.

2.11 Coupled chains

Let us look at the condition for conclusive transfer in the more general scenario indicated by Fig. 2.10: Alice and Bob have a black box acting as an amplitude damping channel in the following way. It has two inputs and two outputs. If Alice puts in state in the dual rail,

$$|\psi\rangle = \alpha|01\rangle + \beta|10\rangle, \quad (2.54)$$

where α and β are *arbitrary and unknown* normalised amplitudes, then the output at Bob is given by

$$p|\phi\rangle\langle\phi| + (1-p)|00\rangle\langle 00|, \quad (2.55)$$

with a normalised "success" state

$$|\phi\rangle = \frac{1}{\sqrt{p}} \left[\alpha f|01\rangle + \beta g|10\rangle + \alpha \tilde{f}|10\rangle + \beta \tilde{g}|01\rangle \right]. \quad (2.56)$$

This black box describes the behaviour of an arbitrarily coupled qubit system that conserves the number of excitations and that is initialised in the all zero state, including parallel uncoupled chains, and coupled chains.

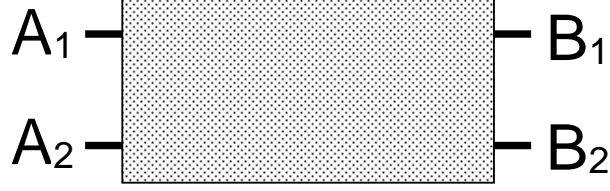


Figure 2.10: Most general setting for conclusive transfer: A *black box* with two inputs and two outputs, acting as an amplitude damping channel defined by Eqs. (2.54) and (2.55)

From the normalisation of $|\phi\rangle$ it follows that

$$p = p(\alpha, \beta) = |\alpha f + \beta \tilde{g}|^2 + |\beta g + \alpha \tilde{f}|^2. \quad (2.57)$$

We are interested in conclusive transfer: by measuring the observable $|00\rangle\langle 00|$ the Bob can project the output onto either the failure state $|00\rangle$ or $|\phi\rangle$. This is clearly possible, but the question is if the output $|\phi\rangle$ and the input $|\psi\rangle$ are related by a *unitary* operation.

If Bob is able to recover the full information that Alice sent, then $p(\alpha, \beta)$ must be *independent of α and β* (otherwise, some information on these amplitudes could be obtained by the measurement already, which contradicts the non-cloning theorem [2]). This implies that $p(1, 0) = p(0, 1)$, i.e.

$$|f|^2 + |\tilde{f}|^2 = |\tilde{g}|^2 + |g|^2. \quad (2.58)$$

Because

$$p\left(\frac{1}{\sqrt{2}}, \frac{1}{\sqrt{2}}\right) = \frac{1}{2}|f + \tilde{g}|^2 + \frac{1}{2}|g + \tilde{f}|^2 \quad (2.59)$$

$$= p(1, 0) + \text{Re}\{f^* \tilde{g} + g \tilde{f}^*\} \quad (2.60)$$

it also implies that

$$\text{Re}\{f^* \tilde{g} + g \tilde{f}^*\} = 0. \quad (2.61)$$

Using the same trick for $p\left(\frac{1}{\sqrt{2}}, \frac{i}{\sqrt{2}}\right)$ we get that $\text{Im}\{f^*\tilde{g} + g\tilde{f}^*\} = 0$ and therefore

$$f^*\tilde{g} + g\tilde{f}^* = 0. \quad (2.62)$$

If we write $|\psi\rangle = U|\phi\rangle$ we get

$$U = \frac{1}{\sqrt{p}} \begin{pmatrix} f & \tilde{f} \\ \tilde{g} & g \end{pmatrix}, \quad (2.63)$$

which is a unitary operator if Eq. (2.58) and (2.62) hold. We thus come to the conclusion that conclusive transfer with the black box defined above is possible if and only if the probability p is independent of α and β . It is interesting to note that a vertical mirror symmetry of the system does not guarantee this. A counterexample is sketched in Fig. 2.11: clearly the initial (“dark”) state $|01\rangle - |10\rangle$ does not evolve, whereas $|01\rangle + |10\rangle$ *does*. Hence the probability must depend on α and β . A trivial case where conclusive transfer works is given by two uncoupled chains, at times where $|f|^2 = |g|^2$. This was discussed in Sect. 2.8. A non-trivial example is given by the coupled system sketched in Fig. 2.12. This can be seen by splitting the Hamiltonian in a horizontal and vertical component,

$$H = H_v + H_z. \quad (2.64)$$

By applying $H_v H_z$ and $H_z H_v$ on single-excitation states it is easily checked that they commute in the first excitation sector (this is not longer true in higher sectors). Since the probability is independent of α and β in the uncoupled case it must also be true in the coupled case (a rotation in the subspace $\{|01\rangle, |10\rangle\}$ does not harm).

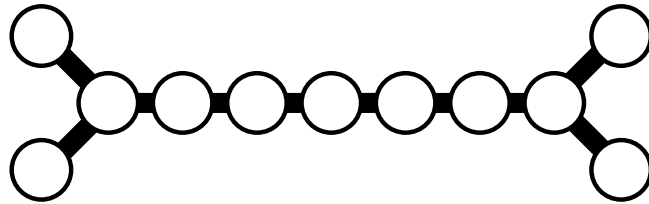


Figure 2.11: A simple counterexample for a vertically symmetric system where dual rail encoding is not possible. The black lines represent exchange couplings.

A final remark - as Alice and Bob always only deal with the states $\{|00\rangle, |10\rangle, |01\rangle\}$ it is obvious that the encoding used in this chapter is really living on *qutrits*. In some sense it would be more natural to consider permanently coupled systems of qutrits,

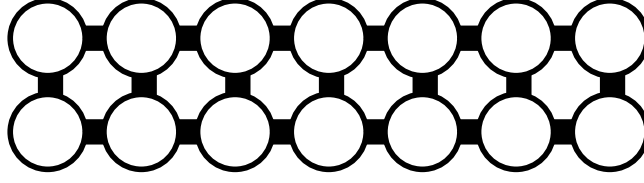


Figure 2.12: An example for a vertically symmetric system where dual rail encoding is possible. The black lines represent exchange couplings of *equal strength*.

such as $SU(3)$ chains [102, 123–125]. The first level of the qutrit $|0\rangle$ is then used as a marker for “no information here”, whereas the information is encoded in the states $|1\rangle$ and $|2\rangle$. One would have to ensure that there is no transition between $|0\rangle$ and $|1\rangle, |2\rangle$, and that the system is initialised in the all zero state.

2.12 Conclusion

In conclusion, we have presented a simple scheme for conclusive and arbitrarily perfect quantum state transfer. To achieve this, two parallel spin chains (individually amplitude damping channels) have been used as one *amplitude delaying channel*. We have shown that our scheme is more robust to decoherence and imperfect timing than the single chain schemes. We have also shown that the scheme is applicable to disordered and coupled chains. The scheme can be used as a way of improving any of the other schemes from the introduction. For instance, one may try to engineer the couplings to have a very high probability of success already at the first measurement, and use further measurements to compensate the errors of implementing the correct values for the couplings. We remark that the dual rail protocol is unrelated to error filtration [126] where parallel channels are used for filtering out environmental effects on flying qubits, whereas the purpose of the dual rail protocol is to ensure the *arrival* of the qubit. Indeed one could combine both protocols to send a qubit on say four rails to ensure the arrival *and* filter errors. Finally, we note that in some recent work [80] it was shown that our encoding can be used to perform quantum gates while the state is transferred, and that it can increase the convergence speed if one performs measurements at intermediate positions [110, 127].

3 Multi Rail encoding

3.1 Introduction

In quantum information theory the rate R of transferred qubits per channel is an important efficiency parameter [70]. Therefore one question that naturally arises is whether or not there is any special meaning in the $1/2$ value of R achieved in the dual rail protocol of the last chapter. We will show now that this is not the case, because there is a way of bringing R arbitrarily close to 1 by considering multi rail encodings. Furthermore, in Section 2.3 it was still left open for which Hamiltonians the probability of success can be made arbitrarily close to 1. Here, we give a sufficient and easily attainable condition for achieving this goal.

This chapter is organised as follows: the model and the notation are introduced in Sec. 3.2. The efficiency and the fidelity of the protocol are discussed in Sec. 3.3 and in Sec. 3.4, respectively. Finally in Sec. 3.5 we prove a theorem which provides us with a sufficient condition for achieving efficient and perfect state transfer in quantum chains.

3.2 The model

Assume that the two communicating parties operate on M independent (i.e. non interacting) copies of the chain. This is quite a common attitude in quantum information theory [70] where successive uses of a memoryless channel are formally described by introducing many parallel copies of the channel (see [54] for a discussion on the possibility of applying this formal description to quantum chain models). Moreover for the case at hand the assumption of Alice and Bob dealing with “real” parallel chains seems reasonable also from a practical point of view [48, 49]. The idea is to use these copies to improve the overall fidelity of the communication. As usual, we assume Alice and Bob to control respectively the first and last qubit of each chain (see Fig. 3.1). By preparing any superposition of her spins Alice can in principle transfer up to M logical qubits. However, in order to improve the communication fidelity the two parties will find it more convenient to redundantly encode only a small number (say $Q(M) \leq M$)

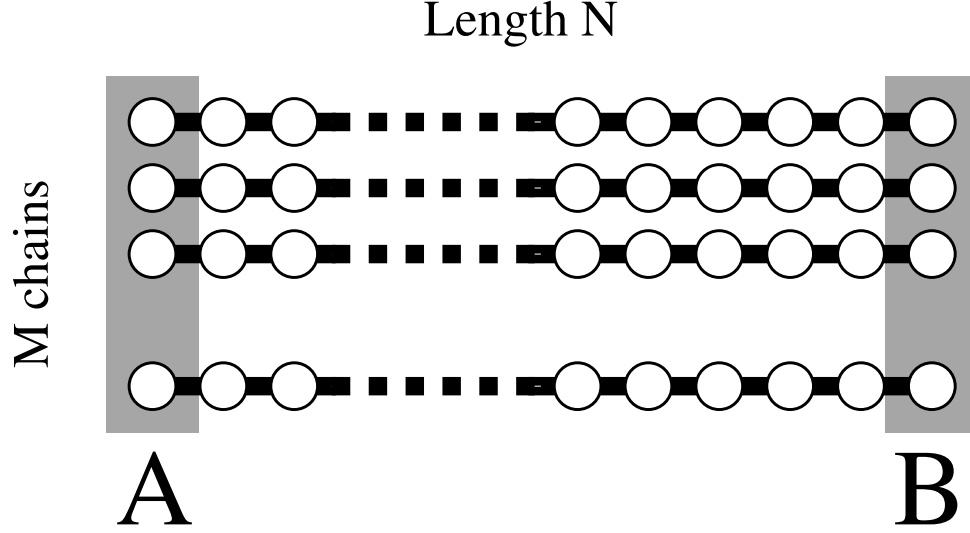


Figure 3.1: Schematic of the system: Alice and Bob operate M chains, each containing N spins. The spins belonging to the same chain interact through the Hamiltonian H which accounts for the transmission of the signal in the system. Spins of different chains do not interact. Alice encodes the information in the first spins of the chains by applying unitary transformations to her qubits. Bob recovers the message in the last spins of the chains by performing joint measurements.

of logical qubits in the M spins. By adopting these strategies Alice and Bob are effectively sacrificing the efficiency $R(M) = Q(M)/M$ of their communication line in order to increase its fidelity. This is typical of any communication scheme and it is analogous to what happens in quantum error correction theory, where a single logical qubit is stored in many physical qubits. In the last chapter we have seen that for $M = 2$ it is possible to achieve perfect state transfer of a single logical qubit with an efficiency equal to $1/2$. Here we will generalise such result by proving that there exist an optimal encoding-decoding strategy which asymptotically allows to achieve perfect state transfer *and* optimal efficiency, i.e.

$$\lim_{M \rightarrow \infty} R(M) = 1. \quad (3.1)$$

Our strategy requires Alice to prepare superpositions of the M chains where $\sim M/2$ of them have a single excitation in the first location while the remaining are in $|0\rangle$. Since in the limit $M \gg 1$ the number of qubit transmitted is $\log \binom{M}{M/2} \approx M$, this architecture guarantees optimal efficiency (3.1). On the other hand, our protocol requires Bob to perform collective measurements on his spins to determine if all the $\sim M/2$ excitations Alice is transmitting arrived at his location. We will prove that

by repeating these detections many times, Bob is able to recover the messages with asymptotically perfect fidelity.

Before beginning the analysis let us introduce some notation. The following definitions *look* more complicated than they really *are*; unfortunately we need them to carefully define the states that Alice uses for encoding the information. In order to distinguish the M different chains we introduce the label $m = 1, \dots, M$: in this formalism $|\mathbf{n}\rangle_m$ represents the state of m -th chain with a single excitation in the n -th spin. In the following we will be interested in those configurations of the whole system where K chains have a single excitation while the remaining $M - K$ are in $|\mathbf{0}\rangle$, as in the case

$$|\mathbf{1}\rangle_1 \otimes |\mathbf{1}\rangle_2 \cdots \otimes |\mathbf{1}\rangle_K \otimes |\mathbf{0}\rangle_{K+1} \cdots \otimes |\mathbf{0}\rangle_M \quad (3.2)$$

where for instance the first K chains have an excitation in the first chain location. Another more general example is given in Fig. 3.2. The complete characterisation of these vectors is obtained by specifying *i)* *which* chains possess a single excitation and *ii)* *where* these excitations are located horizontally along the chains. In answering to the point *i)* we introduce the K -element subsets S_ℓ , composed by the labels of those chains that contain an excitation. Each of these subsets S_ℓ corresponds to a subspace of the Hilbert space $\mathcal{H}(S_\ell)$ with a dimension N^K . The total number of such subsets is equal to the binomial coefficient $\binom{M}{K}$, which counts the number of possibilities in which K objects (excitations) can be distributed among M parties (parallel chains). In particular for any $\ell = 1, \dots, \binom{M}{K}$ the ℓ -th subset S_ℓ will be specified by assigning its K elements, i.e. $S_\ell \equiv \{m_1^{(\ell)}, \dots, m_K^{(\ell)}\}$ with $m_j^{(\ell)} \in \{1, \dots, M\}$ and $m_j^{(\ell)} < m_{j+1}^{(\ell)}$ for all $j = 1, \dots, K$. To characterise the location of the excitations, point *ii)*, we will introduce instead the K -dimensional vectors $\vec{n} \equiv (n_1, \dots, n_K)$ where $n_j \in \{1, \dots, N\}$. We can then define

$$|\vec{n}; \ell\rangle \equiv \bigotimes_{j=1}^K |\mathbf{n}_j\rangle_{m_j^{(\ell)}} \bigotimes_{m' \in \overline{S}_\ell} |\mathbf{0}\rangle_{m'}, \quad (3.3)$$

where \overline{S}_ℓ is the complementary of S_ℓ to the whole set of chains.

The state (3.3) represents a configuration where the j -th chain of the subset S_ℓ is in $|\mathbf{n}_j\rangle$ while the chains that do not belong to S_ℓ are in $|\mathbf{0}\rangle$ (see Fig. 3.2 for an explicit example). The kets $|\vec{n}; \ell\rangle$ are a natural generalisation of the states $|\mathbf{n}\rangle_1 \otimes |\mathbf{0}\rangle_2$ and $|\mathbf{0}\rangle_1 \otimes |\mathbf{n}\rangle_2$ which were used for the dual rail encoding. They are useful for our purposes because they are mutually orthogonal, i.e.

$$\langle\langle \vec{n}; \ell | \vec{n}'; \ell' \rangle\rangle = \delta_{\ell\ell'} \delta_{\vec{n}\vec{n}'}, \quad (3.4)$$

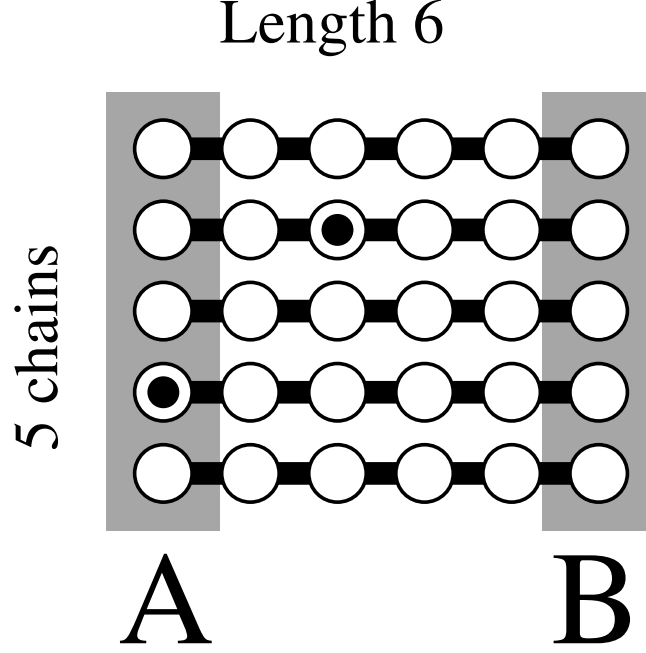


Figure 3.2: Example of our notation for $M = 5$ chains of length $N = 6$ with $K = 2$ excitations. The state above, given by $|\mathbf{0}\rangle_1 \otimes |\mathbf{3}\rangle_2 \otimes |\mathbf{0}\rangle_3 \otimes |\mathbf{1}\rangle_4 \otimes |\mathbf{0}\rangle_5$, has excitations in the chains $m_1 = 2$ and $m_2 = 4$ at the horizontal position $n_1 = 3$ and $n_2 = 1$. It is in the Hilbert space $\mathcal{H}(S_6)$ corresponding to the subset $S_6 = \{2, 4\}$ (assuming that the sets S_ℓ are ordered in a canonical way, i.e. $S_1 = \{1, 2\}$, $S_2 = \{1, 3\}$ and so on) and will be written as $|(3, 1); 6\rangle$. There are $\binom{5}{2} = 10$ different sets S_ℓ and the number of qubits one can transfer using these states is $\log_2 10 \approx 3$. The efficiency is thus given by $R \approx 3/5$ which is already bigger than in the dual rail scheme.

and their time evolution under the Hamiltonian does not depend on ℓ . Among the vectors (3.3) those where all the K excitations are located at the beginning of the S_ℓ chains play an important role in our analysis. Here $\vec{n} = \vec{1} \equiv (1, \dots, 1)$ and we can write

$$|\vec{1}; \ell\rangle \equiv \bigotimes_{m \in S_\ell} |\mathbf{1}\rangle_m \bigotimes_{m' \in \bar{S}_\ell} |\mathbf{0}\rangle_{m'}. \quad (3.5)$$

According to Eq. (3.4), for $\ell = 1, \dots, \binom{M}{K}$ these states form orthonormal set of $\binom{M}{K}$ elements. Analogously by choosing $\vec{n} = \vec{N} \equiv (N, \dots, N)$ we obtain the orthonormal set of $\binom{M}{K}$ vectors

$$|\vec{N}; \ell\rangle \equiv \bigotimes_{m \in S_\ell} |\mathbf{N}\rangle_m \bigotimes_{m' \in \bar{S}_\ell} |\mathbf{0}\rangle_{m'}, \quad (3.6)$$

where all the K excitations are located at the end of the chains.

3.3 Efficient encoding

If all the M chains of the system are originally in $|\mathbf{0}\rangle$, the vectors (3.5) can be prepared by Alice by locally operating on her spins. Moreover since these vectors span a $\binom{M}{K}$ dimensional subspace, Alice can encode in the chain $Q(M, K) = \log_2 \binom{M}{K}$ qubits of logical information by preparing the superpositions,

$$|\Phi\rangle\rangle = \sum_{\ell} A_{\ell} |\vec{\mathbf{1}}; \ell\rangle\rangle, \quad (3.7)$$

with A_{ℓ} complex coefficients. The efficiency of such encoding is hence $R(M, K) = \frac{\log_2 \binom{M}{K}}{M}$ which maximised with respect to K gives,

$$R(M) = \frac{1}{M} \begin{cases} \log_2 \binom{M}{M/2} & \text{for } M \text{ even} \\ \log_2 \binom{M}{(M-1)/2} & \text{for } M \text{ odd.} \end{cases} \quad (3.8)$$

The Stirling approximation can then be used to prove that this encoding is asymptotically efficient (3.1) in the limit of large M , e.g.

$$\log_2 \binom{M}{M/2} \approx \log_2 \frac{M^M}{(M/2)^M} = M. \quad (3.9)$$

Note that already for $M = 5$ the encoding is more efficient (cf. Fig. 3.2) than in the dual rail encoding. In the remaining of the chapter we show that the encoding (3.7) provides perfect state transfer by allowing Bob to perform joint measurements at his end of the chains.

3.4 Perfect transfer

Since the M chains do not interact with each other and possess the same free Hamiltonian H , the unitary evolution of the whole system is described by $U(t) \equiv \otimes_m u_m(t)$, with $u_m(t)$ being the operator acting on the m -th chain. The time evolved of the input $|\vec{\mathbf{1}}; \ell\rangle\rangle$ of Eq. (3.5) is thus equal to

$$U(t)|\vec{\mathbf{1}}; \ell\rangle\rangle = \sum_{\vec{n}} F[\vec{n}, \vec{\mathbf{1}}; t] |\vec{n}; \ell\rangle\rangle, \quad (3.10)$$

where the sum is performed for all $n_j = 1, \dots, N$ and

$$F[\vec{n}, \vec{n}'; t] \equiv f_{n_1, n'_1}(t) \cdots f_{n_K, n'_K}(t), \quad (3.11)$$

is a quantity which does *not* depend on ℓ . In Eq. (3.10) the term $\vec{n} = \vec{N}$ corresponds to having all the K excitations in the last locations of the chains. We can thus write

$$U(t)|\vec{\mathbf{I}}; \ell\rangle = \gamma_1(t)|\vec{N}; \ell\rangle + \sqrt{1 - |\gamma_1(t)|^2} |\xi(t); \ell\rangle , \quad (3.12)$$

where

$$\gamma_1(t) \equiv \langle\langle \vec{N}; \ell | U(t) | \vec{\mathbf{I}}; \ell \rangle\rangle = F[\vec{N}, \vec{\mathbf{I}}; t] \quad (3.13)$$

is the probability amplitude that all the K excitation of $|\vec{\mathbf{I}}; \ell\rangle$ arrive at the end of the chains, and

$$|\xi(t); \ell\rangle \equiv \sum_{\vec{n} \neq \vec{N}} F_1[\vec{n}, \vec{\mathbf{I}}; t] |\vec{n}; \ell\rangle , \quad (3.14)$$

with

$$F_1[\vec{n}, \vec{\mathbf{I}}; t] \equiv \frac{F[\vec{n}, \vec{\mathbf{I}}; t]}{\sqrt{1 - |\gamma_1(t)|^2}}, \quad (3.15)$$

is a superposition of terms where the number of excitations arrived to the end of the communication line is strictly less than K . It is worth noticing that Eq. (3.4) yields the following relations,

$$\langle\langle \vec{N}; \ell | \xi(t); \ell' \rangle\rangle = 0, \quad \langle\langle \xi(t); \ell | \xi(t); \ell' \rangle\rangle = \delta_{\ell\ell'} , \quad (3.16)$$

which shows that $\{|\xi(t); \ell\rangle\}$ is an orthonormal set of vectors which spans a subspace orthogonal to the states $|\vec{N}; \ell\rangle$. The time evolution of the input state (3.7) follows by linearity from Eq. (3.12), i.e.

$$|\Phi(t)\rangle\rangle = \gamma_1(t) |\Psi\rangle\rangle + \sqrt{1 - |\gamma_1(t)|^2} |\bar{\Psi}(t)\rangle\rangle , \quad (3.17)$$

with

$$\begin{aligned} |\bar{\Psi}(t)\rangle\rangle &\equiv \sum_{\ell} A_{\ell} |\xi(t); \ell\rangle , \\ |\Psi\rangle\rangle &\equiv \sum_{\ell} A_{\ell} |\vec{N}; \ell\rangle . \end{aligned} \quad (3.18)$$

The vectors $|\Psi\rangle\rangle$ and $|\bar{\Psi}(t)\rangle\rangle$ are unitary transformations of the input message (3.7) where the orthonormal set $\{|\vec{\mathbf{I}}; \ell\rangle\}$ has been rotated into $\{|\vec{N}; \ell\rangle\}$ and $\{|\xi(t); \ell\rangle\}$ respectively. Moreover $|\Psi\rangle\rangle$ is the configuration we need to have for perfect state

transfer at the end of the chain. In fact it is obtained from the input message (3.7) by replacing the components $|\mathbf{1}\rangle$ (excitation in the first spin) with $|\mathbf{N}\rangle$ (excitation in the last spin). From Eq. (3.16) we know that $|\Psi\rangle\rangle$ and $|\bar{\Psi}(t)\rangle\rangle$ are orthogonal. This property helps Bob to recover the message $|\Psi\rangle\rangle$ from $|\Phi(t)\rangle\rangle$: he only needs to perform a collective measurement on the M spins he is controlling to establish if there are K or less excitations in those locations. The above is clearly a projective measurement that can be performed without destroying the quantum coherence associated with the coefficients A_ℓ . Formally this can be described by introducing the observable

$$\Theta \equiv 1 - \sum_{\ell} |\vec{N}; \ell\rangle\rangle \langle\langle \vec{N}; \ell|. \quad (3.19)$$

A single measurement of Θ on $|\Phi(t_1)\rangle\rangle$ yields the outcome 0 with probability $p_1 \equiv |\gamma_1(t_1)|^2$, and the outcome +1 with probability $1 - p_1$. In the first case the system will be projected in $|\Psi\rangle\rangle$ and Bob will get the message. In the second case instead the state of the system will become $|\bar{\Psi}(t_1)\rangle\rangle$. Already at this stage the two communicating parties have a success probability equal to p_1 . Moreover, as in the dual rail protocol, the channels have been transformed into a quantum erasure channel [113] where the receiver knows if the transfer was successful. Just like the dual rail encoding, this encoding can be used as a simple entanglement purification method in quantum chain transfer (see end of Section 2.2). The rate of entanglement that can be distilled is given by

$$R(M) \left| F[\vec{N}, \vec{1}; t] \right|^2 = R(M) p(t)^{\lfloor M/2 \rfloor}, \quad (3.20)$$

where we used Eq. (3.11) and $p(t) \equiv |f_{N,1}(t)|^2$. As we can see, increasing M on one hand increases $R(M)$, but on the other hand decreases the factor $p(t)^{\lfloor M/2 \rfloor}$. Its maximum with respect to M gives us a lower bound of the entanglement of distillation for a single spin chain, as shown in Fig. 1.11. We can also see that it becomes worth encoding on more than *three* chains for conclusive transfer only when $p(t) > 0.8$.

Consider now what happens when Bob fails to get the right answer from the measurement. The state on which the chains is projected is explicitly given by

$$|\bar{\Psi}(t_1)\rangle\rangle = \sum_{\vec{n} \neq \vec{N}} F_1[\vec{n}, \vec{1}; t_1] \sum_{\ell} A_{\ell} |\vec{n}; \ell\rangle\rangle. \quad (3.21)$$

Let us now consider the evolution of this state for another time interval t_2 . By repeating the same analysis given above we obtain an expression similar to (3.17), i.e.

$$|\Phi(t_2, t_1)\rangle\rangle = \gamma_2 |\Psi\rangle\rangle + \sqrt{1 - |\gamma_2|^2} |\bar{\Psi}(t_2, t_1)\rangle\rangle, \quad (3.22)$$

where now the probability amplitude of getting all excitation in the N -th locations is described by

$$\gamma_2 \equiv \sum_{\vec{n} \neq \vec{N}} F[\vec{N}, \vec{n}; t_2] F_1[\vec{n}, \vec{1}; t_1]. \quad (3.23)$$

In this case $|\bar{\Psi}(t)\rangle\rangle$ is replaced by

$$|\bar{\Psi}(t_2, t_1)\rangle\rangle = \sum_{\ell} A_{\ell} |\xi(t_2, t_1); \ell\rangle\rangle, \quad (3.24)$$

with

$$|\xi(t_2, t_1); \ell\rangle\rangle = \sum_{\vec{n} \neq \vec{N}} F_2[\vec{n}, \vec{1}; t_2, t_1] |\vec{n}; \ell\rangle\rangle, \quad (3.25)$$

and F_2 defined as in Eq. (3.27) (see below). In other words, the state $|\Phi(t_2, t_1)\rangle\rangle$ can be obtained from Eq. (3.17) by replacing γ_1 and F_1 with γ_2 and F_2 . Bob can hence try to use the same strategy he used at time t_1 : i.e. he will check whether or not his M qubits contain K excitations. With (conditional) probability $p_2 \equiv |\gamma_2|^2$ he will get a positive answer and his quantum register will be projected in the state $|\Psi\rangle\rangle$ of Eq. (3.18). Otherwise he will let the system evolve for another time interval t_3 and repeat the protocol. By reiterating the above analysis it is possible to give a recursive expression for the conditional probability of success $p_q \equiv |\gamma_q|^2$ after $q - 1$ successive unsuccessful steps. The quantity γ_q is the analogue of γ_2 and γ_1 of Eqs. (3.13) and (3.22). It is given by

$$\gamma_q \equiv \sum_{\vec{n} \neq \vec{N}} F[\vec{N}, \vec{n}; t_q] F_{q-1}[\vec{n}, \vec{1}, t_{q-1}, \dots, t_1], \quad (3.26)$$

where

$$\begin{aligned} F_{q-1}[\vec{n}, \vec{1}; t_{q-1}, \dots, t_1] \\ \equiv \sum_{\vec{n}' \neq \vec{N}} \frac{F[\vec{N}, \vec{n}'; t_{q-1}]}{\sqrt{1 - |\gamma_{q-1}|^2}} F_{q-2}[\vec{n}', \vec{1}; t_{q-2}, \dots, t_1] \end{aligned} \quad (3.27)$$

and $F_1[\vec{n}, \vec{1}, t]$ is given by Eq. (3.15). In these equations t_q, \dots, t_1 are the *time-intervals* that occurred between the various protocol steps. Analogously the conditional probability of failure at the step q is equal to $1 - p_q$. The probability of having $j - 1$ failures and a success at the step j -th can thus be expressed as

$$\pi(j) = p_j(1 - p_{j-1})(1 - p_{j-2}) \cdots (1 - p_1), \quad (3.28)$$

while the total probability of success after q steps is obtained by the sum of $\pi(j)$ for all $j = 1, \dots, q$, i.e.

$$P_q = \sum_{j=1}^q \pi(j) . \quad (3.29)$$

Since $p_j \geq 0$, Eq. (3.29) is a monotonic function of q . As a matter of fact in the next section we prove that under a very general hypothesis on the system Hamiltonian, the probability of success P_q converges to 1 in the limit of $q \rightarrow \infty$. This means that by repeating many times the collective measure described by Θ Bob is guaranteed to get, sooner or later, the answer 0 and hence the message Alice sent to him. In other words our protocol allows perfect state transfer in the limit of repetitive collective measures. Notice that the above analysis applies for all classes of subsets S_ℓ . The only difference between different choices of K is in the velocity of the convergence of $P_q \rightarrow 1$. In any case, by choosing $K \sim M/2$ Alice and Bob can achieve perfect fidelity *and* optimal efficiency.

3.5 Convergence theorem

Theorem 3.1 (Arbitrarily perfect transfer) *If there is no eigenvector $|e_m\rangle$ of the quantum chain Hamiltonian H which is orthogonal to $|\mathbf{N}\rangle$, then there is a choice of the times intervals t_q, t_{q-1}, \dots, t_1 such that the fidelity converges to 1 as $q \rightarrow \infty$.*

Before proving this Theorem, let us give an intuitive reasoning for the convergence. The unitary evolution can be thought of of a *rotation* in some abstract space, while the measurement corresponds to a *projection*. The dynamics of the system is then represented by alternating rotations and projections. In general this will decrease the norm of each vector to null, unless the rotation axis is *the same* as the projection axis.

PROOF The state of the system at a time interval of t_q after the $(q-1)$ -th failure can be expressed in compact form as follows

$$|\Phi(t_q, \dots, t_1)\rangle\rangle = \frac{U(t_q)\Theta U(t_{q-1})\Theta \dots U(t_1)\Theta |\Phi\rangle\rangle}{\sqrt{(1-p_{q-1}) \dots (1-p_1)}} \quad (3.30)$$

with $U(t)$ the unitary time evolution generated by the system Hamiltonian, and with

Θ the projection defined in Eq. (3.19). One can verify for instance that for $q = 2$, the above equation coincides with Eq. (3.22). [For $q = 1$ this is just (3.17) evaluated at time t_1]. By definition the conditional probability of success at step q -th is equal to

$$p_q \equiv |\langle\langle\Psi|\Phi(t_q, \dots, t_1)\rangle\rangle|^2. \quad (3.31)$$

Therefore, Eq. (3.28) yields

$$\begin{aligned} \pi(q) &= |\langle\langle\Psi|U(t_q)\Theta U(t_{q-1})\Theta \cdots U(t_1)\Theta|\Phi\rangle\rangle|^2 \\ &= |\langle\langle\vec{\mathbf{N}}; \ell|U(t_q)\Theta U(t_{q-1})\Theta \cdots U(t_1)\Theta|\vec{\mathbf{I}}; \ell\rangle\rangle|^2, \end{aligned} \quad (3.32)$$

where the second identity stems from the fact that, according to Eq. (3.4), $U(t)\Theta$ preserves the orthogonality relation among states $|\vec{\mathbf{n}}; \ell\rangle$ with distinct values of ℓ . In analogy to the cases of Eqs. (3.11) and (3.13), the second identity of (3.32) establishes that $\pi(q)$ can be computed by considering the transfer of the input $|\vec{\mathbf{I}}; \ell\rangle$ for *arbitrary* ℓ . The expression (3.32) can be further simplified by noticing that for a given ℓ the chains of the subset \overline{S}_ℓ contribute with a unitary factor to $\pi(q)$ and can be thus neglected (according to (3.5) they are prepared in $|\mathbf{0}\rangle$ and do not evolve under $U(t)\Theta$). Identify $|\vec{\mathbf{I}}\rangle_\ell$ and $|\vec{\mathbf{N}}\rangle_\ell$ with the components of $|\vec{\mathbf{I}}; \ell\rangle$ and $|\vec{\mathbf{N}}; \ell\rangle$ relative to the chains belonging to the subset S_ℓ . In this notation we can rewrite Eq. (3.32) as

$$\pi(q) = |\ell\langle\langle\vec{\mathbf{N}}|U_\ell(t_q)\Theta_\ell \cdots U_\ell(t_1)\Theta_\ell|\vec{\mathbf{I}}\rangle\rangle_\ell|^2, \quad (3.33)$$

where $\Theta_\ell = 1 - |\vec{\mathbf{N}}\rangle_\ell\langle\langle\vec{\mathbf{N}}|$ and $U_\ell(t)$ is the unitary operator $\otimes_{m \in S_\ell} u_m(t)$ which describes the time evolution of the chains of S_ℓ . To prove that there exist suitable choices of t_ℓ such that the series (3.29) converges to 1 it is sufficient to consider the case $t_\ell = t > 0$ for all $j = 1, \dots, q$: this is equivalent to selecting decoding protocols with constant measuring intervals. By introducing the operator $T_\ell \equiv U_\ell(t)\Theta_\ell$, Eq. (3.33) becomes thus

$$\begin{aligned} \pi(q) &= |\ell\langle\langle\vec{\mathbf{N}}|(T_\ell)^q|\vec{\mathbf{I}}\rangle\rangle_\ell|^2 \\ &= {}_\ell\langle\langle\vec{\mathbf{I}}|(T_\ell^\dagger)^q|\vec{\mathbf{N}}\rangle\rangle_\ell\langle\langle\vec{\mathbf{N}}|(T_\ell)^q|\vec{\mathbf{I}}\rangle\rangle_\ell = w(q) - w(q+1), \end{aligned} \quad (3.34)$$

where

$$w(j) \equiv {}_\ell\langle\langle\vec{\mathbf{I}}|(T_\ell^\dagger)^j(T_\ell)^j|\vec{\mathbf{I}}\rangle\rangle_\ell = \|(T_\ell)^j|\vec{\mathbf{I}}\rangle_\ell\|^2, \quad (3.35)$$

is the norm of the vector $(T_\ell)^j |\vec{\mathbf{I}}\rangle_\ell$. Substituting Eq. (3.34) in Eq. (3.29) yields

$$P_q = \sum_{j=1}^q [w(j) - w(j+1)] = 1 - w(q+1) \quad (3.36)$$

where the property $w(1) = {}_\ell \langle \vec{\mathbf{I}} | \Theta_\ell | \vec{\mathbf{I}} \rangle_\ell = 1$ was employed. Proving the thesis is hence equivalent to prove that for $q \rightarrow \infty$ the succession $w(q)$ nullifies. This last relation can be studied using properties of power bounded matrices [128]. In fact, by introducing the norm of the operator $(T_\ell)^q$ we have,

$$w(q) = \|(T_\ell)^q |\vec{\mathbf{I}}\rangle_\ell\|^2 \leq \|(T_\ell)^q\|^2 \leq c \left(\frac{1 + \rho(T_\ell)}{2} \right)^{2q} \quad (3.37)$$

where c is a positive constant which does not depend on q (if S is the similarity transformation that puts T_ℓ into the Jordan canonical form, i.e. $J = S^{-1} T_\ell S$, then c is given explicitly by $c = \|S\| \|S^{-1}\|$) and where $\rho(T_\ell)$ is the spectral radius of T_ℓ , i.e. the eigenvalue of T_ℓ with maximum absolute value (N.B. even when T_ℓ is not diagonalisable this is a well defined quantity). Equation (3.37) shows that $\rho(T_\ell) < 1$ is a sufficient condition for $w(q) \rightarrow 0$. In our case we note that, given any normalised eigenvector $|\lambda\rangle_\ell$ of T_ℓ with eigenvalue λ we have

$$|\lambda| = \|T_\ell |\lambda\rangle_\ell\| = \|\Theta_\ell |\lambda\rangle_\ell\| \leq 1, \quad (3.38)$$

where the inequality follows from the fact that Θ_ℓ is a projector. Notice that in Eq. (3.38) the identity holds only if $|\lambda\rangle_\ell$ is also an eigenvector of Θ_ℓ with eigenvalue $+1$, i.e. only if $|\lambda\rangle_\ell$ is orthogonal to $|\vec{\mathbf{N}}\rangle_\ell$. By definition $|\lambda\rangle_\ell$ is eigenvector $T_\ell = U_\ell(t) \Theta_\ell$: therefore the only possibility to have the equality in Eq. (3.38) is that *i*) $|\lambda\rangle_\ell$ is an eigenvector of $U_\ell(t)$ (i.e. an eigenvector of the Hamiltonian¹ H_ℓ^{tot} of the chain subset S_ℓ) and *ii*) it is orthogonal to $|\vec{\mathbf{N}}\rangle_\ell$. By negating the above statement we get a sufficient condition for the thesis. Namely, if all the eigenvectors $|\vec{E}\rangle_\ell$ of H_ℓ^{tot} are not orthogonal to $|\vec{\mathbf{N}}\rangle_\ell$ than the absolute values of the eigenvalues λ of T_ℓ are strictly smaller than 1 which implies $\rho(T_\ell) < 1$ and hence the thesis. Since the S_ℓ channels are identical and do not interact, the eigenvectors $|\vec{E}\rangle_\ell \equiv \bigotimes_{m \in S_\ell} |e_m\rangle_m$ are tensor product of eigenvectors $|e_m\rangle$ of the single chain Hamiltonians H . Therefore the

¹Notice that strictly speaking the eigenvectors of the Hamiltonian are not the same as those of the time evolution operators. The latter still can have evolution times at which additional degeneracy can increase the set of eigenstates. A trivial example is given for $t = 0$ where *all* states become eigenstates. But it is always possible to find times t at which the eigenstates of $U(t)$ coincide with those of H .

sufficient condition becomes

$${}_{\ell}\langle\langle\vec{E}|\vec{N}\rangle\rangle_{\ell} = \prod_{m \in S_{\ell}} m \langle \mathbf{N} | e_m \rangle_m \neq 0, \quad (3.39)$$

which can be satisfied only if $\langle \mathbf{N} | e_m \rangle \neq 0$ for all eigenvectors $|e_m\rangle$ of the single chain Hamiltonian H . ■

Remark 3.1 While we have proven here that for equal time intervals the probability of success is converging to unity, in practice one may use *optimal* measuring time intervals t_i for a faster transfer (see also Section 2.4). We also point out that timing errors may delay the transfer, but will not decrease its fidelity.

3.6 Quantum chains with nearest-neighbour interactions

It is worth noticing that Eq. (3.39) is a very weak condition, because eigenstates of Hamiltonians are typically entangled. For instance, it holds for open chains with nearest neighbour-interactions:

Theorem 3.2 (Multi rail protocol) *Let H be the Hamiltonian of an open nearest-neighbour quantum chain that conserves the number of excitations. If there is a time t such that $f_{1,N}(t) \neq 0$ (i.e. the Hamiltonian is capable of transport between Alice and Bob) then the state transfer can be made arbitrarily perfect by using the multi rail protocol.*

PROOF We show by contradiction that the criterion of Theorem 3.1 is fulfilled. Assume there exists a normalised eigenvector $|e\rangle$ of the single chain Hamiltonian H such that

$$\langle \mathbf{N} | e \rangle = 0. \quad (3.40)$$

Because $|e\rangle$ is an eigenstate, we can conclude that also

$$\langle e | H | \mathbf{N} \rangle = 0. \quad (3.41)$$

If we act with the Hamiltonian on the ket in Eq. (3.41) we may get some term proportional to $\langle e | \mathbf{N} \rangle$ (corresponding to an Ising-like interaction) and some part proportional to $\langle e | \mathbf{N} - \mathbf{1} \rangle$ (corresponding to a hopping term; if this term did not exist, then clearly

$f_{1,N}(t) = 0$ for all times). We can thus conclude that

$$\langle e | \mathbf{N} - \mathbf{1} \rangle = 0. \quad (3.42)$$

Note that for a closed chain, e.g. a ring, this need not be the case, because then also a term proportional to $\langle e | \mathbf{N} + \mathbf{1} \rangle = \langle e | \mathbf{1} \rangle$ would occur. If we insert the Hamiltonian into Eq. (3.42) again, we can use the same reasoning to see that

$$\langle e | \mathbf{N} - \mathbf{2} \rangle = \dots = \langle e | \mathbf{1} \rangle = 0 \quad (3.43)$$

and hence $|e\rangle = 0$, which is a contradiction to $|e\rangle$ being normalised. ■

3.7 Comparison with Dual Rail

As we have seen above, the Multi Rail protocol allows us in principle to reach in principle a rate arbitrarily close to one. However for a fair comparison with the Dual Rail protocol, we should also take into account the time-scale of the transfer. For the conclusive transfer of entanglement, we have seen in Section 3.4 that only for chains which have a success probability higher than $p(t) = 0.8$ it is worth encoding on more than three rails. The reason is that if the probability of success for a single excitation is p , then the probability of success for $\lfloor M/2 \rfloor$ excitations on M parallel chains is lowered to $p^{\lfloor M/2 \rfloor}$. The protocol for three rails is always more efficient than on two, as still only one excitation is being used, but three complex amplitudes can be transferred per usage.

For arbitrarily perfect transfer, the situation is slightly more complicated as the optimal choice of M also depends on the joint probability of failure that one plans to achieve. Let us assume that at each step of the protocol, the success probability on a single chain is p . Then the number of steps to achieve a given probability of failure P using M chains is given by

$$\ell(P, M) = \max \left\{ \frac{\ln P}{\ln(1 - p^{\lfloor M/2 \rfloor})}, 1 \right\}. \quad (3.44)$$

If we assume that the total time-scale of the transfer is proportional to the number of steps, then the number of qubits that can be transferred per time interval is given by

$$v(P, M) \propto R(M)/\ell(P, M). \quad (3.45)$$

Optimising this rate with respect to M we find three different regimes of the joint

probability of failure (see Fig. 3.3). If one is happy with a large P , then the Multi Rail protocol becomes superior to the Dual Rail for medium p . For intermediate P , the threshold is comparable to the threshold of $p = 0.8$ for conclusive transfer of entanglement. Finally for very low P the Multi Rail only becomes useful for p very close to one. In all three cases the threshold is higher than the $p(t)$ that can usually achieved with unmodulated Heisenberg chains. We can thus conclude that the Multi Rail protocol only becomes useful for chains which already have a very good performance.

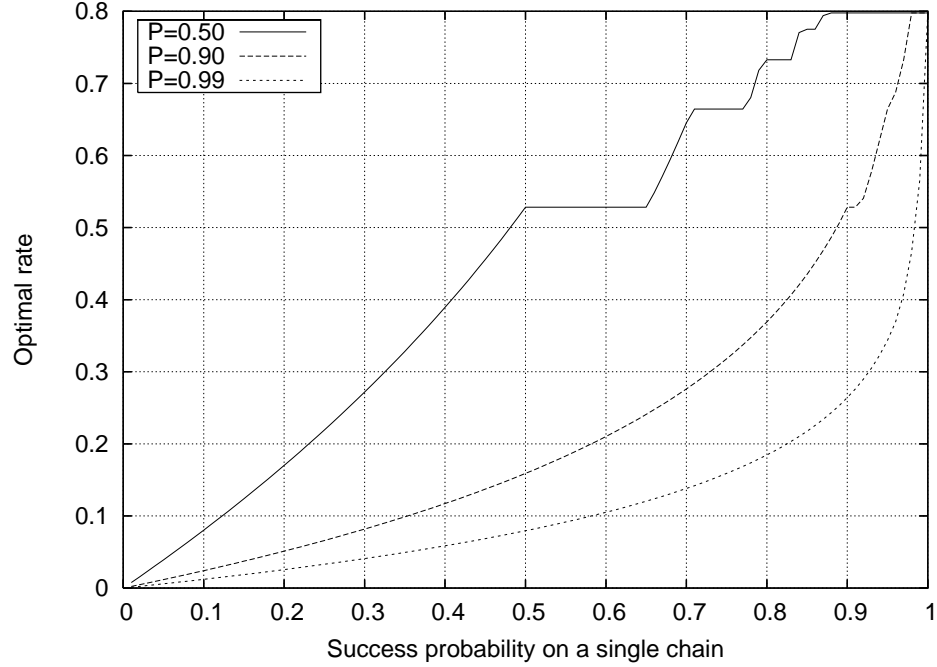


Figure 3.3: Optimal rates (maximisation of Eq. (3.45 with respect to M) for the Multi Rail protocol. Shown are three curves corresponding to different values of the joint probability of failure P one plans to achieve.

3.8 Conclusion

We thus conclude that any nearest-neighbour Hamiltonian that can transfer quantum information with nonzero fidelity (including the Heisenberg chains analysed above) is capable of efficient *and* perfect transfer when used in the context of parallel chains. Hamiltonians with non-nearest neighbour interactions [81,89] can also be used as long as the criterion of Theorem 3.1 is fulfilled.

4 Ergodicity and mixing

4.1 Introduction

We have seen above that by applying measurements at the end of parallel chains, the state of the chain is converging to the ground state, and the quantum information is transferred to the receiver. Indeed, repetitive application of the same transformation is the key ingredient of many controls techniques. Beside quantum state transfer, they have been exploited to inhibit the decoherence of a system by frequently perturbing its dynamical evolution [129–133] (*Bang-Bang control*) or to improve the fidelity of quantum gates [134] by means of frequent measurements (*quantum Zeno-effect* [135]). Recently analogous strategies have also been proposed in the context of state preparation [136–142]. In Refs. [138, 139] for instance, a *homogenisation* protocol was presented which allows one to transform any input state of a qubit into a some pre-fixed target state by repetitively coupling it with an external bath. A similar *thermalisation* protocol was discussed in Ref. [140] to study the efficiency of simulating classical equilibration processes on a quantum computer. In Refs. [141, 142] repetitive interactions with an externally monitored environment were exploited instead to implement *purification* schemes which would allow one to extract pure state components from arbitrary mixed inputs.

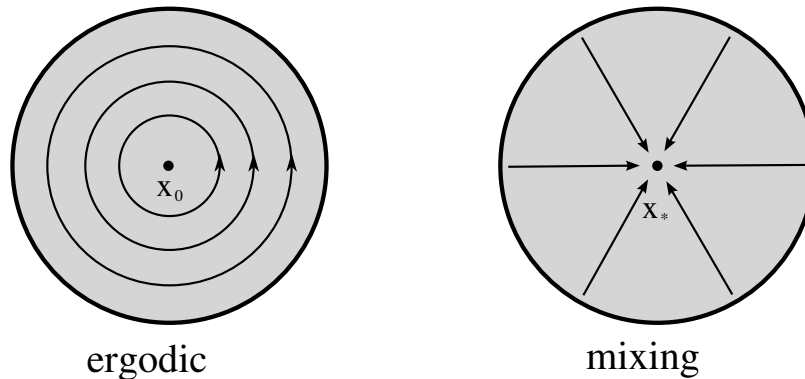


Figure 4.1: Schematic examples of the orbits of an ergodic and a mixing map.

The common trait of the proposals [136–142] and the dual and multi rail protocols is the requirement that repeated applications of a properly chosen quantum operation τ converges to a fixed density matrix x_* independently from the input state x of the system, i.e.

$$\tau^n(x) \equiv \underbrace{\tau \circ \tau \circ \dots \circ \tau}_n(x) \Big|_{n \rightarrow \infty} \longrightarrow x_* , \quad (4.1)$$

with “ \circ ” representing the composition of maps. Following the notation of Refs. [143, 144] we call Eq. (4.1) the *mixing* property of τ . It is related with another important property of maps, namely *ergodicity* (see Fig. 4.1). The latter requires the existence of a unique input state x_0 which is left invariant under a single application of the map¹, i.e.

$$\tau(x) = x \quad \Longleftrightarrow \quad x = x_0 . \quad (4.2)$$

Ergodicity and the mixing property are of high interest not only in the context of the above quantum information schemes. They also occur on a more fundamental level in statistical mechanics [147] and open quantum systems [121, 148], where one would like to study irreversibility and relaxation to thermal equilibrium.

In the case of quantum transformations one can show that mixing maps with convergence point x_* are also ergodic with fixed point $x_0 = x_*$. The opposite implication however is not generally true since there are examples of ergodic quantum maps which are not mixing (see the following). Sufficient conditions for mixing have been discussed both in the specific case of quantum channel [140, 143, 146] and in the more abstract case of maps operating on topological spaces [147]. In particular the Lyapunov direct method [147] allows one to prove that an ergodic map τ is mixing if there exists a continuous functional S which, for all points but the fixed one, is strictly increasing under τ . Here we strengthen this criterion by weakening the requirement on S : our *generalised* Lyapunov functions are requested only to have limiting values $S(\tau^n(x))|_{n \rightarrow \infty}$ which differ from $S(x)$ for all $x \neq x_0$. It turns out that the existence of such S is not just a *sufficient* condition but also a *necessary* condition for mixing. Exploiting this fact one can easily generalise a previous result on *strictly contractive* maps [143]

¹Definition (4.2) may sound unusual for readers who are familiar with a definition of ergodicity from statistical mechanics, where a map is ergodic if its invariant sets have measure 0 or 1. The notion of ergodicity used here is completely different, and was introduced in [143, 145, 146]. The set \mathcal{X} one should have in mind here is not a measurable space, but the compact convex set of quantum states. A perhaps more intuitive definition of ergodicity based on the time average of observables is given by Lemma 4.5).

by showing that maps which are *asymptotic deformations* (see Definition 4.14) are mixing. This has, unlike contractivity, the advantage of being a property independent of the choice of metric (see however [144] for methods of finding “tight” norms). In some cases, the generalised Lyapunov method permits also to derive an optimal mixing condition for quantum channels based on the quantum relative entropy. Finally a slightly modified version of our approach which employs *multi-central* Lyapunov functions yields a characterisation of (not necessarily mixing) maps which in the limit of infinitely many applications move all points toward a proper *subset* (rather than a single point) of the input space.

The introduction of a generalised Lyapunov method seems to be sound not only from a mathematical point of view, but also from a physical point of view. In effect, it often happens that the informations available on the dynamics of a system are only those related on its asymptotic behaviour (e.g. its thermalisation process), its finite time evolution being instead difficult to characterise. Since our method is explicitly constructed to exploit asymptotic features of the mapping, it provides a more effective way to probe the mixing property of the process.

Presenting our results we will not restrict ourself to the case of quantum operations. Instead, following [147] we will derive them in the more general context of continuous maps operating on topological spaces [149]. This approach makes our results stronger by allowing us to invoke only those hypotheses which, to our knowledge, are strictly necessary for the derivation. It is important to stress however that, as a particular instance, all the Theorems and Lemmas presented in this chapter hold for any linear, completely positive, trace preserving map (i.e. quantum channels) operating on a compact subset of normed vectors (i.e. the space of the density matrices of a finite dimensional quantum system). Therefore readers who are not familiar with topological spaces can simply interpret our derivations as if they were just obtained for quantum channels acting on a finite dimensional quantum system.

This chapter is organised as follows. In Sec. 4.3 the generalised Lyapunov method along with some minor results is presented in the context of topological spaces. Then quantum channels are analysed in Sec. 4.4 providing a comprehensive summary of the necessary and sufficient conditions for the mixing property of these maps. Conclusions and remarks form the end of the chapter in Sec. 4.5.

4.2 Topological background

Let us first introduce some basic topological background required for this chapter. A more detailed introduction is given in [149]. Topological spaces are a very elegant way

of defining compactness, convergence and continuity without requiring more than the following structure:

Definition 4.1 A *topological space* is a pair $(\mathcal{X}, \mathcal{O})$ of a set \mathcal{X} and a set \mathcal{O} of subsets of \mathcal{X} (called *open sets*) such that

1. \mathcal{X} and \emptyset are open
2. Arbitrary unions of open sets are open
3. Intersections of two open sets are open

Example 4.1 If \mathcal{X} is an arbitrary set, and $\mathcal{O} = \{\mathcal{X}, \emptyset\}$, then $(\mathcal{X}, \mathcal{O})$ is a topological space. \mathcal{O} is called the *trivial topology*.

Definition 4.2 A topological space \mathcal{X} is *compact* if any open cover (i.e. a set of open sets such that \mathcal{X} is contained in their union) contains a finite sub-cover.

Definition 4.3 A sequence $x_n \in \mathcal{X}$ is *convergent* with limit x_* if each open neighbourhood $O(x_*)$ (i.e. a set such that $x_* \in O(x_*) \in \mathcal{O}$) contains all but finitely many points of the sequence.

Definition 4.4 A map on a topological space is *continuous* if the preimage of any open set is open.

This is already all we require to make useful statements about ergodicity and mixing. However, there are some subtleties which we need to take care of:

Definition 4.5 A topological space is *sequentially compact* if every sequence has a convergent subsequence.

Sequentially compactness is in general not related to compactness! Another subtlety is that with the above definition, a sequence can converge to many different points. For example, in the trivial topology, *any* sequence converges to *any* point. This motivates

Definition 4.6 A topological space is *Hausdorff* if any two distinct points can be separated by open neighbourhoods.

A limit of a sequence in a Hausdorff space is unique. All these problems disappear in metrical spaces:

Definition 4.7 A *metric space* is a pair (\mathcal{X}, d) of a set \mathcal{X} and a function $d : \mathcal{X} \times \mathcal{X} \rightarrow \mathbb{R}$ such that

1. $d(x, y) \geq 0$ and $d(x, y) = 0 \Leftrightarrow x = y$
2. $d(x, y) = d(y, x)$
3. $d(x, z) \leq d(x, y) + d(y, z)$

A metric space becomes a topological space with the canonical topology

Definition 4.8 A subset O of a metric space \mathcal{X} is *open* if $\forall x \in O$ there is an $\epsilon > 0$ such that $\{y \in \mathcal{X} | d(x, y) \leq \epsilon\} \subset O$.

In a metric space with the canonical topology, compactness and sequentially compactness become equivalent. Furthermore, it is automatically Hausdorff (see Fig. 4.2).

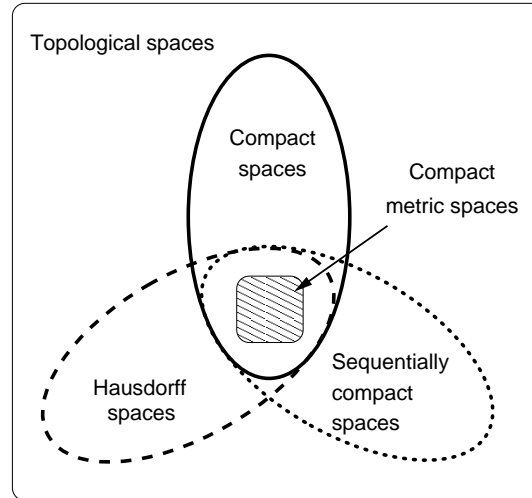


Figure 4.2: Relations between topological spaces [149]. The space of density matrices on which quantum channels are defined, is a compact and convex subset of a normed vectors space (the space of linear operators of the system) which, in the above graphical representation fits within the set of compact metric spaces.

4.3 Generalised Lyapunov Theorem

4.3.1 Topological spaces

In this section we introduce the notation and derive our main result (the Generalised Lyapunov Theorem).

Definition 4.9 Let \mathcal{X} be a topological space and let $\tau : \mathcal{X} \rightarrow \mathcal{X}$ be a map. The sequence $x_n \equiv \tau^n(x)$, where τ^n is a short-hand notation for the n -fold composition of τ , is called the *orbit* of x . An element $x_* \in \mathcal{X}$ is called a *fixed point* of τ if and only if

$$\tau(x_*) = x_* . \quad (4.3)$$

τ is called *ergodic* if and only if it has exactly one fixed point. τ is called *mixing* if and only if there exists a *convergence* point $x_* \in \mathcal{X}$ such that any orbit converges to it, i.e.

$$\lim_{n \rightarrow \infty} x_n = x_* \quad \forall x \in \mathcal{X} . \quad (4.4)$$

A direct connection between ergodicity and mixing can be established as follows.

Lemma 4.1 *Let $\tau : \mathcal{X} \rightarrow \mathcal{X}$ be a continuous mixing map on a topological Hausdorff space \mathcal{X} . Then τ is ergodic.*

PROOF Let x_* be the convergence point of τ and let $x \in \mathcal{X}$ arbitrary. Since τ is continuous we can perform the limit in the argument of τ , i.e.

$$\tau(x_*) = \tau \left(\lim_{n \rightarrow \infty} \tau^n(x) \right) = \lim_{n \rightarrow \infty} \tau^{n+1}(x) = x_* , \quad (4.5)$$

which shows that x_* is a fixed point of τ . To prove that it is unique assume by contradiction that τ possesses a second fixed point $y_* \neq x_*$. Then $\lim_{n \rightarrow \infty} \tau^n(y_*) = y_* \neq x_*$, so τ could not be mixing (since the limit is unique in a Hausdorff space – see Fig. 4.2). Hence τ is ergodic. ■

Remark 4.1 The converse is not true in general, i.e. not every ergodic map is mixing (not even in Hausdorff topological spaces). A simple counterexample is given by $\tau : [-1, 1] \rightarrow [-1, 1]$ with $\tau(x) \equiv -x$ and the usual topology of \mathbb{R} , which is ergodic with fixed point 0, but not mixing since for $x \neq 0$, $\tau^n(x) = (-1)^n x$ is alternating between two points. A similar counterexample will be discussed in the quantum channel section (see Example 4.2).

A well known criterion for mixing is the existence of a *Lyapunov function* [147].

Definition 4.10 Let $\tau : \mathcal{X} \rightarrow \mathcal{X}$ be a map on a topological space \mathcal{X} . A continuous map $S : \mathcal{X} \rightarrow \mathbb{R}$ is called a (strict) *Lyapunov function* for τ around $x_* \in \mathcal{X}$ if and only if

$$S(\tau(x)) > S(x) \quad \forall x \neq x_* . \quad (4.6)$$

Remark 4.2 At this point it is neither assumed that x_* is a fixed point, nor that τ is ergodic. Both follow from the theorem below.

Theorem 4.1 (Lyapunov function) *Let $\tau : \mathcal{X} \rightarrow \mathcal{X}$ be a continuous map on a sequentially compact topological space \mathcal{X} . Let $S : \mathcal{X} \rightarrow \mathbb{R}$ be a Lyapunov function for τ around x_* . Then τ is mixing with the fixed point x_* .*

The proof of this theorem is given in [147]. We will not reproduce it here, because we will provide a general theorem that includes this as a special case. In fact, we will show that the requirement of the strict monotonicity can be *much* weakened, which motivates the following definition.

Definition 4.11 Let $\tau : \mathcal{X} \rightarrow \mathcal{X}$ be a map on a topological space \mathcal{X} . A continuous map $S : \mathcal{X} \rightarrow \mathbb{R}$ is called a *generalised Lyapunov function for τ around $x_* \in \mathcal{X}$* if and only if the sequence $S(\tau^n(x))$ is point-wise convergent² for any $x \in \mathcal{X}$ and S fulfils

$$S_*(x) \equiv \lim_{n \rightarrow \infty} S(\tau^n(x)) \neq S(x) \quad \forall x \neq x_*. \quad (4.7)$$

In general it may be difficult to prove the point-wise convergence. However if S is monotonic under the action of τ and the space is compact, the situation becomes considerably simpler. This is summarised in the following Lemma.

Lemma 4.2 *Let $\tau : \mathcal{X} \rightarrow \mathcal{X}$ be a map on a compact topological space. A continuous map $S : \mathcal{X} \rightarrow \mathbb{R}$ which fulfils*

$$S(\tau(x)) \geq S(x) \quad \forall x \in \mathcal{X}, \quad (4.8)$$

and

$$S_*(x) \equiv \lim_{n \rightarrow \infty} S(\tau^n(x)) > S(x) \quad \forall x \neq x_*. \quad (4.9)$$

for some fixed $x_ \in \mathcal{X}$ is a generalised Lyapunov function for τ around x_* .*

PROOF It only remains to show the (point-wise) convergence of $S(\tau^n(x))$. Since S is a continuous function on a compact space, it is bounded. By Eq. (4.8) the sequence is monotonic. Any bounded monotonic sequence converges. ■

Corollary 4.1 *Let $\tau : \mathcal{X} \rightarrow \mathcal{X}$ be a map on a compact topological space. A continuous map $S : \mathcal{X} \rightarrow \mathbb{R}$ which fulfils*

$$S(\tau(x)) \geq S(x) \quad \forall x \in \mathcal{X}, \quad (4.10)$$

²Point-wise convergence in this context means that for any fixed x the sequence $S_n \equiv S(\tau^n(x))$ is convergent.

and

$$S(\tau^N(x)) > S(x) \quad \forall x \neq x_*, \quad (4.11)$$

for some fixed $N \in \mathbb{N}$ and for some $x_* \in \mathcal{X}$ is a generalised Lyapunov function for τ around x_* .

Remark 4.3 This implies that a strict Lyapunov function is a generalised Lyapunov function (with $N = 1$).

We can now state the main result of this section:

Theorem 4.2 (Generalized Lyapunov function) *Let $\tau : \mathcal{X} \rightarrow \mathcal{X}$ be a continuous map on a sequentially compact topological space \mathcal{X} . Let $S : \mathcal{X} \rightarrow \mathbb{R}$ be a generalised Lyapunov function for τ around x_* . Then τ is mixing with fixed point x_* .*

PROOF Consider the orbit $x_n \equiv \tau^n(x)$ of a given $x \in \mathcal{X}$. Because \mathcal{X} is sequentially compact, the sequence x_n has a convergent subsequence (see Fig. 4.2), i.e. $\lim_{k \rightarrow \infty} x_{n_k} \equiv \tilde{x}$. Let us assume that $\tilde{x} \neq x_*$ and show that this leads to a contradiction. By Eq. (4.7) we know that there exists a finite $N \in \mathbb{N}$ such that

$$S(\tau^N(\tilde{x})) \neq S(\tilde{x}). \quad (4.12)$$

Since τ^N is continuous we can perform the limit in the argument, i.e.

$$\lim_{k \rightarrow \infty} \tau^N(x_{n_k}) = \tau^N(\tilde{x}). \quad (4.13)$$

Likewise, by continuity of S we have

$$\lim_{k \rightarrow \infty} S(x_{n_k}) = S(\tilde{x}), \quad (4.14)$$

and on the other hand

$$\lim_{k \rightarrow \infty} S(x_{N+n_k}) = \lim_{k \rightarrow \infty} S(\tau^N(x_{n_k})) = S(\tau^N \tilde{x}), \quad (4.15)$$

where the second equality stems from the continuity of the map S and τ^N . Because S is a generalised Lyapunov function, the sequence $S(x_n)$ is convergent. Therefore the subsequences (4.14) and (4.15) must have the same limit. We conclude that

$S(\tau^N \tilde{x}) = S(\tilde{x})$ which contradicts Eq. (4.12). Hence $\tilde{x} = x_*$. Since we have shown that any convergent subsequence of $\tau^n(x)$ converges to the same limit x_* , it follows by Lemma 4.3 that $\tau^n(x)$ is converging to x_* . Since that holds for arbitrary x , it follows that τ is mixing. ■

Lemma 4.3 *Let x_n be a sequence in a sequentially compact topological space \mathcal{X} such that any convergent subsequence converges to x_* . Then the sequence converges to x_* .*

PROOF We prove by contradiction: assume that the sequence does not converge to x_* . Then there exists an open neighbourhood $O(x_*)$ of x_* such that for all $k \in \mathbb{N}$, there is a n_k such that $x_{n_k} \notin O(x_*)$. Thus the subsequence x_{n_k} is in the closed space $\mathcal{X} \setminus O(x_*)$, which is again sequentially compact. x_{n_k} has a convergent subsequence with a limit in $\mathcal{X} \setminus O(x_*)$, in particular this limit is not equal to x_* . ■

There is an even more general way of defining Lyapunov functions which we state here for completeness. It requires the concept of the quotient topology [149].

Definition 4.12 Let $\tau : \mathcal{X} \rightarrow \mathcal{X}$ be a map on a topological space \mathcal{X} . A continuous map $S : \mathcal{X} \rightarrow \mathbb{R}$ is called a *multi-central Lyapunov function for τ around $\mathcal{F} \subseteq \mathcal{X}$* if and only if the sequence $S(\tau^n(x))$ is point-wise convergent for any $x \in \mathcal{X}$ and if S and τ fulfil the following three conditions: S is constant on \mathcal{F} , $\tau(\mathcal{F}) \subseteq \mathcal{F}$, and

$$S_*(x) \equiv \lim_{n \rightarrow \infty} S(\tau^n(x)) \neq S(x) \quad \forall x \notin \mathcal{F}. \quad (4.16)$$

For these functions we cannot hope that the orbit is mixing. We can however show that the orbit is “converging” to the set \mathcal{F} in the following sense:

Theorem 4.3 (Multi-central Lyapunov function) *Let $\tau : \mathcal{X} \rightarrow \mathcal{X}$ be a continuous map on a sequentially compact topological space \mathcal{X} . Let $S : \mathcal{X} \rightarrow \mathbb{R}$ be a multi-central Lyapunov function for τ around \mathcal{F} . Let $\varphi : \mathcal{X} \rightarrow \mathcal{X}/\mathcal{F}$ be the continuous mapping into the quotient space (i.e. $\varphi(x) = [x]$ for $x \in \mathcal{X} \setminus \mathcal{F}$ and $\varphi(x) = [\mathcal{F}]$ for $x \in \mathcal{F}$). Then $\tilde{\tau} : \mathcal{X}/\mathcal{F} \rightarrow \mathcal{X}/\mathcal{F}$ given by $\tilde{\tau}([x]) = \varphi(\tau(\varphi^{-1}([x])))$ is mixing with fixed point $[\mathcal{F}]$.*

PROOF First note that $\tilde{\tau}$ is well defined because φ is invertible on $\mathcal{X}/\mathcal{F} \setminus [\mathcal{F}]$ and $\tau(\mathcal{F}) \subseteq \mathcal{F}$, so that $\tilde{\tau}([\mathcal{F}]) = [\mathcal{F}]$. Since \mathcal{X} is sequentially compact, the quotient space \mathcal{X}/\mathcal{F} is also sequentially compact. Note that for O open, $\tilde{\tau}^{-1}(O) = \varphi(\tau^{-1}(\varphi^{-1}(O)))$ is the image of φ of an open set in \mathcal{X} and therefore (by definition of the quotient topology) open in \mathcal{X}/\mathcal{F} . Hence $\tilde{\tau}$ is continuous. The function $\tilde{S}([x]) : \mathcal{X}/\mathcal{F} \rightarrow \mathbb{R}$ given by $\tilde{S}([x]) = S(\varphi^{-1}([x]))$ is continuous and easily seen to be a generalised Lyapunov function around $[\mathcal{F}]$. By Theorem 4.2 it follows that $\tilde{\tau}$ is mixing. ■

4.3.2 Metric spaces

We now show that for the particular class of compact topological sets which posses a metric, the existence of a generalised Lyapunov function is also a necessary condition for mixing.

Theorem 4.4 (Lyapunov criterion) *Let $\tau : \mathcal{X} \rightarrow \mathcal{X}$ be a continuous map on a compact metric space \mathcal{X} . Then τ is mixing with fixed point x_* if and only if a generalised Lyapunov function around x_* exists.*

PROOF Firstly, in metric spaces compactness and sequential compactness are equivalent, so the requirements of Theorem 4.2 are met. Secondly, for any mixing map τ with fixed point x_* , a generalised Lyapunov function around x_* is given by $S(x) \equiv d(x_*, x)$. In fact, it is continuous because of the continuity of the metric and satisfies

$$\lim_{n \rightarrow \infty} S(\tau^n(x)) = d(x_*, x_*) = 0 \leq d(x_*, x) = S(x), \quad (4.17)$$

where the equality holds if and only $x = x_*$. We call $d(x_*, x)$ the *trivial generalised Lyapunov function*. ■

Remark 4.1 In the above Theorem we have not used all the properties of the metric. In fact a continuous *semi-metric* (i.e. without the triangle inequality) would suffice.

The trivial Lyapunov function requires knowledge of the fixed point of the map. There is another way of characterising mixing maps as those which bring elements closer to *each other* (rather than closer to the fixed point).

Definition 4.13 A map $\tau : \mathcal{X} \rightarrow \mathcal{X}$ on a metric space is called a *non-expansive map* if and only if

$$d(\tau(x), \tau(y)) \leq d(x, y) \quad \forall x, y \in \mathcal{X}, \quad (4.18)$$

a *weak contraction* if and only if

$$d(\tau(x), \tau(y)) < d(x, y) \quad \forall x, y \in \mathcal{X}, x \neq y, \quad (4.19)$$

and a *strict contraction* if and only if there exists a $k < 1$ such that

$$d(\tau(x), \tau(y)) \leq k d(x, y) \quad \forall x, y \in \mathcal{X}. \quad (4.20)$$

Remark 4.2 The notation adopted here is slightly different from the definitions used by other Authors [5, 143, 150] who use contraction to indicate our non-expansive maps.

Our choice is motivated by the need to clearly distinguish between non-expansive transformation and weak contractions.

We can generalise the above definition in the following way:

Definition 4.14 A map $\tau : \mathcal{X} \rightarrow \mathcal{X}$ on a metric space is called an *asymptotic deformation* if and only if the sequence $d(\tau^n(x), \tau^n(y))$ converges point-wise for all $x, y \in \mathcal{X}$ and

$$\lim_{n \rightarrow \infty} d(\tau^n(x), \tau^n(y)) \neq d(x, y) \quad \forall x, y \in \mathcal{X}, x \neq y. \quad (4.21)$$

Lemma 4.4 Let $\tau : \mathcal{X} \rightarrow \mathcal{X}$ be a non-expansive map on a metric space \mathcal{X} , and let

$$d(\tau^N(x), \tau^N(y)) < d(x, y) \quad \forall x, y \in \mathcal{X}, x \neq y \quad (4.22)$$

for some fixed $N \in \mathbb{N}$. Then τ is an asymptotic deformation. Then τ is an asymptotic deformation.

PROOF The existence of the limit $\lim_{n \rightarrow \infty} d(\tau^n(x), \tau^n(y))$ follows from the monotonicity and the fact the any metric is lower bounded. ■

Remark 4.4 Any weak contraction is an asymptotic deformation (with $N = 1$).

Theorem 4.5 (Asymptotic deformations) Let $\tau : \mathcal{X} \rightarrow \mathcal{X}$ be a continuous map on a compact metric space \mathcal{X} with at least one fixed point. Then τ is mixing if and only if τ is an asymptotic deformation.

PROOF Firstly assume that τ is an asymptotic deformation. Let x_* be a fixed point and define $S(x) = d(x_*, x)$.

$$\begin{aligned} \lim_{n \rightarrow \infty} S(\tau^n(x)) &= \lim_{n \rightarrow \infty} d(x_*, \tau^n(x)) \\ &= \lim_{n \rightarrow \infty} d(\tau^n(x_*), \tau^n(x)) \neq d(x_*, x) = S(x) \quad \forall x \neq x_*, \end{aligned} \quad (4.23)$$

hence $S(x)$ is a generalised Lyapunov function. By Theorem 4.2 it follows that τ is mixing. Secondly, if τ is mixing, then

$$\lim_{n \rightarrow \infty} d(\tau^n(x), \tau^n(y)) = d(x_*, x_*) = 0 \neq d(x, y) \quad \forall x, y \in \mathcal{X}, x \neq y, \quad (4.24)$$

so τ is an asymptotic deformation. ■

Remark 4.5 Note that the existence of a fixed point is assured if τ is a weak contraction on a compact space [151], or if the metric space is convex compact [152].

As a special case, we get the following result:

Corollary 4.2 *Any weak contraction τ on a compact metric space is mixing.*

PROOF Since the space is compact τ has at least one fixed point. Moreover from Lemma 4.4 we know that τ is an asymptotic deformation. Then Theorem 4.5 applies. ■

Remark 4.6 This result can be seen as an instance of Banach contraction principle on compact spaces. In the second part of the chapter we will present a counterexample which shows that weak contractivity is only a sufficient criterion for mixing (see Example 4.3). In the context of quantum channels an analogous criterion was suggested in [143, 146] which applied to strict contractions. We also note that for weak and strict contractions, the trivial generalised Lyapunov function (Theorem 4.4) is a strict Lyapunov function.

Lemma 4.5 states the ergodic theorem by Birkhoff [153] which, in the context of normed vector spaces, shows the equivalence between the definition of ergodicity of Eq. (4.4) and the standard time average definition.

Lemma 4.5 *Let \mathcal{X} be a convex and compact subset of a normed vector space, and let $\tau : \mathcal{X} \rightarrow \mathcal{X}$ be a continuous map. If τ is ergodic with fixed point x_* , then*

$$\lim_{n \rightarrow \infty} \frac{1}{n+1} \sum_{\ell=0}^n \tau^\ell(x) = x_* . \quad (4.25)$$

PROOF Define the sequence $A_n \equiv \frac{1}{n+1} \sum_{\ell=0}^n \tau^\ell(x)$. Let then M be the upper bound for the norm of vectors in \mathcal{X} , i.e. $M \equiv \sup_{x \in \mathcal{X}} \|x\| < \infty$. which exists because \mathcal{X} is compact. The sequence A_n has a convergent subsequence A_{n_k} with limit \tilde{A} . Since τ is continuous one has $\lim_{k \rightarrow \infty} \tau(A_{n_k}) = \tau(\tilde{A})$. On the other hand, we have

$$\|\tau(A_{n_k}) - A_{n_k}\| = \frac{1}{n_k+1} \|\tau^{n_k+1}(x) - x\| \leq \frac{\|\tau^{n_k+1}(x)\| + \|x\|}{n_k+1} \leq \frac{2M}{n_k+1}, \quad (4.26)$$

so the two sequences must have the same limit, i.e. $\tau(\tilde{A}) = \tilde{A}$. Since τ is ergodic, we have $\tilde{A} = x_*$ and $\lim_{n \rightarrow \infty} A_n = x_*$ by Lemma 4.3. ■

Remark 4.7 Note that if τ has a second fixed point $y_* \neq x_*$, then for all n one has $\frac{1}{n+1} \sum_{\ell=0}^n \tau^\ell(y_*) = y_*$, so Eq. (4.25) would not apply.

4.4 Quantum Channels

In this Section we discuss the mixing properties of quantum channels [2] which account for the most general evolution a quantum system can undergo including measurements and coupling with external environments. In this context solving the mixing problem (4.1) is equivalent to determine if repetitive application of a certain physical transformation will drive any input state of the system (i.e. its density matrices) into a unique output configuration. The relationship between the different mixing criteria one can obtain in this case is summarised in Fig. 4.3.

At a mathematical level quantum channels correspond to linear maps acting on the density operators ρ of the system and satisfying the requirement of being completely positive and trace preserving (CPT). For a formal definition of these properties we refer the reader to [5, 154, 155]: here we note only that a necessary and sufficient condition to being CPT is to allow Kraus decomposition [154] or, equivalently, Stinespring dilation [156]. Our results are applicable if the underlying Hilbert space is finite-dimensional. In such regime there is no ambiguity in defining the convergence of a sequence since all operator norms are equivalent (i.e. given two norms one can construct an upper and a lower bound for the first one by properly scaling the second one). Also the set of bounded operators and the set of operators of Hilbert-Schmidt class coincide. For the sake of definiteness, however, we will adopt the trace-norm which, given the linear operator $\Theta : \mathcal{H} \rightarrow \mathcal{H}$, is defined as $\|\Theta\|_1 = \text{Tr}[\sqrt{\Theta^\dagger \Theta}]$ with $\text{Tr}[\cdots]$ being the trace over \mathcal{H} and Θ^\dagger being the adjoint of Θ . This choice is in part motivated by the fact [150] that any quantum channel is non-expansive with respect to the metric induced³ by $\|\cdot\|_1$ (the same property does not necessarily apply to other operator norms, e.g. the Hilbert-Schmidt norm, also when these are equivalent to $\|\cdot\|_1$).

We start by showing that the mixing criteria discussed in the first half of the chapter do apply to the case of quantum channel. Then we will analyse these maps by studying their linear extensions in the whole vector space formed by the linear operators of \mathcal{H} .

4.4.1 Mixing criteria for Quantum Channels

Let \mathcal{H} be a finite dimensional Hilbert space and let $\mathcal{S}(\mathcal{H})$ be the set of its density matrices ρ . The latter is a convex and compact subset of the larger normed vector space $\mathcal{L}(\mathcal{H})$ composed by the linear operators $\Theta : \mathcal{H} \rightarrow \mathcal{H}$ of \mathcal{H} . From this and from the fact that CPT maps are continuous (indeed they are linear) it follows that for

³This is just the trace distance $d(\rho, \sigma) = \|\rho - \sigma\|_1$.

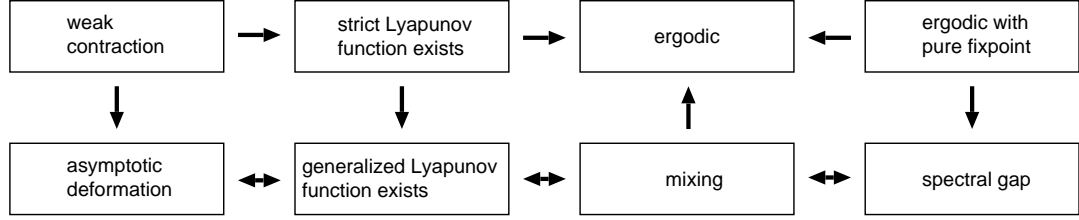


Figure 4.3: Relations between the different properties of a quantum channel.

a quantum channel there always exists at least one density operator which is a fixed point [140]. It also follows that all the results of the previous section apply to quantum channels. In particular Lemma 4.1 holds, implying that any mixing quantum channel must be ergodic. The following example shows, however, that it is possible to have ergodic quantum channels which are not mixing.

Example 4.2 Consider the qubit quantum channel τ obtained by cascading a completely decoherent channel with a NOT gate. Explicitly τ is defined by the transformations $\tau(|0\rangle\langle 0|) = |1\rangle\langle 1|$, $\tau(|1\rangle\langle 1|) = |0\rangle\langle 0|$, and $\tau(|0\rangle\langle 1|) = \tau(|1\rangle\langle 0|) = 0$ with $|0\rangle, |1\rangle$ being the computational basis of the qubit. This map is ergodic with fixed point given by the completely mixed state $(|0\rangle\langle 0| + |1\rangle\langle 1|)/2$. However it is trivially not mixing since, for instance, repetitive application of τ on $|0\rangle\langle 0|$ will oscillate between $|0\rangle\langle 0|$ and $|1\rangle\langle 1|$.

Theorem 4.5 implies that a quantum channel $\tau : \mathcal{S}(\mathcal{H}) \rightarrow \mathcal{S}(\mathcal{H})$ is mixing if and only if it is an asymptotic deformation. As already pointed out in the introduction, this property is *metric independent* (as opposed to contractivity). Alternatively, if the fixed point of a quantum channel is known, then one may use the trivial generalised Lyapunov function (Theorem 4.4) to check if it is mixing. However both criteria depend on the metric distance, which usually has no easy physical interpretation. A more useful choice is the quantum relative entropy, which is defined as

$$H(\rho, \sigma) \equiv \text{Tr} \rho (\log \rho - \log \sigma). \quad (4.27)$$

The quantum relative entropy is continuous in finite dimension [157] and can be used as a measure of *distance* (though it is not a metric). It is finite if the support of ρ is contained in the support of σ . To ensure that it is a continuous function on a compact space, we choose σ to be faithful:

Theorem 4.6 (Relative entropy criterion) *A quantum channel with faithful fixed point ρ_* is mixing if and only if the quantum relative entropy with respect to ρ_* is a*

generalised Lyapunov function.

PROOF Because of Theorem 4.2 we only need to prove the second part of the thesis, i.e. that mixing channels admit the quantum relative entropy with respect to the fixed point, $S(\rho) \equiv H(\rho, \rho_*)$, as a generalised Lyapunov function. Firstly notice that the quantum relative entropy is monotonic under quantum channels [158, 159]. Therefore the limit $S_*(\rho) \equiv \lim_{n \rightarrow \infty} S(\tau^n(\rho))$ does exist and satisfies the condition $S_*(\rho) \geq S(\rho)$. Suppose now there exists a ρ such that $S_*(\rho) = S(\rho)$. Because τ is mixing and S is continuous we have

$$S(\rho) = S_*(\rho) = \lim_{n \rightarrow \infty} S(\tau^n(\rho)) = S(\rho_*) = 0, \quad (4.28)$$

and hence $H(\rho, \rho_*) = 0$. Since $H(\rho, \sigma) = 0$ if and only if $\rho = \sigma$ it follows that S is a Lyapunov function around ρ_* . ■

Another important investigation tool is Corollary 4.2: weak contractivity of a quantum channel is a sufficient condition for mixing. As already mentioned in the previous section, unfortunately this not a necessary condition. Here we present an explicit counterexample based on a quantum channel introduced in Ref. [140].

Example 4.3 Consider a three-level quantum system characterised by the orthogonal vectors $|0\rangle, |1\rangle, |2\rangle$ and the quantum channel τ defined by the transformations $\tau(|2\rangle\langle 2|) = |1\rangle\langle 1|$, $\tau(|1\rangle\langle 1|) = \tau(|0\rangle\langle 0|) = |0\rangle\langle 0|$, and $\tau(|i\rangle\langle j|) = 0$ for all $i \neq j$. Its easy to verify that after just two iterations any input state ρ will be transformed into the vector $|0\rangle\langle 0|$. Therefore the map is mixing. On the other hand it is explicitly not a weak contraction with respect to the trace norm since, for instance, one has

$$\|\tau(|2\rangle\langle 2|) - \tau(|0\rangle\langle 0|)\|_1 = \||1\rangle\langle 1| - |0\rangle\langle 0|\|_1 = \||2\rangle\langle 2| - |0\rangle\langle 0|\|_1, \quad (4.29)$$

where in the last identity we used the invariance of $\|\cdot\|_1$ with respect to unitary transformations.

4.4.2 Beyond the density matrix operator space: spectral properties

Exploiting linearity quantum channels can be extended beyond the space $\mathcal{S}(\mathcal{H})$ of density operators to become maps defined on the full vector space $\mathcal{L}(\mathcal{H})$ of the linear operators of the system, in which basic linear algebra results hold. This allows one to simplify the analysis even though the mixing property (4.1) is still defined with respect to the density operators of the system.

Mixing conditions for quantum channels can be obtained by considering the structure of their eigenvectors in the extended space $\mathcal{L}(\mathcal{H})$. For example, it is easily shown that the spectral radius [160] of any quantum channel is equal to unity [140], so its eigenvalues are contained in the unit circle. The eigenvalues λ on the unit circle (i.e. $|\lambda| = 1$) are referred to as *peripheral eigenvalues*. Also, as already mentioned, since $\mathcal{S}(\mathcal{H})$ is compact and convex, CPT maps have always at least one fixed point which is a density matrix [140].

Theorem 4.7 (Spectral gap criterion) *Let τ be a quantum channel. τ is mixing if and only if its only peripheral eigenvalue is 1 and this eigenvalue is simple.*

PROOF The "if" direction of the proof is a well known result from linear algebra (see for example [160, Lemma 8.2.7]). Now let us assume τ is mixing towards ρ_* . Let Θ be a generic operator in $\mathcal{L}(\mathcal{H})$. Then Θ can be decomposed in a finite set of non-orthogonal density operators⁴, i.e. $\Theta = \sum_{\ell} c_{\ell} \rho_{\ell}$, with $\rho_{\ell} \in \mathcal{S}(\mathcal{H})$ and c_{ℓ} complex. Since $\text{Tr}[\rho_{\ell}] = 1$, we have $\text{Tr}[\Theta] = \sum_{\ell} c_{\ell}$. Moreover since τ is mixing we have $\lim_{n \rightarrow \infty} \tau^n(\rho_{\ell}) = \rho_*$ for all ℓ , with convergence with respect to the trace-norm. Because of linearity this implies

$$\lim_{n \rightarrow \infty} \tau^n(\Theta) = \sum_{\ell} c_{\ell} \rho_* = \text{Tr}[\Theta] \rho_* . \quad (4.30)$$

If there existed any other eigenvector Θ_* of τ with eigenvalue on the unit circle, then $\lim_{n \rightarrow \infty} \tau^n(\Theta_*)$ would not satisfy Eq. (4.30). ■

The speed of convergence can also be estimated by [140]

$$\|\tau^n(\rho) - \rho_*\|_1 \leq C_N n^N \kappa^n , \quad (4.31)$$

where N is the dimensionality of the underlying Hilbert space, κ is the second largest eigenvalue of τ , and C_N is some constant depending only on N and on the chosen norm. Hence, for $n \gg N$ the convergence becomes exponentially fast. As mentioned in [143], the criterion of Theorem 4.7 is in general difficult to check. This is because one has to find all eigenvalues of the quantum channel, which is hard especially in the high dimensional case. Also, if one only wants to check if a particular channel

⁴To show that this is possible, consider an arbitrary operator basis of $\mathcal{L}(\mathcal{H})$. If N is the finite dimension of \mathcal{H} the basis will contain N^2 elements. Each element of the basis can then be decomposed into two Hermitian operators, which themselves can be written as linear combinations of at most N projectors. Therefore there exists a generating set of at most $2N^3$ positive operators, which can be normalised such that they are quantum states. There even exists a basis (i.e. a minimal generating set) consisting of density operators, but in general it cannot be orthogonalised.

is mixing or not, then the amount of information obtained is much higher than the required amount.

Example 4.4 As an application consider the non mixing CPT map of Example 4.2. One can verify that apart from the eigenvalue 1 associated with its fixed point (i.e. the completely mixed state), it possess another peripheral eigenvalue. This is $\lambda = -1$ which is associated with the Pauli operator $|0\rangle\langle 0| - |1\rangle\langle 1|$.

Corollary 4.3 *The convergence speed of any mixing quantum channel is exponentially fast for sufficiently high values of n .*

PROOF From Theorem 4.7 mixing channels have exactly one peripheral eigenvalue, which is also simple. Therefore the derivation of Ref. [140] applies and Eq. (4.31) holds. ■

This result should be compared with the case of strictly contractive quantum channels whose convergence was shown to be exponentially fast along to whole trajectory [143, 146].

4.4.3 Ergodic channels with pure fixed points

An interesting class of ergodic quantum channel is formed by those CPT maps whose fixed point is a *pure* density matrix. Among them we find for instance the maps employed in the communication protocols discussed in this thesis or those of the purification schemes of Refs. [141, 142]. We will now show that within this particular class, ergodicity and mixing are indeed equivalent properties.

We first need the following Lemma, which discusses a useful property of quantum channels (see also [161]).

Lemma 4.6 *Let τ be a quantum channel and Θ be an eigenvector of τ with peripheral eigenvalue $\lambda = e^{i\varphi}$. Then, given $g = \text{Tr} [\sqrt{\Theta^\dagger \Theta}] > 0$, the density matrices $\rho = \sqrt{\Theta \Theta^\dagger}/g$ and $\sigma = \sqrt{\Theta^\dagger \Theta}/g$ are fixed points of τ .*

PROOF Use the left polar decomposition to write $\Theta = g \rho U$ where U is a unitary operator. The operator ρU is clearly an eigenvector of τ with eigenvalue $e^{i\varphi}$, i.e.

$$\tau(\rho U) = \lambda \rho U . \tag{4.32}$$

Hence introducing a Kraus set $\{K_n\}_n$ of τ [154] and the spectral decomposition of the density matrix $\rho = \sum_j p_j |\psi_j\rangle\langle\psi_j|$ with $p_j > 0$ being its positive eigenvalues, one gets

$$\lambda = \text{Tr}[\tau(\rho U)U^\dagger] = \sum_{j,\ell,n} p_j \langle\phi_\ell|K_n|\psi_j\rangle\langle\psi_j|UK_n^\dagger U^\dagger|\phi_\ell\rangle, \quad (4.33)$$

where the trace has been performed with respect to an orthonormal basis $\{|\phi_\ell\rangle\}_\ell$ of \mathcal{H} . Taking the absolute values of both terms gives

$$\begin{aligned} |\lambda| &= \left| \sum_{j,\ell,n} p_j \langle\phi_\ell|K_n|\psi_j\rangle\langle\psi_j|UK_n^\dagger U^\dagger|\phi_\ell\rangle \right| \\ &\leq \sqrt{\sum_{j,\ell,n} p_j \langle\phi_\ell|K_n|\psi_j\rangle\langle\psi_j|K_n^\dagger|\phi_\ell\rangle} \sqrt{\sum_{j,\ell,n} p_j \langle\phi_\ell|UK_n U^\dagger|\psi_j\rangle\langle\psi_j|UK_n^\dagger U^\dagger|\phi_\ell\rangle} \\ &= \sqrt{\text{Tr}[\tau(\rho)]} \sqrt{\text{Tr}[\tilde{\tau}(\rho)]} = 1, \end{aligned} \quad (4.34)$$

where the inequality follows from the Cauchy-Schwartz inequality. The last identity instead is a consequence of the fact that the transformation $\tilde{\tau}(\rho) = U\tau(U^\dagger\rho U)U^\dagger$ is CPT and thus trace preserving. Since $|\lambda| = 1$ it follows that the inequality must be replaced by an identity. This happens if and only if there exist $e^{i\vartheta}$ such that

$$\sqrt{p_j}\{\langle\phi_\ell|K_n|\psi_j\rangle\}^* = \sqrt{p_j}\langle\psi_j|K_n^\dagger|\phi_\ell\rangle = e^{i\vartheta}\sqrt{p_j}\langle\psi_j|UK_n^\dagger U^\dagger|\phi_\ell\rangle, \quad (4.35)$$

for all j, ℓ and n . Since the $|\phi_\ell\rangle$ form a basis of \mathcal{H} , and $p_j > 0$ this implies

$$\langle\psi_j|K_n^\dagger = e^{i\vartheta}\langle\psi_j|UK_n^\dagger U^\dagger \Rightarrow \langle\psi_j|UK_n^\dagger = e^{-i\vartheta}\langle\psi_j|K_n^\dagger U, \quad (4.36)$$

for all n and for all the not null eigenvectors $|\psi_j\rangle$ of ρ . This yields

$$\begin{aligned} \tau(\rho U) &= \sum_j p_j \sum_n K_n |\psi_j\rangle\langle\psi_j| UK_n^\dagger = e^{-i\vartheta} \sum_j p_j \sum_n K_n |\psi_j\rangle\langle\psi_j| K_n^\dagger U \\ &= e^{-i\vartheta} \tau(\rho) U \end{aligned} \quad (4.37)$$

which, replaced in (4.32) gives $e^{-i\vartheta} \tau(\rho) = e^{i\varphi} \rho$, whose only solution is $e^{-i\vartheta} = e^{i\varphi}$. Therefore $\tau(\rho) = \rho$ and ρ is a fixed point of τ . The proof for σ goes along similar lines: simply consider the right polar decomposition of Θ instead of the left polar decomposition. \blacksquare

Corollary 4.4 *Let τ be an ergodic quantum channel. It follows that its eigenvectors associated with peripheral eigenvalues are normal operators.*

PROOF Let Θ be an eigenoperator with peripheral eigenvalue $e^{i\varphi}$ such that $\tau(\Theta) = e^{i\varphi} \Theta$. By Lemma 4.6 we know that, given $g = \text{Tr}[\sqrt{\Theta^\dagger \Theta}]$ the density matrices $\rho = \sqrt{\Theta \Theta^\dagger}/g$ and $\sigma = \sqrt{\Theta^\dagger \Theta}/g$ must be fixed points of τ . Since the map is ergodic we must have $\rho = \sigma$, i.e. $\Theta \Theta^\dagger = \Theta^\dagger \Theta$. ■

Theorem 4.8 (Purely ergodic maps) *Let $|\psi_1\rangle\langle\psi_1|$ be the pure fixed point of an ergodic quantum channel τ . It follows that τ is mixing.*

PROOF We will use the spectral gap criterion showing that $|\psi_1\rangle\langle\psi_1|$ is the only peripheral eigenvector of τ . Assume in fact that $\Theta \in L(\mathcal{H})$ is an eigenvector of τ with peripheral eigenvalue, i.e.

$$\tau(\Theta) = e^{i\varphi} \Theta. \quad (4.38)$$

From Lemma 4.6 we know that the density matrix

$$\rho = \sqrt{\Theta \Theta^\dagger}/g, \quad (4.39)$$

with $g = \text{Tr}[\sqrt{\Theta^\dagger \Theta}] > 0$, must be a fixed point of τ . Since this is an ergodic map we must have $\rho = |\psi_1\rangle\langle\psi_1|$. This implies $\Theta = g|\psi_1\rangle\langle\psi_2|$, with $|\psi_2\rangle$ some normalised vector of \mathcal{H} . Replacing it into Eq. (4.38) and dividing both terms by g yields $\tau(|\psi_1\rangle\langle\psi_2|) = e^{i\varphi}|\psi_1\rangle\langle\psi_2|$ and

$$|\langle\psi_1|\tau(|\psi_1\rangle\langle\psi_2|)|\psi_2\rangle| = 1. \quad (4.40)$$

Introducing a Kraus set $\{K_n\}_n$ of τ and employing Cauchy-Schwartz inequality one can then write

$$\begin{aligned} 1 &= |\langle\psi_1|\tau(|\psi_1\rangle\langle\psi_2|)|\psi_2\rangle| = \left| \sum_n \langle\psi_1|K_n|\psi_1\rangle\langle\psi_2|K_n^\dagger|\psi_2\rangle \right| \\ &\leq \sqrt{\sum_n \langle\psi_1|K_n|\psi_1\rangle\langle\psi_1|K_n^\dagger|\psi_1\rangle} \sqrt{\sum_n \langle\psi_2|K_n|\psi_2\rangle\langle\psi_2|K_n^\dagger|\psi_2\rangle} \\ &= \sqrt{\langle\psi_1|\tau(|\psi_1\rangle\langle\psi_1|)|\psi_1\rangle} \sqrt{\langle\psi_2|\tau(|\psi_2\rangle\langle\psi_2|)|\psi_2\rangle} = \sqrt{\langle\psi_2|\tau(|\psi_2\rangle\langle\psi_2|)|\psi_2\rangle}, \end{aligned} \quad (4.41)$$

where we used the fact that $|\psi_1\rangle$ is the fixed point of τ . Since τ is CPT the quantity $\langle\psi_2|\tau(|\psi_2\rangle\langle\psi_2|)|\psi_2\rangle$ is upper bounded by 1. Therefore in the above expression the

inequality must be replaced by an identity, i.e.

$$\langle \psi_2 | \tau(|\psi_2\rangle\langle\psi_2|) | \psi_2 \rangle = 1 \quad \Longleftrightarrow \quad \tau(|\psi_2\rangle\langle\psi_2|) = |\psi_2\rangle\langle\psi_2|. \quad (4.42)$$

Since τ is ergodic, we must have $|\psi_2\rangle\langle\psi_2| = |\psi_1\rangle\langle\psi_1|$. Therefore $\Theta \propto |\psi_1\rangle\langle\psi_1|$ which shows that $|\psi_1\rangle\langle\psi_1|$ is the only eigenvector of τ with peripheral eigenvalue of. ■

An application of the previous Theorem is obtained as follows.

Lemma 4.7 *Let $M_{AB} = M_A \otimes 1_B + 1_A \otimes M_B$ be an observable of the composite system $\mathcal{H}_A \otimes \mathcal{H}_B$ and τ the CPT linear map on \mathcal{H}_A of Stinespring form [156]*

$$\tau(\rho) = \text{Tr}_B \left[U (\rho \otimes |\phi\rangle_B \langle\phi|) U^\dagger \right], \quad (4.43)$$

(here $\text{Tr}_X[\dots]$ is the partial trace over the system X , and U is a unitary operator of $\mathcal{H}_A \otimes \mathcal{H}_B$). Assume that $[M_{AB}, U] = 0$ and that $|\phi\rangle_B$ is the eigenvector corresponding to a non-degenerate maximal or minimal eigenvalue of M_B . Then τ is mixing if and only if U has one and only one eigenstate that factorises as $|\nu\rangle_A \otimes |\phi\rangle_B$.

PROOF Let ρ be an arbitrary fixed point of τ (since τ is CPT it has always at least one), i.e. $\text{Tr}_B [U (\rho \otimes |\phi\rangle_B \langle\phi|) U^\dagger] = \rho$. Since M_{AB} is conserved and $\text{Tr}_A [M_A \rho] = \text{Tr}_A [M_A \tau(\rho)]$, the system B must remain in the maximal state, which we have assumed to be unique and pure, i.e.

$$U (\rho \otimes |\phi\rangle_B \langle\phi|) U^\dagger = \rho \otimes |\phi\rangle_B \langle\phi| \quad \Longrightarrow \quad [U, \rho \otimes |\phi\rangle_B \langle\phi|] = 0. \quad (4.44)$$

Thus there exists a orthonormal basis $\{|u_k\rangle\}_k$ of $\mathcal{H}_A \otimes \mathcal{H}_B$ diagonalising simultaneously both U and $\rho \otimes |\phi\rangle_B \langle\phi|$. We express the latter in this basis, i.e. $\rho \otimes |\phi\rangle_B \langle\phi| = \sum_k p_k |u_k\rangle\langle u_k|$ with $p_k > 0$, and compute the von Neumann entropy of subsystem B . This yields

$$0 = H(|\phi\rangle_B \langle\phi|) = H \left(\text{Tr}_A \left[\sum_k p_k |u_k\rangle\langle u_k| \right] \right) \geq \sum_k p_k H(\text{Tr}_A [|u_k\rangle\langle u_k|]) \quad (4.45)$$

From the convexity of the von Neumann entropy the above inequality leads to a contradiction unless $\text{Tr}_A [|u_k\rangle\langle u_k|] = |\phi\rangle_B \langle\phi|$ for all k . The $|u_k\rangle$ must therefore be factorising,

$$|u_k\rangle = |\nu_k\rangle_A \otimes |\phi\rangle_B. \quad (4.46)$$

If the factorising eigenstate of U is unique, it must follow that $\rho = |\nu\rangle\langle\nu|$ for some $|\nu\rangle$ and that τ is ergodic. By Theorem 4.8 it then follows that τ is also mixing. If on

the other hand there exists more than one factorising eigenstate, than all states of the form of Eq. (4.46) correspond to a fixed point $\rho_k = |\nu_k\rangle\langle\nu_k|$ and τ is neither ergodic nor mixing. ■

Remark 4.3 An application of this Lemma is the protocol for read and write access by local control discussed in the next chapter.

4.5 Conclusion

In reviewing some known results on the mixing property of continuous maps, we obtained a stronger version of the direct Lyapunov method. For compact metric spaces (including quantum channels operating over density matrices) it provides a necessary and sufficient condition for mixing. Moreover it allows us to prove that asymptotic deformations with at least one fixed point must be mixing.

In the specific context of quantum channels we employed the generalised Lyapunov method to analyse the mixing properties. Here we also analysed different mixing criteria. In particular we have shown that an ergodic quantum channel with a pure fixed point is also mixing.

5 Read and write access by local control

5.1 Introduction

The unitarity of Quantum Mechanics implies that information is conserved. Whatever happens to a quantum system - as long as it is unitary, the original state can in principle be recovered by applying the inverse unitary transformation. However it is well known that in open quantum systems [121] the reduced dynamics is no longer unitary. The reduced dynamics is described by a completely positive, trace preserving maps, and we have seen in the last chapter that there are extreme examples, namely *mixing* maps, where all information about the initial state is eventually lost. Where has it gone? If the whole system evolves unitary, then this information must have been transferred in the *correlations* between reduced system and environment [162], and/or in the environment. We can see that this may be useful for quantum state transfer, in particular the case where all information is transferred into the "environment", which could be another quantum system (the receiver). A particularly useful case is given by mixing maps with pure convergence points, because a pure state cannot be correlated, and because we have a simple convergence criterion in this case (Subsection 4.4.3). This is an example of *homogenisation* [138, 139]. Furthermore, if the mixing property arises from some operations, we can expect that by applying the inverse operations, information can also be transferred back to the system. This property was used in [137, 163] to generate arbitrary states of a cavity field by sending atoms through the cavity. The crucial difference is that in our system control is only assumed to be available on a subsystem (such as, for example, the ends of a quantum chain). Hence we will show in this chapter how arbitrary quantum states can be written to (i.e. prepared on) a large system, and read from it, by *local* control only. This is similar in spirit to universal quantum interfaces [164], but our different approach allows us to specify explicit protocols and to give lower bounds for fidelities. We also demonstrate how this can be used to significantly improve the quantum communication between two parties if the receiver is allowed to store the received signals in a quantum memory

before decoding them. In the limit of an infinite memory, the transfer is perfect. We prove that this scheme allows the transfer of arbitrary multi-partite states along Heisenberg chains of spin-1/2 particles with random coupling strengths.

Even though the convergence of a mixing map is essentially exponentially fast (Corollary 4.3), we still have to deal with infinite limits. Looking at the environment this in turn would require to study states on an infinite dimensional Hilbert space, and unfortunately this can introduce many mathematical difficulties. We are mainly interested in bounds for the finite case: if the protocol stops after finitely many steps, what is the fidelity of the reading/writing? Which encoding and decoding operations must be applied? By stressing on these questions, we can actually avoid the infinite dimensional case, but the price we have to pay is that our considerations become a bit technically involved.

5.2 Protocol

We consider a tripartite finite dimensional Hilbert space given by $\mathcal{H} = \mathcal{H}_C \otimes \mathcal{H}_{\bar{C}} \otimes \mathcal{H}_M$. We assume that full control (the ability to prepare states and apply unitary transformations) is possible on system C and M , but no control is available on system \bar{C} . However, we assume that C and \bar{C} are coupled by some time-independent Hamiltonian H . We show here that under certain assumptions, if the system $C\bar{C}$ is initialised in some arbitrary state we can transfer ("read") this state into the system M by applying some operations between M and C . Likewise, by initialising the system M in the correct state, we can prepare ("write") arbitrary states on the system $C\bar{C}$. The system M functions as a *quantum memory* and must be at least as large as the system $C\bar{C}$. As sketched in Fig. 5.1 we can imagine it to be split into sectors M_ℓ , I.e..

$$\mathcal{H}_M = \bigotimes_{\ell=1}^L \mathcal{H}_{M_\ell} \quad (5.1)$$

with

$$\dim \mathcal{H}_{M_\ell} = \dim \mathcal{H}_C. \quad (5.2)$$

For the reading case, we assume that the memory is initialised in the state

$$|0\rangle_M \equiv \bigotimes_{\ell} |0\rangle_{M_\ell} \quad (5.3)$$

where $|0\rangle$ can stand for some generic state¹. Like in the multi rail protocols considered in Chapter 3, we let the system evolve for a while, perform an operation, let it evolve again and so forth, only that now the operation is not a measurement, but a *unitary gate*. More specifically, at step ℓ of the protocol we perform a unitary swap S_ℓ between system C and systems M_ℓ . After the L th swap operation the protocol stops. The protocol for reading is thus represented by the unitary operator

$$W \equiv S_L U S_{L-1} U \cdots S_\ell U \cdots S_1 U, \quad (5.4)$$

where $U \in \mathcal{L}(\mathcal{H}_{C\bar{C}})$ is the time-evolution operator $U = \exp\{-iHt\}$ for some fixed time interval t . As we will see in the next section, the reduced evolution of the system \bar{C} under the protocol can be expressed in terms of the CPT map

$$\tau(\rho_{\bar{C}}) \equiv \text{tr}_C \left[U (\rho_{\bar{C}} \otimes |0\rangle_C \langle 0|) U^\dagger \right], \quad (5.5)$$

where $|0\rangle_C$ is the state that is swapped in from the memory. Our main assumption now is that τ is ergodic with a pure fixed point (which we denote as $|0\rangle_{\bar{C}}$). By Theorem 4.8 this implies that τ is mixing, and therefore asymptotically all information is transferred into the memory.

For writing states on the system, we just make use of the unitarity of W . Roughly speaking, we initialise the memory in the state that it *would have ended up in* after applying W if system $C\bar{C}$ had started in the state we want to initialise. Then we apply the *inverse* of W given by

$$W^\dagger = U^\dagger S_1 \cdots U^\dagger S_\ell \cdots U^\dagger S_{L-1} U^\dagger S_L. \quad (5.6)$$

We will see in Section 5.4 how this gives rise to a unitary coding transformation on the memory system, such that arbitrary and unknown states can be initialised on the system. The reader has probably noticed that the inverse of W is generally unphysical in the sense that it requires backward time evolution, i.e. one has to wait *negative* time steps between the swaps. But we will see later how this can be fixed by a simple transformation. For the moment, we just assume that W^\dagger is physical.

¹Later on we will give an example where $|0\rangle$ represents a multi-qubit state with all qubits aligned, but here we don't need to assume this.

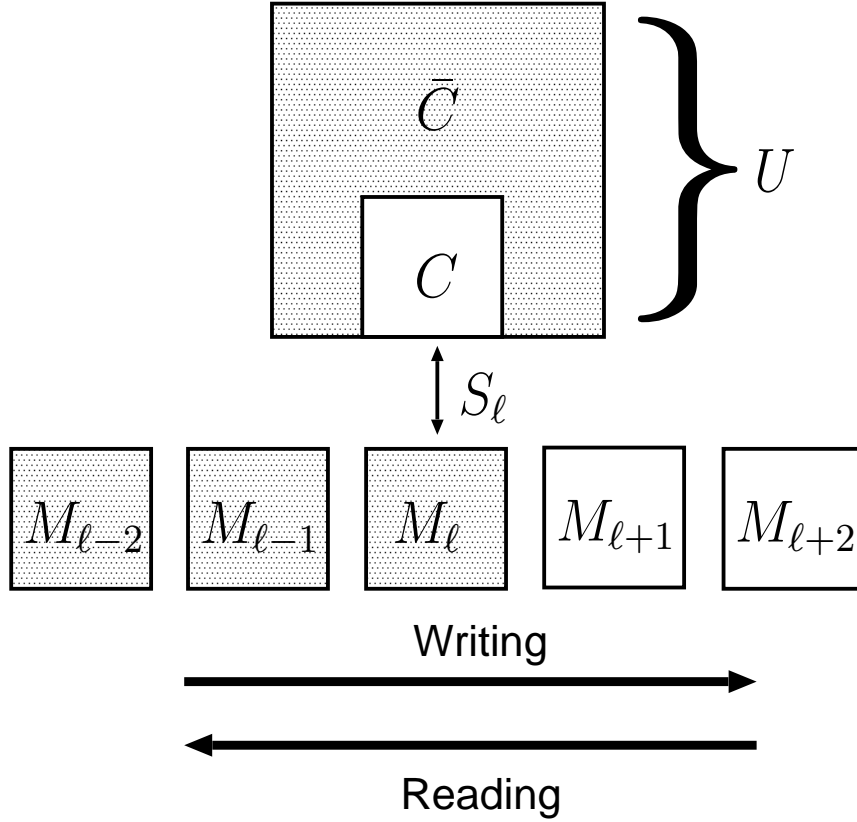


Figure 5.1: The system $C\bar{C}$ can only be controlled by acting on a (small) subsystem C . However system C is coupled to system \bar{C} by a unitary operator $U = \exp\{-iHt\}$. This coupling can - in some cases - *mediate* the local control on C to the full system $C\bar{C}$. In our case, system C is controlled by performing regular swap operations S_ℓ between it and a quantum memory M_ℓ .

5.3 Decomposition equations

In this section we give a decomposition of the state after applying the protocol which will allow us to estimate the fidelities for state transfer in terms of the mixing properties of the map τ . Let $|\psi\rangle_{C\bar{C}} \in \mathcal{H}_{C\bar{C}}$ be an arbitrary state. We notice that the C component of $W|\psi\rangle_{C\bar{C}}|0\rangle_M$ is always $|0\rangle_C$. Therefore we can decompose it as follows

$$W|\psi\rangle_{C\bar{C}}|0\rangle_M = |0\rangle_C \otimes \left[\sqrt{\eta}|0\rangle_{\bar{C}}|\phi\rangle_M + \sqrt{1-\eta}|\Delta\rangle_{\bar{C}M} \right] \quad (5.7)$$

with $|\Delta\rangle_{\bar{C}M}$ being a normalised vector of \bar{C} and M which satisfies the identity

$$\bar{C}\langle 0|\Delta\rangle_{\bar{C}M} = 0. \quad (5.8)$$

It is worth stressing that in the above expression η , $|\phi\rangle_M$ and $|\Delta\rangle_{\bar{C}M}$ are depending on $|\psi\rangle_{C\bar{C}}$. We decompose W^\dagger acting on the first term of Eq. (5.7) as

$$W^\dagger|0\rangle_{C\bar{C}}|\phi\rangle_M = \sqrt{\tilde{\eta}} |\psi\rangle_{C\bar{C}}|0\rangle_M + \sqrt{1-\tilde{\eta}} |\tilde{\Delta}\rangle_{C\bar{C}M}, \quad (5.9)$$

where $|\tilde{\Delta}\rangle_{C\bar{C}M}$ is the orthogonal complement of $|\psi\rangle_{C\bar{C}}|0\rangle_M$, i.e.

$$\bar{C}_C \langle \psi |_M \langle 0 | \tilde{\Delta} \rangle_{C\bar{C}M} = 0. \quad (5.10)$$

Multiplying Eq. (5.9) from the left with ${}_{C\bar{C}}\langle \psi |_M \langle 0 |$ and using the conjugate of Eq. (5.7) we find that $\eta = \tilde{\eta}$. An expression of η in terms of τ can be obtained by noticing that for any vector $|\psi\rangle_{\bar{C}C}$ the following identity applies

$$\tau(\rho_{\bar{C}}) = \text{tr}_C \left[U (\rho_{\bar{C}} \otimes |0\rangle_C \langle 0|) U^\dagger \right] = \text{tr}_{CM} \left[U S_\ell (|\psi\rangle_{\bar{C}C} \langle \psi| \otimes |0\rangle_M \langle 0|) S_\ell U^\dagger \right], \quad (5.11)$$

with $\rho_{\bar{C}}$ being the reduced density matrix $\text{tr}_C [|\psi\rangle_{\bar{C}C} \langle \psi|]$. Reiterating this expression one gets

$$\text{tr}_{CM} \left[W (|\psi\rangle_{C\bar{C}} \langle \psi| \otimes |0\rangle_M \langle 0|) W^\dagger \right] = \tau^{L-1} (\rho'_{\bar{C}}) \quad (5.12)$$

with $\rho'_{\bar{C}} = \text{tr}_C [U (|\psi\rangle_{\bar{C}C} \langle \psi|) U^\dagger]$. Therefore from Eq. (5.7) and the orthogonality relation (5.8) it follows that

$$\eta = {}_{\bar{C}}\langle 0 | \tau^{L-1} (\rho'_{\bar{C}}) | 0 \rangle_{\bar{C}}, \quad (5.13)$$

which, since τ is mixing, shows that $\eta \rightarrow 1$ for $L \rightarrow \infty$. Moreover we can use Eq. (4.31) to claim that

$$\begin{aligned} |\eta - 1| &= |{}_{\bar{C}}\langle 0 | \tau^{L-1} (\rho'_{\bar{C}}) | 0 \rangle_{\bar{C}} - 1| \\ &\leq \| \tau^{L-1} (\rho'_{\bar{C}}) - |0\rangle_{\bar{C}} \langle 0| \|_1 \leq R (L-1)^{d_{\bar{C}}} \kappa^{L-1}, \end{aligned} \quad (5.14)$$

where R is a constant which depends upon $d_{\bar{C}} \equiv \dim \mathcal{H}_{\bar{C}}$ and where $\kappa \in]0, 1[$ is the second largest eigenvalue of τ .

5.4 Coding transformation

Here we derive the decoding/encoding transformation that relates states on the memory M to the states that are on the system $C\bar{C}$. We first apply the above decomposi-

tions Eqs. (5.7) and (5.9) to a fixed orthonormal basis $\{|\psi_k\rangle_{C\bar{C}}\}$ of $\mathcal{H}_{C\bar{C}}$, i.e.

$$\begin{aligned} W|\psi_k\rangle_{C\bar{C}}|0\rangle_M &= |0\rangle_C \otimes \left[\sqrt{\eta_k}|0\rangle_{\bar{C}}|\phi_k\rangle_M + \sqrt{1-\eta_k}|\Delta_k\rangle_{\bar{C}M} \right] \\ W^\dagger|0\rangle_{C\bar{C}}|\phi_k\rangle_M &= \sqrt{\eta_k}|\psi_k\rangle_{C\bar{C}}|0\rangle_M + \sqrt{1-\eta_k}|\tilde{\Delta}_k\rangle_{C\bar{C}M}. \end{aligned} \quad (5.15)$$

Define a linear operator D on \mathcal{H}_M which performs the following transformation

$$D|\psi_k\rangle_M = |\phi_k\rangle_M. \quad (5.16)$$

Here $|\psi_k\rangle_M$ are orthonormal vectors of M which represent the states $\{|\psi_k\rangle_{C\bar{C}}\}$ of $\mathcal{H}_{C\bar{C}}$ (formally they are obtained by a partial isometry from $\bar{C}C$ to M). The vectors $|\phi_k\rangle_M$ are defined through Eq. (5.15) - typically they will not be orthogonal. We first show that for large L they become approximately orthogonal.

From the unitarity of W^\dagger and from Eq. (5.15) we can establish the following identity

$$\begin{aligned} {}_M\langle\phi_k|\phi_{k'}\rangle_M &= \sqrt{\eta_k \eta_{k'}} \delta_{kk'} + \sqrt{\eta_k (1-\eta_{k'})} {}_{\bar{C}CM}\langle\psi_k 0|\tilde{\Delta}_{k'}\rangle_{\bar{C}CM} \\ &+ \sqrt{\eta_{k'} (1-\eta_k)} {}_{\bar{C}CM}\langle\tilde{\Delta}_k|\psi_{k'} 0\rangle_{\bar{C}CM} + \sqrt{(1-\tilde{\eta}_k)(1-\tilde{\eta}_{k'})} {}_{C\bar{C}M}\langle\tilde{\Delta}_k|\tilde{\Delta}_{k'}\rangle_{C\bar{C}M}. \end{aligned} \quad (5.17)$$

Defining $\eta_0 \equiv \min_k \eta_k$ it follows for $k \neq k'$ that

$$|{}_M\langle\phi_k|\phi_{k'}\rangle_M| \leq \sqrt{\eta_k (1-\eta_{k'})} |{}_{\bar{C}CM}\langle\psi_k 0|\tilde{\Delta}_{k'}\rangle_{\bar{C}CM}| \quad (5.18)$$

$$\begin{aligned} &+ \sqrt{\eta_{k'} (1-\eta_k)} |{}_{\bar{C}CM}\langle\tilde{\Delta}_k|\psi_{k'} 0\rangle_{\bar{C}CM}| \\ &+ \sqrt{(1-\tilde{\eta}_k)(1-\tilde{\eta}_{k'})} |{}_{C\bar{C}M}\langle\tilde{\Delta}_k|\tilde{\Delta}_{k'}\rangle_{C\bar{C}M}| \\ &\leq 2\sqrt{1-\eta_0} + (1-\eta_0) \leq 3\sqrt{1-\eta_0}. \end{aligned} \quad (5.19)$$

Therefore for all k, k' the inequality

$$|{}_M\langle\phi_k|\phi_{k'}\rangle_M - \delta_{k,k'}| \leq 3\sqrt{1-\eta_0} \quad (5.20)$$

holds. It is worth noticing that, since Eq. (5.14) applies for all input states $|\psi\rangle_{\bar{C}C}$, we have

$$|\eta_0 - 1| \leq C (L-1)^{d_{\bar{C}}} \kappa^{L-1}. \quad (5.21)$$

Eq. (5.20) allows us to make an estimation of the eigenvalues λ_k of $D^\dagger D$ as

$$|\lambda_k - 1| \leq 3 d_{C\bar{C}} \sqrt{1-\eta_0}, \quad (5.22)$$

with $d_{C\bar{C}} \equiv \dim \mathcal{H}_{C\bar{C}}$. We now take a polar decomposition $D = PV$ of D . V is the *best unitary approximation* to D [160, p 432] and we have

$$\begin{aligned} \|D - V\|_2^2 &= \sum_k \left[\sqrt{\lambda_k} - 1 \right]^2 \\ &\leq \sum_k |\lambda_k - 1| \\ &\leq 3 d_{C\bar{C}}^2 \sqrt{1 - \eta_0}. \end{aligned} \quad (5.23)$$

Therefore

$$\boxed{\|D - V\|_2 \leq \sqrt{3} d_{C\bar{C}} (1 - \eta_0)^{1/4}}, \quad (5.24)$$

which, thanks to Eq. (5.21), shows that D can be approximated arbitrary well by a unitary operator V for $L \rightarrow \infty$.

5.5 Fidelities for reading and writing

In what follows we will use V^\dagger and V as our reading and writing transformation, respectively. In particular, V^\dagger will be used to recover the input state $|\psi\rangle_{C\bar{C}}$ of the chain after we have (partially) transferred it into M through the unitary W (i.e. we first act on $|\psi\rangle_{C\bar{C}} \otimes |0\rangle_M$ with W , and then we apply V^\dagger on M). Vice-versa, in order to prepare a state $|\psi\rangle_{C\bar{C}}$ on $C\bar{C}$ we first prepare M into $|\psi\rangle_M$, then we apply to it the unitary transformation V and finally we apply W^\dagger . We now give bounds on the fidelities for both procedures.

The fidelity for reading the state $|\psi\rangle_M$ is given by

$$F_r(\psi) \equiv {}_M \langle \psi | V^\dagger R_M V | \psi \rangle_M \quad (5.25)$$

where R_M is the state of the memory after W , i.e.

$$R_M \equiv \text{tr}_{C\bar{C}} \left[W(|\psi\rangle_{C\bar{C}} \langle \psi| \otimes |0\rangle_M \langle 0|) W^\dagger \right] = \eta |\phi\rangle_M \langle \phi| + (1 - \eta) \sigma_M. \quad (5.26)$$

In the above expression we used Eqs. (5.7) and (5.8) and defined $\sigma_M = \text{tr}_{\bar{C}}[|\Delta\rangle_{\bar{C}M} \langle \Delta|]$. Therefore by linearity we get

$$F_r(\psi) = \eta |{}_M \langle \phi | V | \psi \rangle_M|^2 + (1 - \eta) {}_M \langle \psi | V^\dagger \sigma_M V | \psi \rangle_M \geq \eta |{}_M \langle \phi | V | \psi \rangle_M|^2. \quad (5.27)$$

Notice that

$$|_M \langle \phi | V | \psi \rangle_M| = |_M \langle \phi | V - D + D | \psi \rangle_M| \geq |_M \langle \phi | D | \psi \rangle_M| - |_M \langle \phi | D - V | \psi \rangle_M|. \quad (5.28)$$

Now we use the inequality (5.24) to write

$$|_M \langle \phi | D - V | \psi \rangle_M| \leq \|D - V\|_2 \leq \sqrt{3} d_{C\bar{C}} (1 - \eta_0)^{1/4}. \quad (5.29)$$

If $|\psi\rangle_M$ was a basis state $|\psi_k\rangle_M$, then $|_M \langle \phi | D | \psi \rangle_M| = 1$ by the definition Eq. (5.16) of D . For *generic* $|\psi\rangle_M$ we can use the linearity to find after some algebra that

$$\sqrt{\eta} |_M \langle \phi | D | \psi \rangle_M| \geq \sqrt{\eta_0} - 3 d_{C\bar{C}} \sqrt{1 - \eta_0}. \quad (5.30)$$

Therefore Eq. (5.28) gives

$$\sqrt{\eta} |_M \langle \phi | V | \psi \rangle_M| > \sqrt{\eta_0} - 5 d_{C\bar{C}} (1 - \eta_0)^{1/4}. \quad (5.31)$$

By Eq. (5.27) it follows that

$$F_r \geq \eta_0 - 10 d_{C\bar{C}} (1 - \eta_0)^{1/4}. \quad (5.32)$$

The fidelity for writing a state $|\psi\rangle_{\bar{C}C}$ into $\bar{C}C$ is given by

$$F_w(\psi) \equiv {}_{C\bar{C}} \langle \psi | \text{tr}_M \left[W^\dagger V (|\psi\rangle_M \langle \psi| \otimes |0\rangle_{\bar{C}C} \langle 0|) V^\dagger W \right] |\psi\rangle_{C\bar{C}}. \quad (5.33)$$

A lower bound for this quantity is obtained by replacing the trace over M with the expectation value on $|0\rangle_M$, i.e.

$$\begin{aligned} F_w(\psi) &\geq {}_{C\bar{C}} \langle \psi | {}_M \langle 0 | W^\dagger V (|\psi\rangle_M \langle \psi| \otimes |0\rangle_{\bar{C}C} \langle 0|) V^\dagger W | 0 \rangle_M |\psi\rangle_{C\bar{C}} \\ &= \left| {}_{C\bar{C}} \langle 0 | {}_M \langle \psi | V^\dagger W | 0 \rangle_M |\psi\rangle_{C\bar{C}} \right|^2 \\ &= \eta \left| {}_M \langle \psi | V^\dagger | \phi \rangle_M \right|^2 = \eta |_M \langle \phi | V | \psi \rangle_M|^2 \end{aligned} \quad (5.34)$$

where Eqs. (5.7) and the orthogonality relation (5.8) have been employed to derive the second identity. Notice that the last term of the inequality (5.34) coincides with the lower bound (5.27) of the reading fidelity. Therefore, by applying the same derivation of the previous section we can write

$$\boxed{F \geq \eta_0 - 10 d_{C\bar{C}} (1 - \eta_0)^{1/4}}, \quad (5.35)$$



Figure 5.2: Alice and Bob control the spins N_A and N_B interconnected by the spins N_R . At time jt Bob performs a swap S_j between his spins and the memory M_j .

which shows that the reading and writing fidelities converge to 1 in the limit of large L . Note that this lower bound can probably be largely improved.

5.6 Application to spin chain communication

We now show how the above protocol can be used to improve quantum state transfer on a spin chain. The main advantage of using such a memory protocol is that - opposed to all other schemes - Alice can send arbitrary multi-qubit states with a single usage of the channel. She needs no encoding, all the work is done by Bob. The protocol proposed here can be used to improve the performances of any scheme mentioned in Section 1.5, and it works for a large class of Hamiltonians, including Heisenberg and XY models with arbitrary (also randomly distributed) coupling strengths.

Consider a chain of spin-1/2 particles described by a Hamiltonian H which conserves the number of excitations. The chain is assumed to be divided in three portions A (Alice), B (Bob) and R (the remainder of the chain, connecting Alice and Bob) containing respectively the first N_A spins of the chain, the last N_B spins and the intermediate N_R spins, and the total length of the chain is $N = N_A + N_R + N_B$ (see Fig 5.2). Bob has access also to a collection of quantum memories $M_1, \dots, M_j, \dots, M_L$ isomorphic with B , i.e. each having dimension equal to the dimension 2^{N_B} of B . We assume that Bob's memory is initialised in the zero excitation state $|0\rangle_M$. Alice prepares an arbitrary and unknown state $|\psi\rangle_A$ on her N_A qubits. By defining the (from Bob's perspective) controlled part of system $C = B$ and the uncontrolled part $\bar{C} = AR$, we can apply the results of the last sections and get the following

Theorem 5.1 (Memory swapping) *Let H be the Hamiltonian of an open nearest-neighbour quantum chain that conserves the number of excitations. If there is a time t such that $f_{1,N}(t) \neq 0$ (i.e. the Hamiltonian is capable of transport between Alice and Bob) then the state transfer can be made arbitrarily perfect by using the memory swapping protocol.*

PROOF We only have to show that the reduced dynamics on the chain is mixing with a pure fixed point. Using the number of excitations as a conserved additive observable, we can use the criterion of Lemma 4.7: If there exists exactly one eigenstate $|E\rangle$ of factorising form with $|0\rangle_B$, i.e.

$$\exists_1 |\lambda\rangle_{AR} : H|\lambda\rangle_{AR} \otimes |0\rangle_B = E|\lambda\rangle_{AR} \otimes |0\rangle_B, \quad (5.36)$$

then the reduced dynamics is mixing toward $|0\rangle_{AR}$. Assume by contradiction that has an eigenvector $|E\rangle_{AR} \neq |0\rangle_{AR}$ which falsifies Eq. (5.36). Such an eigenstate can be written as

$$|E\rangle_{AR} \otimes |0\rangle_B = a|\mu\rangle_{AR} \otimes |0\rangle_B + b|\bar{\mu}\rangle_{AR} \otimes |0\rangle_B, \quad (5.37)$$

where a and b are complex coefficients and where the spin just before the section B (with position $N_A + N_R$) is in the state $|0\rangle$ for $|\mu\rangle_{AR}$ and in the state $|1\rangle$ for $|\bar{\mu}\rangle_{AR}$. Since the interaction between this spin and the first spin of section B includes an exchange term (otherwise $f_{1,N}(t)=0$ for all t), then the action of H on the second term of (5.37) yields exactly one state which contains an excitation in the sector B . It cannot be compensated by the action of H on the first term of (5.37). But by assumption $|E\rangle_{AR} \otimes |0\rangle_B$ is an eigenstate of H , so we conclude that $b = 0$. This argument can be repeated for the second last spin of section R , the third last spin, and so on, to finally yield $|E\rangle_{AR} = |0\rangle_{AR}$, as long as all the nearest neighbour interactions contain exchange parts. ■

Remark 5.1 Theorem 5.1 should be compared to Theorem 3.2 for the multi rail protocol. They are indeed very similar. However the current theorem is much stronger, since it allows to send arbitrary multi-excitation states, and also to write states back onto the chain. It is interesting to note that Lemma 4.7 and Theorem 5.1 indicate a connection between the dynamical controllability of a system and its static entanglement properties. It may be interesting to obtain a *quantitative* relation between the amount of entanglement and the convergence speed.

Let us now come back to the question raised in Section 5.2 about the operation W^\dagger being unphysical. As mentioned before, this can be fixed using a simple transformation: if the Hamiltonian H fulfils the requirements of Lemma 4.7, then also the Hamiltonian $-H$ fulfils them. Now derive the coding transformation \tilde{V} as given in Section 5.4 for the Hamiltonian $\tilde{H} = -H$. In this picture, the reading protocol W is unphysical, whereas the writing protocol becomes physical. In the more general case

where the condition of Lemma 4.7 is not valid, but the map

$$\tau(\rho_{\bar{C}}) \equiv \text{tr}_C \left[U (\rho_{\bar{C}} \otimes |0\rangle_C \langle 0|) U^\dagger \right] \quad (5.38)$$

is still ergodic with a pure fixed point, we then require the map

$$\tilde{\tau}(\rho_{\bar{C}}) \equiv \text{tr}_C \left[U^\dagger (\rho_{\bar{C}} \otimes |0\rangle_C \langle 0|) U \right] \quad (5.39)$$

to be also ergodic with pure fixed point to be able to use this trick.

5.7 Conclusion

We have given an explicit protocol for controlling a large permanently coupled system by accessing a small subsystem only. In the context of quantum chain communication this allows us to make use of the quantum memory of the receiving party to improve the fidelity to a value limited only by the size of the memory. We have shown that this scheme can be applied to a Heisenberg spin chain. The main advantage of this method is that arbitrary multi-excitation states can be transferred. Also, our method can be applied to chains that do not conserve the number of excitations in the system, as long as the reduced dynamic is ergodic with a pure fixed point.

It remains an open question how much of our results remain valid if the channel is mixing toward a *mixed* state. In this case, a part of the quantum information will in general remain in the correlations between the system and the memory, and it cannot be expected that the fidelity converges to one. However, by concentrating only on the eigenstate of the fixed point density operator with the largest eigenvalue, it should be possible to derive some bounds of the amount of information that can be extracted.

6 A valve for probability amplitude

6.1 Introduction

We have mainly discussed two methods for quantum state transfer so far. In the first one, multiple chains were used, and in the second one, a single chain was used in combination with a large quantum memory. Can we combine the best of the two schemes, i.e. is it possible to use only a single chain and a single memory qubit? In this chapter we will show that this is indeed the case and that the fidelity can be improved easily by applying in certain time-intervals two-qubit gates at the receiving end of the chain. These gates act as a *valve* which takes probability amplitude out of the system without ever putting it back. The required sequence is determined *a priori* by the Hamiltonian of the system. Such a protocol is *optimal* in terms of resources, because two-qubit gates at the sending and receiving end are required in order to connect the chain to the blocks in *all* above protocols (though often not mentioned explicitly). At the same time, the engineering demands are not higher than for the memory swapping protocol. Our scheme has some similarities with [92], but the gates used here are much simpler, and arbitrarily high fidelity is guaranteed by a convergence theorem for arbitrary coupling strengths and all non-Ising coupling types that conserve the number of excitations. Furthermore, we show numerically that our protocol could also be realised by a simple switchable interaction.

6.2 Arbitrarily Perfect State Transfer

We now show how the receiver can improve the fidelity to an arbitrarily high value by applying two-qubit gates between the end of the chain and a “target qubit” of the block. We label the qubits of the chain by $1, 2, \dots, N$ and the target qubit by $N + 1$ (see Fig. 6.1). The coupling of the chain is described by a Hamiltonian H . We assume that the Hamiltonian H conserves the number of excitations and that the target qubit $N + 1$ is uncoupled,

$$H|N + 1\rangle = 0 \tag{6.1}$$

and set the energy of the ground state $|\mathbf{0}\rangle$ to zero. For what follows we restrict all operators to the $N + 2$ dimensional Hilbert space

$$\mathcal{H} = \text{span} \{|\mathbf{n}\rangle; n = 0, 1, 2, \dots, N + 1\}. \quad (6.2)$$

Our final assumption about the Hamiltonian of the system is that there exists a time t such that

$$f_{N,t}(t) \equiv \langle \mathbf{N} | \exp \{-itH\} | \mathbf{1} \rangle \neq 0. \quad (6.3)$$

Physically this means that the Hamiltonian has the capability of transporting from the first to the last qubit of the chain. As mentioned in the introduction, the fidelity of this transport may be very bad in practice.

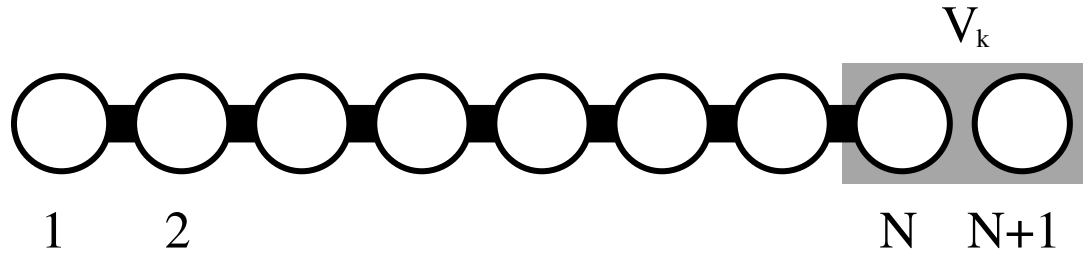


Figure 6.1: A quantum chain (qubits $1, 2, \dots, N$) and a target qubit ($N + 1$). By applying a sequence of two-qubit unitary gates V_k on the last qubit of the chain and the target qubit, arbitrarily high fidelity can be achieved.

We denote the unitary evolution operator for a given time t_k as $U_k \equiv \exp \{-it_k H\}$ and introduce the projector

$$P = 1 - |\mathbf{0}\rangle\langle\mathbf{0}| - |\mathbf{N}\rangle\langle\mathbf{N}| - |\mathbf{N} + \mathbf{1}\rangle\langle\mathbf{N} + \mathbf{1}|. \quad (6.4)$$

A crucial ingredient to our protocol is the operator

$$\begin{aligned} V(c, d) \equiv & P + |\mathbf{0}\rangle\langle\mathbf{0}| + d|\mathbf{N}\rangle\langle\mathbf{N}| + d^*|\mathbf{N} + \mathbf{1}\rangle\langle\mathbf{N} + \mathbf{1}| \\ & + c^*|\mathbf{N} + \mathbf{1}\rangle\langle\mathbf{N}| - c|\mathbf{N}\rangle\langle\mathbf{N} + \mathbf{1}|, \end{aligned} \quad (6.5)$$

where c and d are complex normalised amplitudes. It is easy to check that

$$VV^\dagger = V^\dagger V = 1, \quad (6.6)$$

so V is a unitary operator on \mathcal{H} . V acts as the identity on all but the last two qubits, and can hence be realised by a *local two-qubit gate on the qubits N and $N + 1$* .

Furthermore we have $VP = P$ and

$$V(c, d) [\{c|\mathbf{N}\rangle + d|\mathbf{N} + \mathbf{1}\rangle\}] = |\mathbf{N} + \mathbf{1}\rangle. \quad (6.7)$$

The operator $V(c, d)$ has the role of moving probability amplitude c from the N th qubit to target qubit, without moving amplitude back into the system, and can be thought of as a *valve*. Of course as $V(c, d)$ is unitary, there are also states such that $V(c, d)$ acting on them would move back probability amplitude into the system, but these do not occur in the protocol discussed here.

Using the time-evolution operator and two-qubit unitary gates on the qubits N and $N + 1$ we will now develop a protocol that transforms the state $|\mathbf{1}\rangle$ into $|\mathbf{N} + \mathbf{1}\rangle$. Let us first look at the action of U_1 on $|\mathbf{1}\rangle$. Using the projector P we can decompose this time-evolved state as

$$\begin{aligned} U_1|\mathbf{1}\rangle &= PU_1|\mathbf{1}\rangle + |\mathbf{N}\rangle\langle\mathbf{N}|U_1|\mathbf{1}\rangle \\ &\equiv PU_1|\mathbf{1}\rangle + \sqrt{p_1}\{c_1|\mathbf{N}\rangle + d_1|\mathbf{N} + \mathbf{1}\rangle\}, \end{aligned} \quad (6.8)$$

where $p_1 = |\langle\mathbf{N}|U_1|\mathbf{1}\rangle|^2$, $c_1 = \langle\mathbf{N}|U_1|\mathbf{1}\rangle/\sqrt{p_1}$ and $d_1 = 0$. Let us now consider the action of $V_1 \equiv V(c_1, d_1)$ on the time-evolved state. By Eq. (6.7) it follows that

$$V_1U_1|\mathbf{1}\rangle = PU_1|\mathbf{1}\rangle + \sqrt{p_1}|\mathbf{N} + \mathbf{1}\rangle. \quad (6.9)$$

Hence with a probability of p_1 , the excitation is now in the position $N + 1$, where it is “frozen” (since that qubit is not coupled to the chain. We will now show that at the next step, this probability is increased. Applying U_2 to Eq. (6.9) we get

$$\begin{aligned} U_2V_1U_1|\mathbf{1}\rangle &= PU_2PU_1|\mathbf{1}\rangle + \langle\mathbf{N}|U_2PU_1|\mathbf{1}\rangle|\mathbf{N}\rangle + \sqrt{p_1}|\mathbf{N} + \mathbf{1}\rangle \\ &= PU_2PU_1|\mathbf{1}\rangle + \sqrt{p_2}\{c_2|\mathbf{N}\rangle + d_2|\mathbf{N} + \mathbf{1}\rangle\} \end{aligned} \quad (6.10)$$

with $c_2 = \langle\mathbf{N}|U_2PU_1|\mathbf{1}\rangle/\sqrt{p_2}$, $d_2 = \sqrt{p_1}/\sqrt{p_2}$ and

$$p_2 = p_1 + |\langle\mathbf{N}|U_2PU_1|\mathbf{1}\rangle|^2 \geq p_1. \quad (6.11)$$

Applying $V_2 \equiv V(c_2, d_2)$ we get

$$V_2U_2V_1U_1|\mathbf{1}\rangle = PU_2PU_1|\mathbf{1}\rangle + \sqrt{p_2}|\mathbf{N} + \mathbf{1}\rangle. \quad (6.12)$$

Repeating this strategy ℓ times we get

$$\left(\prod_{k=1}^{\ell} V_k U_k\right) |\mathbf{1}\rangle = \left(\prod_{k=1}^{\ell} P U_k\right) |\mathbf{1}\rangle + \sqrt{p_\ell} |\mathbf{N} + \mathbf{1}\rangle, \quad (6.13)$$

where the products are arranged in the time-ordered way. Using the normalisation of the r.h.s. of Eq. (6.13) we get

$$p_\ell = 1 - \left\| \left(\prod_{k=1}^{\ell} P U_k\right) |\mathbf{1}\rangle \right\|^2. \quad (6.14)$$

From Section 3.5 we know that there exists a $t > 0$ such that for equal time intervals $t_1 = t_2 = \dots = t_k = t$ we have $\lim_{\ell \rightarrow \infty} p_\ell = 1$. Therefore the limit of infinite gate operations for Eq. (6.13) is given by

$$\lim_{\ell \rightarrow \infty} \left(\prod_{k=1}^{\ell} V_k U_k\right) |\mathbf{1}\rangle = |\mathbf{N} + \mathbf{1}\rangle. \quad (6.15)$$

It is also easy to see that $\lim_{k \rightarrow \infty} d_\ell = 1$, $\lim_{k \rightarrow \infty} c_\ell = 0$ and hence the gates V_k converge to the identity operator. Furthermore, since $V_k U_k |\mathbf{0}\rangle = |\mathbf{0}\rangle$ it also follows that arbitrary superpositions can be transferred. As discussed in Theorem 4.31, this convergence is asymptotically exponentially fast in the number of gate applied (a detailed analysis of the relevant scaling can be found in Chapter 2). Equation (6.15) is a surprising result, which shows that *any non-perfect transfer can be made arbitrarily perfect* by only applying two-qubit gates on one end of the quantum chain. It avoids restricting the gate times to specific times (as opposed to the dual rail scheme) while requiring no additional memory qubit (as opposed to the memory swapping scheme).

The sequence V_k that needs to be applied to the end of the chain to perform the state transfer only depends on the Hamiltonian of the quantum chain. The relevant properties can in principle be determined a priori by preceding measurements and tomography on the quantum chain (as discussed in Sect. 2.9).

6.3 Practical Considerations

Motivated by the above result we now investigate how the above protocol may be implemented in practice, well before the realisation of the quantum computing blocks from Fig. 1.4. The two-qubit gates V_k are essentially rotations in the $\{|01\rangle, |10\rangle\}$ space of the qubits N and $N + 1$. It is therefore to be expected that they can be realised (up

to a irrelevant phase) by a switchable Heisenberg or XY type coupling between the N th and the target qubit. However in the above, we have assumed that the gates V_k can be applied instantaneously, i.e. in a time-scale much smaller than the time-scale of the dynamics of the chain. This corresponds to a switchable coupling that is much stronger than the coupling strength of the chain.

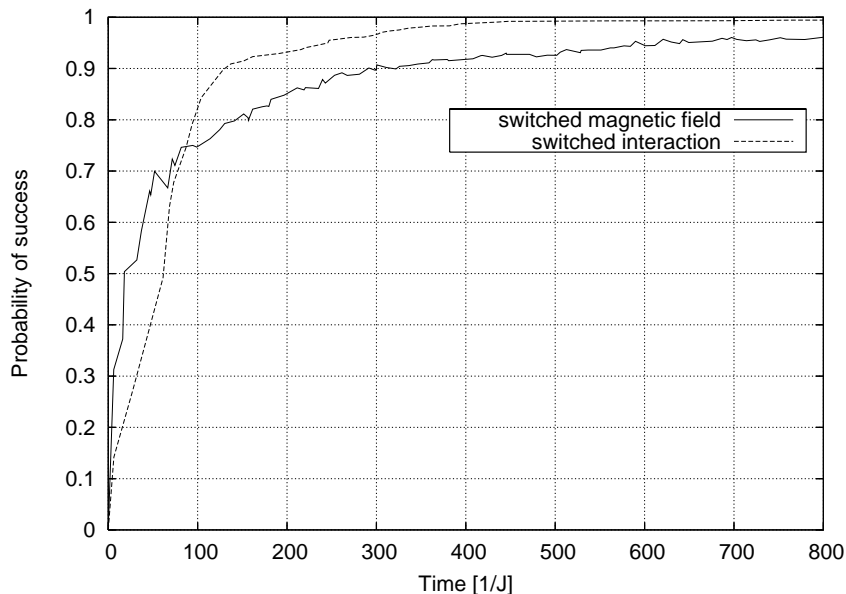


Figure 6.2: Numerical example for the convergence of the success probability. Simulated is a quantum chain of length $N = 20$ with the Hamiltonian from Eq. (6.16) (dashed line) and Eq. (6.17) with $B/J = 20$ (solid line). Using the original protocol [1], the same chain would only reach a success probability of 0.63 in the above time interval.

Here, we numerically investigate if a convergence similar to the above results is still possible when this assumption is not valid. We *do* however assume that the switching of the interaction is still describable by an instantaneous switching (i.e. the sudden approximation is valid). This assumption is mainly made to keep the numerics simple. We do not expect qualitative differences when the switching times become finite as long as the time-dependent Hamiltonian is still conserving the number of excitations in the chain. In fact it has recently been shown that the finite switching time can even *improve* the fidelity [33]. Intuitively, this happens because by gradually decreasing the coupling, he not only receives the probability amplitude of the last qubit of the chain, but can also "swallow" a bit of the dispersed wave-packed (similar to the situation discussed in [92]).

We have investigated two types of switching. For the first type, the coupling itself

is switchable, i.e.

$$H(t) = J \sum_{n=1}^{N-1} \sigma_n^- \sigma_{n+1}^+ + \Delta(t) \sigma_N^- \sigma_{N+1}^+ + \text{h.c.}, \quad (6.16)$$

where $\Delta(t)$ can be 0 or 1. For the second type, the target qubit is *permanently* coupled to the remainder of the chain, but a strong magnetic field on the last qubit can be switched,

$$H(t) = J \sum_{n=1}^N \sigma_n^- \sigma_{n+1}^+ + \text{h.c.} + B\Delta(t)\sigma_{N+1}^z, \quad (6.17)$$

where again $\Delta(t)$ can be 0 or 1 and $B \gg 1$. This suppresses the coupling between the N th and $N + 1$ th qubit due to an energy mismatch.

In both cases, we first numerically optimise the times for unitary evolution t_k over a fixed time interval such that the probability amplitude at the N th qubit is maximal. The algorithm then finds the optimal time interval during which $\Delta(t) = 1$ such that the probability amplitude at the target qubit is increased. In some cases the phases are not correct, and switching on the interaction would result in probability amplitude floating back into the chain. In this situation, the target qubit is left decoupled and the chain is evolved to the next amplitude maximum at the N th qubit. Surprisingly, even when the time-scale of the gates is comparable to the dynamics, near-perfect transfer remains possible (Fig 6.2). In the case of the switched magnetic field, the achievable fidelity depends on the strength of the applied field. This is because the magnetic field does not fully suppress the coupling between the two last qubits. A small amount of probability amplitude is lost during each time evolution U_k , and when the gain by the gate is compensated by this loss, the total success probability no longer increases.

6.4 Conclusion

We have seen that by having a simple switchable interaction acting as a *valve* for probability amplitude, arbitrarily perfect state transfer is possible on a single spin chain. In fact, by using the inverse protocol, arbitrary¹ states in the first excitation sector can also be prepared on the chain. Furthermore, this protocol can easily be adopted to arbitrary graphs connecting multiple senders and receivers (as discussed for weakly coupled systems in [86]).

¹Opposed to the method for state preparation developed in the last chapter this allows the creation of *known* states only (as the valve operations V_k depend explicitly on the state that one wants to prepare).

7 External noise

7.1 Introduction

An important question that was left open so far is what happens to quantum state transfer in the presence of external noise. It is well known from the theory of open quantum systems [121] that this can lead to dissipation and decoherence, which also means that quantum information is lost. The evolution of a closed quantum system is described by the Schrödinger equation

$$\partial_t |\psi\rangle = -iH|\psi\rangle. \quad (7.1)$$

If a system is very strongly coupled to an environment, the dynamic is completely incoherent and described by some simple rate equations for the occupation probabilities,

$$\partial_t P_n = \sum_m k_{n \leftarrow m} P_m - \sum_m k_{m \leftarrow n} P_n. \quad (7.2)$$

In the more general case where the dynamic consists of coherent and incoherent parts, the evolution can sometimes be expressed as a Lindblad equation [121]

$$\partial_t \rho = \mathcal{L}\rho \quad (7.3)$$

for the reduced density matrix. These three regimes are shown in Fig. 7.1. For quantum information theory, coherence is essential [2], and one has to try to isolate the quantum chain as much as possible from the environment. In the partially coherent regime, typically the quantum behaviour decays exponentially with a rate depending on the temperature of the environment. Not surprisingly, this has also been found in the context of quantum state transfer [165–167]. From a theoretical point of view it is perhaps more interesting to look at the low temperature and strong coupling regime, where the dynamics is often non-Markovian [121] and can no longer be expressed as a simple Lindblad equation. This is also interesting from a practical perspective, corresponding to effects of the environment which cannot be avoided by cooling. Here we consider a model where the system is coupled to a spin environment through

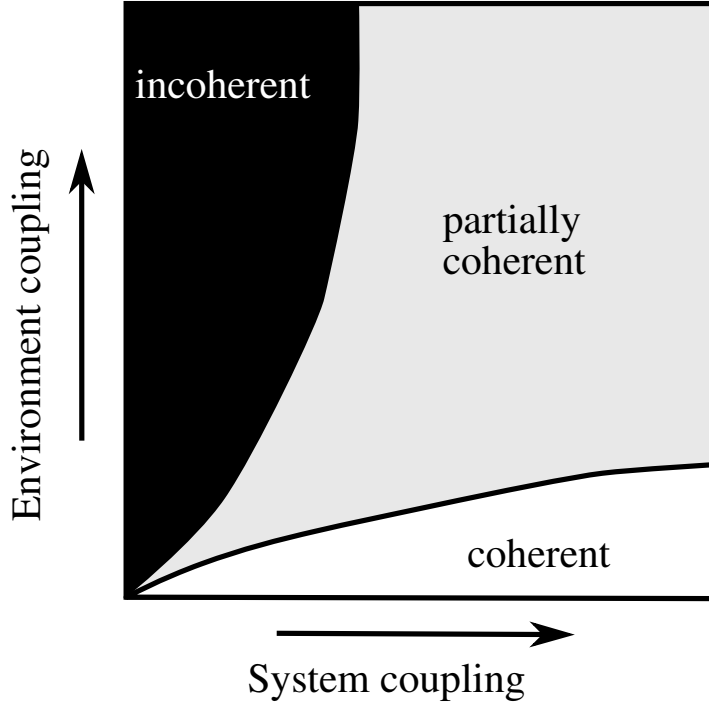


Figure 7.1: Dominant regimes of dynamics depending on the relative strength of the system Hamiltonian and the environmental coupling [47].

an exchange interaction. This coupling offers the unique opportunity of an analytic solution of our problem without *any* approximations regarding the strength of system-environment coupling (in most treatments of the effect of an environment on the evolution of a quantum system, the system-environment coupling is assumed to be weak) and allows us to include inhomogeneous interactions of the bath spins with the system. For such coupling, decoherence is possible for mixed (thermal) initial bath states [168, 169]. However if the system and bath are both initially cooled to their ground states, is there still a non-trivial effect of the environment on the fidelity? In this chapter we find that there are two important effects: the spin transfer functions (Eq. 1.19) are *slowed down* by a factor of two, and *destabilised* by a modulation of $|\cos Gt|$, where G is the mean square coupling to the environment. This has both positive and negative implications for the use of strongly coupled spin systems as quantum communication channels. The spin transfer functions also occur in the charge and energy transfer dynamics in molecular systems [47] and in continuous time random walks [170] to which our results equally apply.

7.2 Model

We choose to start with a specific spin system, i.e. an open spin chain of arbitrary length N , with a Hamiltonian given by

$$H_S = -\frac{1}{2} \sum_{\ell=1}^{N-1} J_{\ell} (X_{\ell} X_{\ell+1} + Y_{\ell} Y_{\ell+1}), \quad (7.4)$$

where J_{ℓ} are some arbitrary couplings and X_{ℓ} and Y_{ℓ} are the Pauli-X and Y matrices for the ℓ th spin. Toward the end of the section we will however show that our results hold for any system where the number of excitations is conserved during dynamical evolution. In addition to the chain Hamiltonian, each spin ℓ of the chain interacts with an independent bath of M_{ℓ} environmental spins (see Fig 7.2) via an inhomogeneous Hamiltonian,

$$H_I^{(\ell)} = -\frac{1}{2} \sum_{k=1}^{M_{\ell}} g_k^{(\ell)} (X_{\ell} X_k^{(\ell)} + Y_{\ell} Y_k^{(\ell)}). \quad (7.5)$$

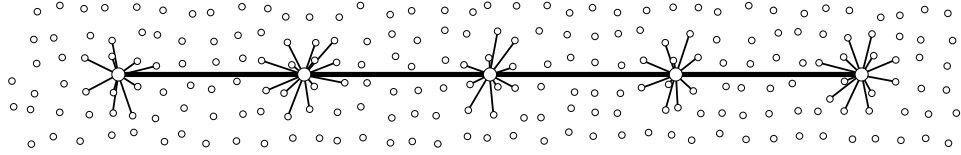


Figure 7.2: A spin chain of length $N = 5$ coupled to independent baths of spins.

In the above expression, the Pauli matrices X_{ℓ} and Y_{ℓ} act on the ℓ th spin of the chain, whereas $X_k^{(\ell)}$ and $Y_k^{(\ell)}$ act on the k th environmental spin attached to the ℓ th spin of the chain. We denote the total interaction Hamiltonian by

$$H_I \equiv \sum_{\ell=1}^N H_I^{(\ell)}. \quad (7.6)$$

The total Hamiltonian is given by $H = H_S + H_I$, where it is important to note that $[H_S, H_I] \neq 0$. We assume that a homogeneous magnetic field along the z-axis is applied. The ground state of the system is then given by the fully polarised state $|0,0\rangle$, with all chain and bath spins aligned along the z-axis. The above Hamiltonian describes an extremely complex and disordered system with a Hilbert space of dimension 2^{N+NM} . In the context of state transfer however, only the dynamics of the first excitation sector is relevant. We proceed by mapping this sector to a much simpler system [171–175].

For $\ell = 1, 2, \dots, N$ we define the states

$$|\ell, 0\rangle \equiv X_\ell |0, 0\rangle \quad (7.7)$$

and

$$|0, \ell\rangle \equiv \frac{1}{G_\ell} \sum_{k=1}^{M_\ell} g_k^{(\ell)} X_k^{(\ell)} |0, 0\rangle \quad (7.8)$$

with

$$G_\ell = \sqrt{\sum_{k=1}^{M_\ell} \left(g_k^{(\ell)}\right)^2}. \quad (7.9)$$

It is easily verified that (setting $J_0 = J_N = 0$)

$$\begin{aligned} H_S |\ell, 0\rangle &= -J_{\ell-1} |\ell-1, 0\rangle - J_\ell |\ell+1, 0\rangle \\ H_S |0, \ell\rangle &= 0, \end{aligned} \quad (7.10)$$

and

$$H_I |\ell, 0\rangle = -G_\ell |0, \ell\rangle \quad (7.11)$$

$$H_I |0, \ell\rangle = -G_\ell |\ell, 0\rangle. \quad (7.12)$$

Hence these states define a $2N$ -dimensional subspace that is invariant under the action of H . This subspace is equivalent to the first excitation sector of a system of $2N$ spin $1/2$ particles, coupled as it is shown in Fig 7.3.

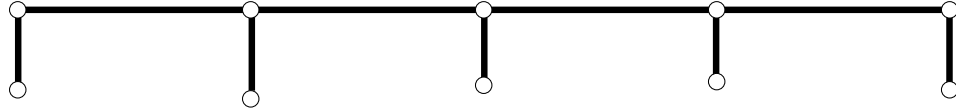


Figure 7.3: In the first excitation sector, the system can be mapped into an effective spin model where the bath spins are replaced by a single effective spin, as indicated here for $N = 5$.

Our main assumption is that the bath couplings are *in effect* the same, i.e. $G_\ell = G$ for all ℓ . Note however that the individual number of bath spins M_ℓ and bath couplings $g_k^{(\ell)}$ may still depend on ℓ and k as long as their means square average is the same. Also, our analytic solution given in the next paragraph relies on this assumption, but numerics show that our main result [Equation (7.28)] remains a good approximation if the G_ℓ slightly vary and we take $G \equiv \langle G_\ell \rangle$. Disorder in the vertical couplings is treated *exactly* in the sense that our results hold for any choice of couplings J_ℓ .

7.3 Results

In this paragraph, we solve the Schrödinger equation for the model outlined above and discuss the spin transfer functions. Firstly, let us denote the orthonormal eigenstates of H_S alone by

$$H_S|\psi_k\rangle = \epsilon_k|\psi_k\rangle \quad (k = 1, 2, \dots, N) \quad (7.13)$$

with

$$|\psi_k\rangle = \sum_{\ell=1}^N a_{k\ell}|\ell, 0\rangle. \quad (7.14)$$

For what follows, it is not important whether analytic expressions for the eigensystem of H_S can be found. Our result holds even for models that are not analytically solvable, such as the randomly coupled chains considered in Section 2.6. We now make an ansatz for the eigenstates of the full Hamiltonian, motivated by the fact that the states

$$|\phi_\ell^n\rangle \equiv \frac{1}{\sqrt{2}}(|\ell, 0\rangle + (-1)^n|0, \ell\rangle) \quad (n = 1, 2) \quad (7.15)$$

are eigenstates of $H_I^{(\ell)}$ with the corresponding eigenvalues $\pm G$ [this follows directly from Eqs. (7.11) and (7.12)]. Define the vectors

$$|\Psi_k^n\rangle \equiv \sum_{\ell=1}^N a_{k\ell}|\phi_\ell^n\rangle \quad (7.16)$$

with $k = 1, 2, \dots, N$ and $n = 0, 1$. The $|\Psi_k^n\rangle$ form an orthonormal basis in which we express the matrix elements of the Hamiltonian. We can easily see that

$$H_I|\Psi_k^n\rangle = -(-1)^n G|\Psi_k^n\rangle \quad (7.17)$$

and

$$H_S|\Psi_k^n\rangle = \frac{\epsilon_k}{\sqrt{2}} \sum_{\ell=1}^N a_{k\ell}|\ell, 0\rangle = \frac{\epsilon_k}{2} (|\Psi_k^0\rangle + |\Psi_k^1\rangle). \quad (7.18)$$

Therefore the matrix elements of the full Hamiltonian $H = H_S + H_I$ are given by

$$\langle\Psi_{k'}^{n'}|H|\Psi_k^n\rangle = \delta_{kk'} \left(-(-1)^n G\delta_{nn'} + \frac{\epsilon_k}{2} \right). \quad (7.19)$$

The Hamiltonian is not diagonal in the states of Eq. (7.16). But H is now block diagonal consisting of N blocks of size 2, which can be easily diagonalised analytically.

The orthonormal eigenstates of the Hamiltonian are given by

$$|E_k^n\rangle = c_{kn}^{-1} \{((-1)^n \Delta_k - 2G) |\Psi_k^0\rangle + \epsilon_k |\Psi_k^1\rangle\} \quad (7.20)$$

with the eigenvalues

$$E_k^n = \frac{1}{2} (\epsilon_k + (-1)^n \Delta_k) \quad (7.21)$$

and the normalisation

$$c_{kn} \equiv \sqrt{((-1)^n \Delta_k - 2G)^2 + \epsilon_k^2}, \quad (7.22)$$

where

$$\Delta_k = \sqrt{4G^2 + \epsilon_k^2}. \quad (7.23)$$

Note that the ansatz of Eq. (7.16) that put H in block diagonal form did not depend on the details of H_S and $H_I^{(\ell)}$. The methods presented here can be applied to a much larger class of systems, including the generalised spin star systems (which include an interaction within the bath) discussed in [175].

After solving the Schrödinger equation, let us now turn to quantum state transfer. The relevant quantity [1, 92] is given by the transfer function

$$\begin{aligned} f_{N,1}(t) &\equiv \langle N, 0 | \exp \{-iHt\} | 1, 0 \rangle \\ &= \sum_{k,n} \exp \{-iE_k^n t\} \langle E_k^n | 1, 0 \rangle \langle N, 0 | E_k^n \rangle. \end{aligned}$$

The modulus of $f_{N,1}(t)$ is between 0 (no transfer) and 1 (perfect transfer) and fully determines the fidelity of state transfer. Since

$$\begin{aligned} \langle \ell, 0 | E_k^n \rangle &= c_{kn}^{-1} \{((-1)^n \Delta_k - 2G) \langle \ell, 0 | \Psi_k^0 \rangle + \epsilon_k \langle \ell, 0 | \Psi_k^1 \rangle\} \\ &= \frac{c_{kn}^{-1}}{\sqrt{2}} ((-1)^n \Delta_k - 2G + \epsilon_k) a_{k\ell} \end{aligned}$$

we get

$$\begin{aligned} f_{N,1}(t) &= \\ &\frac{1}{2} \sum_{k,n} e^{\frac{-it}{2}(\epsilon_k + (-1)^n \Delta_k)} \frac{((-1)^n \Delta_k - 2G + \epsilon_k)^2}{((-1)^n \Delta_k - 2G)^2 + \epsilon_k^2} a_{k1} a_{kN}^*. \end{aligned} \quad (7.24)$$

Eq. (7.24) is the main result of this section, fully determining the transfer of quantum information and entanglement in the presence of the environments. In the limit $G \rightarrow 0$,

we have $\Delta_k \approx \epsilon_k$ and $f_{N,1}(t)$ approaches the usual result without an environment,

$$f_{N,1}^0(t) \equiv \sum_k \exp\{-it\epsilon_k\} a_{k1} a_{kN}^*. \quad (7.25)$$

In fact, a series expansion of Eq. (7.24) yields that the first modification of the transfer function is of the order of G^2 ,

$$G^2 \sum_k a_{k1} a_{kN}^* \left[\exp\{-it\epsilon_k\} \left(-\frac{1}{\epsilon_k^2} - \frac{it}{\epsilon_k} \right) + \frac{1}{\epsilon_k^2} \right]. \quad (7.26)$$

Hence the effect is small for very weakly coupled baths. However, as the chains get longer, the lowest lying energy ϵ_1 usually approaches zero, so the changes become more significant (scaling as $1/\epsilon_k$). For intermediate G , we evaluated Eq. (7.24) numerically and found that the first peak of the transfer function generally becomes slightly lower, and gets shifted to higher times (Figures 7.4 and 7.5). A numeric search in the coupling space $\{J_\ell, \ell = 1, \dots, N-1\}$ however also revealed some rare examples where an environment can also slightly improve the peak of the transfer function (Fig 7.6).

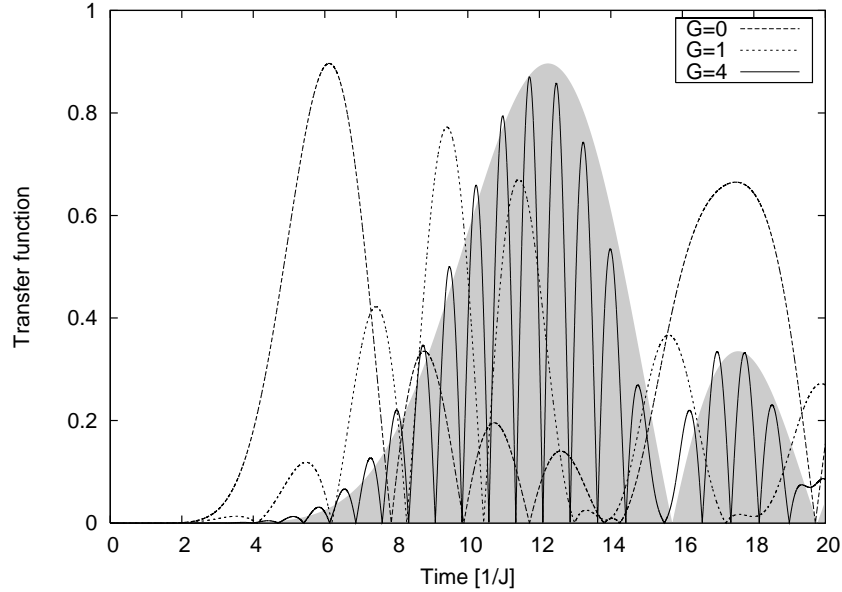


Figure 7.4: The absolute value of the transport function $f_{N,1}(t)$ of an uniform spin chain (i.e. $J_\ell = 1$) with length $N = 10$ for three different values of the bath coupling G . The filled grey curve is the envelope of the limiting function for $G \gg \epsilon_k/2$ given by $|f^0(\frac{t}{2})|$. We can see that Eq. (7.28) becomes a good approximation already at $G = 4$.

In the strong coupling regime $G \gg \epsilon_k/2$, we can approximate Eq. (7.23) by $\Delta_k \approx 2G$.

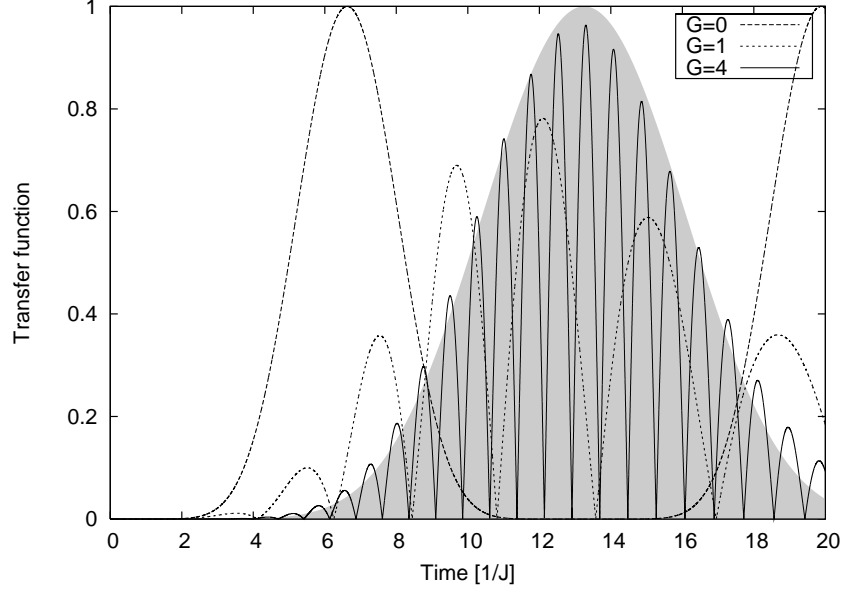


Figure 7.5: The same as Fig. 7.4, but now for an engineered spin chain [i.e. $J_\ell = \sqrt{\ell(N-\ell)}$] as in Subsection 1.5.1. For comparison, we have rescaled the couplings such that $\sum_\ell J_\ell$ is the same as in the uniform coupling case.

Inserting it in Eq. (7.24) then becomes

$$\begin{aligned}
 f_{N,1}(t) &\approx \frac{1}{2}e^{-iGt} \sum_k \exp\left\{-it\epsilon_k \frac{1}{2}\right\} a_{k1} a_{kN}^* + \\
 &\quad + \frac{1}{2}e^{iGt} \sum_k \exp\left\{-it\epsilon_k \frac{1}{2}\right\} a_{k1} a_{kN}^* \\
 &= \cos(Gt) f_{N,1}^0\left(\frac{t}{2}\right).
 \end{aligned} \tag{7.27}$$

This surprisingly simple result consists of the normal transfer function, slowed down by a factor of $1/2$, and modulated by a quickly oscillating term (Figures 7.4 and 7.5). We call this effect *destabilisation*. Our derivation actually did not depend on the indexes of $f(t)$ and we get for the transfer from the n th to the m th spin of the chain that

$$\boxed{f_{n,m}(t) \approx \cos(Gt) f_{n,m}^0\left(\frac{t}{2}\right).} \tag{7.28}$$

It may look surprising that the matrix $f_{n,m}$ is no longer unitary. This is because we are considering the dynamics of the chain only, which is an open quantum system [121]. A heuristic interpretation of Eq. (7.28) is that the excitation oscillates back and forth between the chain and the bath (hence the modulation), and spends half

of the time trapped in the bath (hence the slowing). If the time of the maximum of the transfer function $|f_{n,m}^0(t)|$ for $G = 0$ is a multiple of $\pi/2G$ then this maximum is also reached in the presence of the bath. We remark that this behaviour is strongly non-Markovian [121].

Finally, we want to stress that Eq. (7.28) is *universal* for any spin Hamiltonian that conserves the number of excitations, i.e. with $[H_S, \sum_\ell Z_\ell] = 0$. Thus our restriction to chain-like topology and exchange couplings for H_S is not necessary. In fact the only difference in the whole derivation of Eq. (7.28) for a more general Hamiltonian is that Eq. (7.10) is replaced by

$$H_S|\ell, 0\rangle = \sum_{\ell'} h_{\ell'} |\ell', 0\rangle. \quad (7.29)$$

The Hamiltonian can still be formally diagonalised in the first excitation sector as in Eq. (7.14), and the states of Eq. (7.20) will still diagonalise the total Hamiltonian $H_S + H_I$. Also, rather than considering an exchange Hamiltonian for the interaction with the bath, we could have considered a Heisenberg interaction [176], but only for the special case where all bath couplings $g_k^{(\ell)}$ are all the same [177]. Up to some irrelevant phases, this leads to the same results as for the exchange interaction.

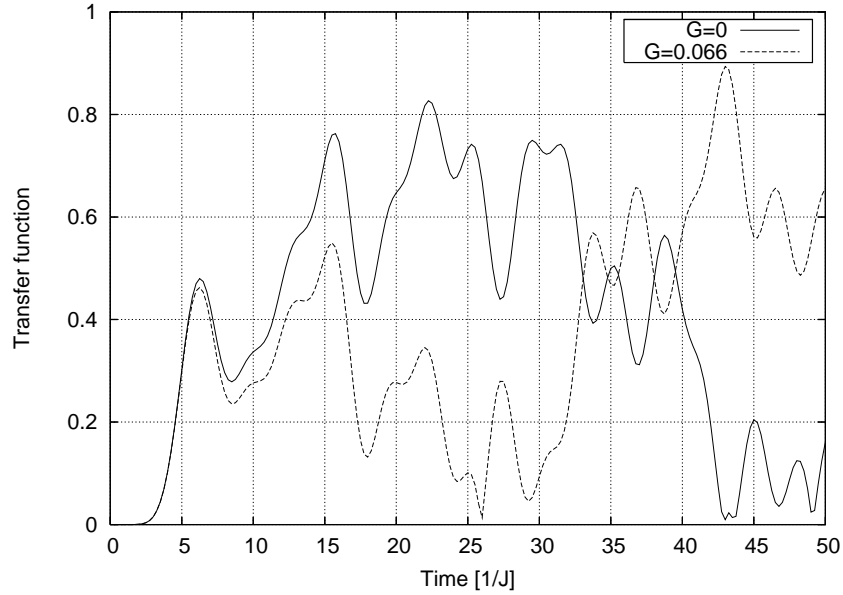


Figure 7.6: A weakly coupled bath may even improve the transfer function for some specific choices of the J_ℓ . This plot shows the transfer function $|f_{N,1}(t)|$ for $N = 10$. The couplings J_ℓ were found numerically.

7.4 Conclusion

We found a surprisingly simple and universal scaling law for the spin transfer functions in the presence of spin environments. In the context of quantum state transfer this result is double-edged: on one hand, it shows that even for very strongly coupled baths quantum state transfer is possible, with the same fidelity and only reasonable slowing. On the other hand, it also shows that the fidelity as a function of time becomes destabilised with a quickly oscillating modulation factor. In practice, this factor will restrict the time-scale in which one has to be able to read the state from the system. The results here are very specific to the simple bath model and do not hold in more general models (such as these discussed in [165, 167], where true decoherence and dissipation takes place). What we intended to demonstrate is that even though a bath coupling need not introduce decoherence or dissipation to the system, it can cause other dynamical processes that can be problematic for quantum information processing. Because the effects observed here cannot be avoided by cooling the bath, they may become relevant in some systems as a low temperature limit.

8 Conclusion and outlook

Our research on quantum state transfer with spin chains has taken us on a journey from a very practical motivation to quite fundamental issues and back again. On one hand, our results are quite abstract and fundamental, and have related state transfer to number theory, topology and quantum convergence. On the other hand, we have developed schemes which are simple and practical, taking into account experimental hurdles such as disorder and restricted control. While the multi rail scheme and the memory swapping scheme will probably become useful only after much further progress in experimental QIT, the dual rail scheme and in particular the valve scheme have some good chances to be realised in the near future.

State transfer with quantum chains has become an area of large interest, with more than seventy articles on the subject over the last three years. The most important goal now is an experiment that demonstrates coherent transfer on a short chain (say of length $N \geq 5$). Such an experiment is not only useful building a quantum computer, but also from a fundamental perspective. For instance, the violation of a Bell-inequality between distant entangled solid state qubits would be a milestone in the field. Since this requires a very high transfer fidelity, the design of such an experiment would probably require system dependent theoretical research on how to overcome specific types of noise and how to improve the fidelity for specific Hamiltonians.

List of Figures

1.1	In areas of universal control, quantum states can easily be transferred by sequences of unitary swap gates $S_{j,k}$ between nearest neighbours. . .	12
1.2	Schematic layout of a quantum computer. The solid arrows represent the flow of quantum information, and the dashed arrows the flow of classical information.	13
1.3	Permanently coupled quantum chains can transfer quantum states without control along the line. Note that the ends still need to be controllable to initialise and read out quantum states.	13
1.4	Small blocks (grey) of qubits (white circles) connected by quantum chains. Each block consists of (say) 13 qubits, 4 of which are connected to outgoing quantum chains (the thick black lines denote their nearest-neighbour couplings). The blocks are connected to the macroscopic world through classical wires (thin black lines with black circles at their ends) through which arbitrary unitary operations can be triggered on the block qubits. The quantum chains require no external control. . .	14
1.5	A quantum chain consisting of $N = 20$ flux qubits [34] (picture and experiment by Floor Paauw, TU Delft). The chain is connected to four larger SQUIDS for readout and gating.	15
1.6	Minimal fidelity $p(t)$ for a Heisenberg chain of length $N = 50$	21
1.7	Snapshots of the time evolution of a Heisenberg chain with $N = 50$. Shown is the distribution $ f_{n,1}(t) ^2$ of the wave-function in space at different times if initially localised at the first qubit.	22
1.8	Mean and variance of the state $ \mathbf{1}\rangle$ as a function of time. Shown is the case $N = 50$ with the y-axis giving the value <i>relative</i> to the mean $N/2 + 1$ and variance $(N^2 - 1)/12$ of an equal distribution $\frac{1}{\sqrt{N}} \sum \mathbf{n}\rangle$	22
1.9	Approximation of the transfer amplitude for $N = 50$ around the first maximum by Bessel and Airy functions [1,61].	23

1.10	$p_M(T)$ as a function of T for different chain lengths. The solid curve is given by $1.82(2T)^{-2/3}$ and corresponds to the first peak of the probability amplitude (Eq. 1.29)	24
1.11	Quantum capacity, entanglement of formation (EOF), a lower bound for the entanglement of distillation (EOD) and the averaged fidelity as a function of $p(t)$. We also show the corresponding chain length which reaches this value as a first peak and the classical threshold $3 - 2\sqrt{2}$. The explicit expression for the quantum capacity plotted here is given in [54], and the lower bound of the entanglement of distillation will be derived in Section 3.4.	28
1.12	Snapshots of the time evolution of a quantum chain with engineered couplings (1.47) for $N = 50$. Shown is the distribution of the wave-function in space at different times if initially localised at the first qubit (compare Fig. 1.7).	30
2.1	Two quantum chains interconnecting A and B . Control of the systems is only possible at the two qubits of either end.	36
2.2	Quantum circuit representation of conclusive and arbitrarily perfect state transfer. The first gate at Alice's qubits represents a NOT gate applied to the second qubit controlled by the first qubit being zero. The qubit $ \psi_A\rangle_1$ on the left hand side represents an arbitrary input state at Alice's site, and the qubit $ \psi_B\rangle_1$ represents the same state, successfully transferred to Bob's site. The t_ℓ -gate represents the unitary evolution of the spin chains for a time interval of t_ℓ	37
2.3	Semilogarithmic plot of the joint probability of failure $P(\ell)$ as a function of the number of measurements ℓ . Shown are Heisenberg spin-1/2-chains with different lengths N . The times between measurements t_ℓ have been optimised numerically.	39
2.4	Time t needed to transfer a state with a given joint probability of failure P across a chain of length N . The points denote exact numerical data, and the fit is given by Eq. (2.15).	41
2.5	The minimal joint probability of failure $P(\ell)$ for chains with length N in the presence of amplitude damping. The parameter J/Γ of the curves is the coupling of the chain (in Kelvin) divided by the decay rate (ns^{-1}).	44
2.6	Two <i>disordered</i> quantum chains interconnecting A and B . Control of the systems is only possible at the two qubits of either end.	46

2.7	The absolute values of the transition amplitudes $f_{N,1}(t)$ and $g_{N,1}(t)$ for two Heisenberg chains of length $N = 10$. The couplings strengths of both chains were chosen randomly from the interval $[0.8J, 1.2J]$. The circles show times where Bob can perform measurements without gaining information on α and β	47
2.8	The relevant properties for conclusive transfer can be determined by measuring the response of the two systems at their ends only.	51
2.9	Time t needed to transfer a state with a given joint probability of failure P across a chain of length N with uncorrelated fluctuations of $\Delta = 0.05$. The points denote numerical data averaged over 100 realisations, and the fit is given by Eq. (2.53). This figure should be compared with Fig. 2.4 where $\Delta = 0$	54
2.10	Most general setting for conclusive transfer: A <i>black box</i> with two inputs and two outputs, acting as an amplitude damping channel defined by Eqs. (2.54) and (2.55)	55
2.11	A simple counterexample for a vertically symmetric system where dual rail encoding is not possible. The black lines represent exchange couplings. 56	
2.12	An example for a vertically symmetric system where dual rail encoding is possible. The black lines represent exchange couplings <i>of equal strength</i> . 57	
3.1	Schematic of the system: Alice and Bob operate M chains, each containing N spins. The spins belonging to the same chain interact through the Hamiltonian H which accounts for the transmission of the signal in the system. Spins of different chains do not interact. Alice encodes the information in the first spins of the chains by applying unitary transformations to her qubits. Bob recovers the message in the last spins of the chains by performing joint measurements.	59
3.2	Example of our notation for $M = 5$ chains of length $N = 6$ with $K = 2$ excitations. The state above, given by $ \mathbf{0}\rangle_1 \otimes \mathbf{3}\rangle_2 \otimes \mathbf{0}\rangle_3 \otimes \mathbf{1}\rangle_4 \otimes \mathbf{0}\rangle_5$, has excitations in the chains $m_1 = 2$ and $m_2 = 4$ at the horizontal position $n_1 = 3$ and $n_2 = 1$. It is in the Hilbert space $\mathcal{H}(S_6)$ corresponding to the subset $S_6 = \{2, 4\}$ (assuming that the sets S_ℓ are ordered in a canonical way, i.e. $S_1 = \{1, 2\}$, $S_2 = \{1, 3\}$ and so on) and will be written as $ (3, 1); 6\rangle$. There are $\binom{5}{2} = 10$ different sets S_ℓ and the number of qubits one can transfer using these states is $\log_2 10 \approx 3$. The efficiency is thus given by $R \approx 3/5$ which is already bigger than in the dual rail scheme.	61

3.3	Optimal rates (maximisation of Eq. (3.45 with respect to M) for the Multi Rail protocol. Shown are three curves corresponding to different values of the joint probability of failure P one plans to achieve.	71
4.1	Schematic examples of the orbits of a ergodic and a mixing map.	72
4.2	Relations between topological spaces [149]. The space of density matrices on which quantum channels are defined, is a compact and convex subset of a normed vectors space (the space of linear operators of the system) which, in the above graphical representation fits within the set of compact metric spaces.	76
4.3	Relations between the different properties of a quantum channel.	85
5.1	The system $C\bar{C}$ can only be controlled by acting on a (small) subsystem C . However system C is coupled to system \bar{C} by a unitary operator $U = \exp \{-iHt\}$. This coupling can - in some cases - <i>mediate</i> the local control on C to the full system $C\bar{C}$. In our case, system C is controlled by performing regular swap operations S_ℓ between it and a quantum memory M_ℓ	96
5.2	Alice and Bob control the spins N_A and N_B interconnected by the spins N_R . At time jt Bob performs a swap S_j between his spins and the memory M_j	101
6.1	A quantum chain (qubits $1, 2, \dots, N$) and a target qubit $(N + 1)$. By applying a sequence of two-qubit unitary gates V_k on the last qubit of the chain and the target qubit, arbitrarily high fidelity can be achieved.	105
6.2	Numerical example for the convergence of the success probability. Simulated is a quantum chain of length $N = 20$ with the Hamiltonian from Eq. (6.16) (dashed line) and Eq. (6.17) with $B/J = 20$ (solid line). Using the original protocol [1], the same chain would only reach a success probability of 0.63 in the above time interval.	108
7.1	Dominant regimes of dynamics depending on the relative strength of the system Hamiltonian and the environmental coupling [47].	111
7.2	A spin chain of length $N = 5$ coupled to independent baths of spins.	112
7.3	In the first excitation sector, the system can be mapped into an effective spin model where the bath spins are replaced by a single effective spin, as indicated here for $N = 5$	113

7.4	The absolute value of the transport function $f_{N,1}(t)$ of an uniform spin chain (i.e. $J_\ell = 1$) with length $N = 10$ for three different values of the bath coupling G . The filled grey curve is the envelope of the limiting function for $G \gg \epsilon_k/2$ given by $ f^0(\frac{t}{2}) $. We can see that Eq. (7.28) becomes a good approximation already at $G = 4$	116
7.5	The same as Fig. 7.4, but now for an engineered spin chain [i.e. $J_\ell = \sqrt{\ell(N - \ell)}$] as in Subsection 1.5.1. For comparison, we have rescaled the couplings such that $\sum_\ell J_\ell$ is the same as in the uniform coupling case.	117
7.6	A weakly coupled bath may even improve the transfer function for some specific choices of the J_ℓ . This plot shows the transfer function $ f_{N,1}(t) $ for $N = 10$. The couplings J_ℓ were found numerically.	118

List of Tables

2.1	The total time t and the number of measurements M needed to achieve a probability of success of 99% for different fluctuation strengths Δ (uncorrelated case). Given is the statistical mean and the standard deviation. The length of the chain is $N = 20$ and the number of random samples is 10. For strong fluctuations $\Delta = 0.1$, we also found particular samples where the success probability could not be achieved within the time range searched by the algorithm.	52
2.2	The total time t and the number of measurements M needed to achieve a probability of success of 99% for different correlations c between the couplings [see Eq. (2.50) and Eq. (2.51)]. Given is the statistical mean and the standard deviation for a fluctuation strength of $\Delta = 0.05$. The length of the chain is $N = 20$ and the number of random samples is 20.	53

Bibliography

- [1] S. Bose, *Quantum Communication through an Unmodulated Spin Chain*, Phys. Rev. Lett. **91**, 207901 (2003).
- [2] M. A. Nielsen and I. L. Chuang, *Quantum Computation and Quantum Information*, Cambridge University Press, Cambridge (2000).
- [3] P. W. Shor, *Polynomial-Time Algorithms for Prime Factorization and Discrete Logarithms on a Quantum Computer*, J. Sci. Statist. Comput. **26**, 1484 (1997).
- [4] D. P. DiVincenzo, *The Physical Implementation of Quantum Computation*, Fortsch.Phys. **48**, 9 (2000).
- [5] R. F. Werner, *Quantum Information Theory - an Invitation*, Springer Tracts Mod.Phys. **173**, 14, quant-ph/0101061 (2001).
- [6] R. Cleve and J. Watrous, *Fast parallel circuits for the quantum Fourier transform*, Annual Symposium on Foundations of Computer Science **41**, 526 (2000).
- [7] R. Jozsa, *On the simulation of quantum circuits*, quant-ph/0603163 (2006).
- [8] N. Yoranand and A. J. Short, *Classical simulation of limited-width cluster-state quantum computation*, quant-ph/0601178 (2006).
- [9] H. Häffner, W. Hänsel, C. F. Roos, J. Benhelm, D. Chekalkar, M. Chwalla, T. Körber, U. D. Rapol, M. Riebe, P. O. Schmidt, C. Becher, O. Gühne, W. Dür, and R. Blatt, *Scalable multiparticle entanglement of trapped ions*, Nature **438**, 643 (2005).
- [10] A. J. Skinner, M. E. Davenport, and B. E. Kane, *Hydrogenic Spin Quantum Computing in Silicon: A Digital Approach*, Phys. Rev. Lett. **90**, 087901 (2003).
- [11] D. Kielpinski, C. Monroe, and D. Wineland, *Architecture for a Large-Scale Ion-Trap Quantum Computer*, Nature **417**, 709 (2002).
- [12] S. Lloyd, *Power of Entanglement in Quantum Communication*, Phys. Rev. Lett. **90**, 167902 (2003).

- [13] F. H. L. Koppens, J. A. Folk, J. M. Elzerman, R. Hanson, L. H. W. van Beveren, I. T. Vink, H. P. Tranitz, W. Wegscheider, L. P. Kouwenhoven, and L. M. K. Vandersypen, *Control and Detection of Singlet-Triplet Mixing in a Random Nuclear Field*, Science **309**, 1346 (2005).
- [14] R. Hanson, L. H. W. van Beveren, I. T. Vink, J. M. Elzerman, W. J. M. Naber, F. H. L. Koppens, L. P. Kouwenhoven, and L. M. K. Vandersypen, *Single-Shot Readout of Electron Spin States in a Quantum Dot Using Spin-Dependent Tunnel Rates*, Phys. Rev. Lett. **94**, 196802 (2005).
- [15] T. Yamamoto, Y. A. Pashkin, O. Astafiev, Y. Nakamura, and J. S. Tsai, *Demonstration of conditional gate operation using superconducting charge qubits*, Nature **425**, 941 (2003).
- [16] I. Chiorescu, P. Bertet, K. Semba, Y. Nakamura, C. J. P. M. Harmans, and J. E. Mooij, *Coherent dynamics of a flux qubit coupled to a harmonic oscillator*, Nature **431**, 159 (2004).
- [17] V. Subrahmanyam and A. Lakshminarayan, *Transport of entanglement through a Heisenberg XY spin chain*, Phys. Lett. A **349**, 164 (2006).
- [18] V. Subrahmanyam, *Entanglement dynamics and quantum-state transport in spin chains*, Phys. Rev. A **69**, 034304 (2004).
- [19] M. B. Plenio, J. Hartley, and J. Eisert, *Dynamics and manipulation of entanglement in coupled harmonic systems with many degrees of freedom*, New. J. Phys. **6**, 36 (2004).
- [20] L. Amico, A. Osterloh, F. Plastina, R. Fazio, and G. M. Palma, *Dynamics of entanglement in one-dimensional spin systems*, Phys. Rev. A **69**, 022304 (2004).
- [21] M. J. Hartmann, M. E. Reuter, and M. B. Plenio, *Excitation and Entanglement Transfer Near Quantum Critical Points*, quant-ph/0608051 (2006).
- [22] M. J. Hartmann, M. E. Reuter, and M. B. Plenio, *Excitation and entanglement transfer versus spectral gap*, New. J. Phys. **8**, 94 (2006).
- [23] F. Verstraete, M. Popp, and J. I. Cirac, *Entanglement versus Correlations in Spin Systems*, Phys. Rev. Lett. **92**, 027901 (2004).
- [24] F. Verstraete, M. A. Martin-Delgado, and J. I. Cirac, *Diverging Entanglement Length in Gapped Quantum Spin Systems*, Phys. Rev. Lett. **92**, 087201 (2004).

- [25] T. Boness, S. Bose, and T. S. Monteiro, *Entanglement and Dynamics of Spin Chains in Periodically Pulsed Magnetic Fields: Accelerator Modes*, Phys. Rev. Lett. **96**, 187201 (2006).
- [26] J. Fitzsimons and J. Twamley, *Superballistic diffusion of entanglement in disordered spin chains*, Phys. Rev. A **72**, 050301 (2005).
- [27] L. F. Santos, G. Rigolin, and C. O. Escobar, *Entanglement versus chaos in disordered spin chains*, Phys. Rev. A **69**, 042304 (2004).
- [28] T. Boness, M. Stocklin, and T. Monteiro, *Quantum chaos with spin-chains in pulsed magnetic fields*, quant-ph/0612074 (2006).
- [29] J. P. Keating, N. Linden, J. C. F. Matthews, and A. Winter, *Localization and its consequences for quantum walk algorithms and quantum communication*, quant-ph/0606205 (2006).
- [30] T. J. G. Apollaro and F. Plastina, *Entanglement localization by a single defect in a spin chain*, Phys. Rev. A **74**, 062316 (2006).
- [31] A. Romito, R. Fazio, and C. Bruder, *Solid-state quantum communication with Josephson arrays*, Phys. Rev. B **71**, 100501(R) (2005).
- [32] D. Tsomokos, M. Hartmann, S. Huelga, and M. B. Plenio, *Dynamics of entanglement in realistic chains of superconducting qubits*, quant-ph/0611077 (2006).
- [33] A. Lyakhov and C. Bruder, *Use of dynamical coupling for improved quantum state transfer*, Phys. Rev. B **74**, 235303 (2006).
- [34] A. Lyakhov and C. Bruder, *Quantum state transfer in arrays of flux qubits*, New. J. Phys. **7**, 181 (2005).
- [35] D. Loss and D. P. DiVincenzo, *Quantum computation with quantum dots*, Phys. Rev. A **57**, 120 (1998).
- [36] A. D. Greentree, J. H. Cole, A. R. Hamilton, and L. C. L. Hollenberg, *Coherent electronic transfer in quantum dot systems using adiabatic passage*, Phys. Rev. B **70**, 235317 (2004).
- [37] I. D'Amico, *Quantum buses and quantum computer architecture based on quantum dots*, cond-mat/0511470 (2005).

-
- [38] T. P. Spiller, I. D'Amico, and B. W. Lovett, *Entanglement distribution for a practical quantum-dot-based quantum processor architecture*, quant-ph/0601124 (2006).
 - [39] J. Zhang, X. Peng, and D. Suter, *Speedup of quantum-state transfer by three-qubit interactions: Implementation by nuclear magnetic resonance*, Phys. Rev. A **73**, 062325 (2006).
 - [40] J. Fitzsimons, L. Xiao, S. C. Benjamin, and J. A. Jones, *Quantum Information Processing with Delocalized Qubits under Global Control*, quant-ph/0606188 (2006).
 - [41] J. Zhang, G. L. Long, W. Zhang, Z. Deng, W. Liu, , and Z. Lu, *Simulation of Heisenberg XY interactions and realization of a perfect state transfer in spin chains using liquid nuclear magnetic resonance*, Phys. Rev. A **72**, 012331 (2005).
 - [42] J. J. Garcia-Ripoll and J. I. Cirac, *Spin dynamics for bosons in an optical lattice*, New. J. Phys. **5**, 76 (2003).
 - [43] M. Paternostro, G. M. Palma, M. S. Kim, and G. Falci, *Quantum-state transfer in imperfect artificial spin networks*, Phys. Rev. A **71**, 042311 (2005).
 - [44] M. Paternostro, *Theoretical proposals on efficient schemes for quantum information processing*, Ph.D. thesis, The Queen's University of Belfast (2005).
 - [45] D. G. Angelakis, M. F. Santos, and S. Bose, *Photon blockade induced Mott transitions and XY spin models in coupled cavity arrays*, quant-ph/0606159 (2006).
 - [46] M. J. Hartmann, F. G. S. L. Brandao, and M. B. Plenio, *Strongly Interacting Polaritons in Coupled Arrays of Cavities*, Nature Physics **2**, 849 (2006).
 - [47] V. May and O. Kühn, *Charge and Energy Transfer Dynamics in Molecular Systems*, Wiley-Interscience, Hoboken (2004).
 - [48] N. Motoyama, H. Eisaki, and S. Uchida, *Magnetic Susceptibility of Ideal Spin 1/2 Heisenberg Antiferromagnetic Chain Systems, Sr₂CuO₃ and SrCuO₂*, Phys. Rev. Lett. **76**, 3212 (1996).
 - [49] P. Gambardella, A. Dallmeyer, K. Maiti, M. C. Malagoli, W. Eberhardt, K. Kern, and C. Carbone, *Ferromagnetism in one-dimensional monatomic metal chains*, Nature **416**, 301 (2002).

- [50] A. Uhlmann, *The 'transition probability' on the state space of a \ast -algebra*, Rep. Math. Phys. **9**, 273 (1976).
- [51] R. Jozsa, *Fidelity for mixed quantum states*, J. Mod. Opt. **41**, 2315 (1994).
- [52] D. Kretschmann and R. F. Werner, *Quantum channels with memory*, Phys. Rev. A **72**, 062323 (2005).
- [53] A. Kay, *Unifying Quantum State Transfer and State Amplification*, Phys. Rev. Lett. **98**, 010501 (2007).
- [54] V. Giovannetti and R. Fazio, *Information-capacity description of spin-chain correlations*, Phys. Rev. A **71**, 032314 (2005).
- [55] J. H. Eberly, B. W. Shore, Z. Bialynicka-Birula, and I. Bialynicki-Birula, *Coherent dynamics of N -level atoms and molecules. I. Numerical experiments**, Phys. Rev. A **16**, 2038 (1977).
- [56] Z. Bialynicka-Birula, I. Bialynicki-Birula, J. H. Eberly, and B. W. Shore, *Coherent dynamics of N -level atoms and molecules. II. Analytic solutions**, Phys. Rev. A **16**, 2048 (1977).
- [57] R. Cook and B. W. Shore, *Coherent dynamics of N -level atoms and molecules. III. An analytically soluble periodic case*, Phys. Rev. A **20**, 539 (1979).
- [58] B. W. Shore and R. J. Cook, *Coherent dynamics of N -level atoms and molecules. IV. Two- and three-level behavior*, Phys. Rev. A **20**, 1958 (1979).
- [59] C. Albanese, M. Christandl, N. Datta, and A. Ekert, *Mirror Inversion of Quantum States in Linear Registers*, Phys. Rev. Lett. **93**, 230502 (2004).
- [60] T. J. Osborne and N. Linden, *Propagation of quantum information through a spin system*, Phys. Rev. A **69**, 052315 (2004).
- [61] M. Abramowitz and I. A. Stegun, *Handbook of Mathematical Functions*, Dover, New York (1972).
- [62] S. Lang, *Algebra*, Addison-Wesley, Boston (1984).
- [63] P. C. Hemmer, L. C. Maximon, and H. Wergeland, *Recurrence Time of a Dynamical System*, Phys. Rev. **111**, 689 (1958).

- [64] M.-H. Yung and S. Bose, *Perfect state transfer, effective gates, and entanglement generation in engineered bosonic and fermionic networks*, Phys. Rev. A **71**, 032310 (2005).
- [65] M. Christandl, N. Datta, T. C. Dorlas, A. Ekert, A. Kay, and A. J. Landahl, *Perfect transfer of arbitrary states in quantum spin networks*, Phys. Rev. A **71**, 032312 (2005).
- [66] S. Bravyi, M. B. Hastings, and F. Verstraete, *Lieb-Robinson bounds and the generation of correlations and topological quantum order*, Phys. Rev. Lett. **97**, 050401 (2006).
- [67] B. Nachtergaele and R. Sims, *Lieb-Robinson Bounds and the Exponential Clustering Theorem*, Commun. Math. Phys. **265**, 119 (2006).
- [68] M. Horodecki, P. Horodecki, and R. Horodecki, *Inseparable Two Spin- $1/2$ Density Matrices Can Be Distilled to a Singlet Form*, Phys. Rev. Lett. **78**, 574 (1997).
- [69] M. Horodecki, P. Horodecki, and . . . R. Horodecki, Phys. Rev. A **60**, *General teleportation channel, singlet fraction, and quasidistillation*, Phys. Rev. A **60**, 1888 (1999).
- [70] C. H. Bennett and P. W. Shor, *Quantum information theory*, IEEE Trans. Inf. Theory **44**, 2724 (1998).
- [71] M. Christandl, N. Datta, A. Ekert, and A. J. Landahl, *Perfect State Transfer in Quantum Spin Networks*, Phys. Rev. Lett. **92**, 187902 (2004).
- [72] G. M. Nikolopoulos, D. Petrosyan, and P. Lambropoulos, *Coherent electron wavepacket propagation and entanglement in array of coupled quantum dots*, Europhys. Lett. **65**, 297 (2004).
- [73] A. Peres, *Reversible logic and quantum computers*, Phys. Rev. A **32**, 3266 (1985).
- [74] M.-H. Yung, *Quantum speed limit for perfect state transfer in one dimension*, Phys. Rev. A **74**, 030303(R) (2006).
- [75] S. Yang, Z. Song, and C. P. Sun, *Quantum state swapping via a qubit network with Hubbard interactions*, Phys. Rev. B **73**, 195122 (2006).
- [76] Z. Song and C. P. Sun, *Quantum information storage and state transfer based on spin systems*, Low Temp.Phys. **31**, 907 (2005).

- [77] T. Shi, Y. Li, Z. Song, and C. P. Sun, *Quantum-state transfer via the ferromagnetic chain in a spatially modulated field*, Phys. Rev. A **71**, 032309 (2005).
- [78] D. Petrosyan and P. Lambropoulos, *Coherent population transfer in a chain of tunnel coupled quantum dots*, Opt.Commun. **264**, 419 (2006).
- [79] G. M. Nikolopoulos, D. Petrosyan, and P. Lambropoulos, *Electron wavepacket propagation in a chain of coupled quantum dots*, J. Phys. C: Condens. Matter **16**, 4991 (2004).
- [80] A. Kay and M. Ericsson, *Geometric effects and computation in spin networks*, New. J. Phys. **7**, 143 (2005).
- [81] A. Kay, *Perfect state transfer: Beyond nearest-neighbor couplings*, Phys. Rev. A **73**, 032306 (2006).
- [82] A. Kay, *Quantum Computation with Minimal Control*, Ph.D. thesis, University of Cambridge, <http://cam.qubit.org/users/Alastair/thesis.pdf> (2006).
- [83] P. Karbach and J. Stolze, *Spin chains as perfect quantum state mirrors*, Phys. Rev. A **72**, 030301(R) (2005).
- [84] L. Dan and Z. Jing-Fu, *Effect of disturbance in perfect state transfer*, Chin.Phys. **15**, 272 (2006).
- [85] M. B. Plenio and F. L. Semião, *High efficiency transfer of quantum information and multiparticle entanglement generation in translation-invariant quantum chains*, New. J. Phys. **7**, 73 (2005).
- [86] A. Wójcik, T. Łuczak, P. Kurzyński, A. Grudka, T. Gdala, and M. Bednarska, *Multiuser quantum communication networks*, quant-ph/0608107 (2006).
- [87] A. Wójcik, T. Łuczak, P. Kurzyński, A. Grudka, T. Gdala, and M. Bednarska, *Unmodulated spin chains as universal quantum wires*, Phys. Rev. A **72**, 034303 (2005).
- [88] Y. Li, T. Shi, B. Chen, Z. Song, and C. P. Sun, *Quantum-state transmission via a spin ladder as a robust data bus*, Phys. Rev. A **71**, 022301 (2005).
- [89] M. Avellino, A. J. Fisher, and S. Bose, *Quantum communication in spin systems with long-range interactions*, Phys. Rev. A **74**, 012321 (2006).

- [90] M. Avellino, A. J. Fisher, and S. Bose, *Erratum: Quantum communication in spin systems with long-range interactions [Phys. Rev. A 74, 012321 (2006)]*, Phys. Rev. A **74**, 039901 (2006).
- [91] S. Paganelli, F. de Pasquale, and G. L. Giorgi, *Faithful state transfer through a quantum channel*, Phys. Rev. A **74**, 012316 (2006).
- [92] H. L. Haselgrove, *Optimal state encoding for quantum walks and quantum communication over spin systems*, Phys. Rev. A **72**, 062326 (2005).
- [93] J. Fitzsimons and J. Twamley, *Globally Controlled Quantum Wires for Perfect Qubit Transport, Mirroring, and Computing*, Phys. Rev. Lett. **97**, 090502 (2006).
- [94] R. Raussendorf, *Quantum computation via translation-invariant operations on a chain of qubits*, Phys. Rev. A **72**, 052301 (2005).
- [95] S. Yang, Z. Song, and C. P. Sun, *Wave-packet transmission of Bloch electrons manipulated by magnetic field*, Phys. Rev. A **73**, 022317 (2006).
- [96] K. Maruyama, T. Iitaka, and F. Nori, *Enhancement of entanglement transfer in a spin chain by phase shift control*, quant-ph/0610103 (2006).
- [97] S. Bose, B. Jin, and V. E. Korepin, *Quantum communication through a spin ring with twisted boundary conditions*, Phys. Rev. A **72**, 022345 (2005).
- [98] S. Yang, Z. Song, and C. Sun, *Quantum dynamics of magnetically controlled network for Bloch electrons*, quant-ph/0602209 (2006).
- [99] G. D. Chiara, D. Rossini, S. Montangero, and R. Fazio, *From perfect to fractal transmission in spin chains*, Phys. Rev. A **72**, 012323 (2005).
- [100] D. Rossini, V. Giovannetti, and R. Fazio, *Information transfer rates in spin quantum channels*, quant-ph/0609022 (2006).
- [101] D. Burgarth and S. Bose, *Universal destabilization and slowing of spin-transfer functions by a bath of spins*, Phys. Rev. A **73**, 062321 (2006).
- [102] D. Burgarth and S. Bose, *Conclusive and arbitrarily perfect quantum-state transfer using parallel spin-chain channels*, Phys. Rev. A **71**, 052315 (2005).
- [103] D. Burgarth and S. Bose, *Perfect quantum state transfer with randomly coupled quantum chains*, New. J. Phys. **7**, 135 (2005).

- [104] D. Burgarth, S. Bose, and V. Giovannetti, *Efficient and perfect state transfer in quantum chains*, Int. J. Quant. Inf. **4**, 405 (2006).
- [105] D. Burgarth and V. Giovannetti, *The Generalized Lyapunov Theorem and its Application to Quantum Channels*, quant-ph/0605197 (2006).
- [106] D. Burgarth, V. Giovannetti, and S. Bose, *State Transfer in Permanently Coupled Quantum Chains*, NATO Sci. Ser. III **199**, 218 (2006).
- [107] D. Burgarth, V. Giovannetti, and S. Bose, *Optimal quantum chain communication by end gates*, quant-ph/0610018 (2006).
- [108] D. Burgarth, V. Giovannetti, and S. Bose, *Efficient and perfect state transfer in quantum chains*, J. Phys. A: Math. Gen. **38**, 6793 (2005).
- [109] V. Giovannetti and D. Burgarth, *Improved Transfer of Quantum Information Using a Local Memory*, Phys. Rev. Lett. **96**, 030501 (2006).
- [110] B. Vaucher, D. Burgarth, and S. Bose, *Arbitrarily perfect quantum communication using unmodulated spin chains, a collaborative approach*, J. Opt. B: Quantum Semiclass. Opt. **7**, S356 (2005).
- [111] R. Raussendorf and H. J. Briegel, *A One-Way Quantum Computer*, Phys. Rev. Lett. **86**, 5188 (2001).
- [112] I. L. Chuang and Y. Yamamoto, *Quantum Bit Regeneration*, Phys. Rev. Lett. **76**, 4281 (1996).
- [113] C. H. Bennett, D. P. DiVincenzo, and J. A. Smolin, *Capacities of Quantum Erasure Channels*, Phys. Rev. Lett. **78**, 3217 (1997).
- [114] J. He, Q. Chen, L. Ding, and S. Wan, *Conclusive quantum-state transfer with a single randomly coupled spin chain*, quant-ph/0606088 (2006).
- [115] D. Vion, A. Aassime, A. Cottet, P. Joyez, H. Pothier, C. Urbina, D. Esteve, and M. H. Devoret, *Manipulating the Quantum State of an Electrical Circuit*, Science **296**, 886 (2002).
- [116] I. Chiorescu, Y. Nakamura, C. J. P. M. Harmans, and J. E. Mooij, *Coherent Quantum Dynamics of a Superconducting Flux Qubit*, Science **299**, 1869 (2003).
- [117] G. M. Palma, K. A. Suominen, and A. K. Ekert, *Quantum Computers and Dissipation*, Proc. Roy. Soc. Lond. A **452**, 567 (1996).

- [118] W. Y. Hwang, H. Lee, D. D. Ahn, and S. W. Hwang, *Efficient schemes for reducing imperfect collective decoherences*, Phys. Rev. A **62**, 062305 (2000).
- [119] A. Beige, D. Braun, and P. Knight, *Driving atoms into decoherence-free states*, New. J. Phys. **2**, 22 (2000).
- [120] M. Plenio and P. Knight, *The quantum-jump approach to dissipative dynamics in quantum optics*, Rev. Mod. Phys. **70**, 101 (1998).
- [121] H.-P. Breuer and F. Petruccione, *The Theory Of Open Quantum Systems*, Oxford University Press, Oxford (2002).
- [122] P. W. Anderson, *Absence of Diffusion in Certain Random Lattices*, Phys. Rev. **109**, 1492 (1958).
- [123] B. Sutherland, *Model for a multicomponent quantum system*, Phys. Rev. B **12**, 3795 (1975).
- [124] C. Hadley, A. Serafini, and S. Bose, *Entanglement creation and distribution on a graph of exchange-coupled qutrits*, Phys. Rev. A **72**, 052333 (2005).
- [125] A. Bayat and V. Karimipour, *Transfer of d-Level quantum states through spin chains by random swapping*, quant-ph/0612144 (2006).
- [126] N. Gisin, N. Linden, S. Massar, and S. Popescu, *Error filtration and entanglement purification for quantum communication*, Phys. Rev. A **72**, 012338 (2005).
- [127] B. Vaucher, *Quantum Communication of Spin-Qubits using a Collaborative Approach*, Master's thesis, Ecole Polytechnique Federale de Lausanne (2005).
- [128] J. R. Schott, *Matrix Analysis for Statistics*, Wiley-Interscience, Hoboken (1996).
- [129] L. Viola and S. Lloyd, *Dynamical suppression of decoherence in two-state quantum systems*, Phys. Rev. A **58**, 2733 (1998).
- [130] L. Viola, E. Knill, and S. Lloyd, *Dynamical Decoupling of Open Quantum Systems*, Phys. Rev. Lett. **82**, 2417 (1999).
- [131] L. Viola, S. Lloyd, and E. Knill, *Universal Control of Decoupled Quantum Systems*, Phys. Rev. Lett. **83**, 4888 (1999).
- [132] D. Vitali and P. Tombesi, *Using parity kicks for decoherence control*, Phys. Rev. A **59**, 4178 (1999).

- [133] J. J. L. Morton, A. M. Tyryshkin, A. Ardavan, S. C. Benjamin, K. Porfyakis, S. A. Lyon, and G. A. D. Briggs, *Bang-bang control of fullerene qubits using ultra-fast phase gates*, Nature Physics **2**, 40 (2006).
- [134] J. D. Franson, B. C. Jacobs, and T. B. Pittman, *Quantum computing using single photons and the Zeno effect*, Phys. Rev. A **70**, 062302 (2004).
- [135] A. Peres, *Quantum Theory: Concepts and Methods*, Kluwer Academic Publishers, Dordrecht (1993).
- [136] B. Kümmerer and H. Maassen, *A scattering theory for Markov Chains*, Inf. Dim. Anal. Quant. Probab. Rel. Top. **3**, 161 (2000).
- [137] T. Wellens, A. Buchleitner, B. Kümmerer, and H. Maassen, *Quantum State Preparation via Asymptotic Completeness*, Phys. Rev. Lett. **85**, 3361 (2000).
- [138] H. V. Scarani, M. Ziman, P. Štelmachovič, N. Gisin, and V. Bužek, *Thermalizing Quantum Machines: Dissipation and Entanglement*, Phys. Rev. Lett. **88**, 097905 (2002).
- [139] M. Ziman, P. Štelmachovič, V. Bužek, M. Hillery, V. Scarani, and N. Gisin, *Diluting quantum information: An analysis of information transfer in system-reservoir interactions*, Phys. Rev. A **65**, 042105 (2002).
- [140] B. M. Terhal and D. P. DiVincenzo, *Problem of equilibration and the computation of correlation functions on a quantum computer*, Phys. Rev. A **61**, 022301 (2000).
- [141] H. Nakazato, T. Takazawa, and K. Yuasa, *Purification through Zeno-Like Measurements*, Phys. Rev. Lett. **90**, 060401 (2003).
- [142] H. Nakazato, M. Unoki, and K. Yuasa, *Preparation and entanglement purification of qubits through Zeno-like measurements*, Phys. Rev. A **70**, 012303 (2004).
- [143] M. Raginsky, *Dynamical Aspects of Information Storage in Quantum-Mechanical Systems*, Ph.D. thesis, Department of Electrical and Computer Engineering, Northwestern University (2002).
- [144] S. Richter and R. F. Werner, *Ergodicity of quantum cellular automata*, J. Stat. Phys. **82**, 963 (1996).
- [145] M. Raginsky, *Entropy production rates of bistochastic strictly contractive quantum channels on a matrix algebra*, J. Phys. A: Math. Gen. **35**, L585 (2002).

- [146] M. Raginsky, *Strictly contractive quantum channels and physically realizable quantum computers*, Phys. Rev. A **65**, 032306 (2002).
- [147] R. F. Streater, *Statistical Dynamics*, Imperial College Press, London (1995).
- [148] R. Alicki, *Irreversible Quantum Dynamics*, volume 622 of *Lect. Notes Phys.*, Springer, New York (2003).
- [149] K. Jänich, *Topology*, Springer, New York (1984).
- [150] M. B. Ruskai, *Beyond Strong Subadditivity? Improved Bounds On The Contractions Of Generalized Relative Entropy*, Rev. Math. Phys. **6**, 1147 (1994).
- [151] I. Stakgold, *Greens Functions and Boundary Value Problems*, Wiley-Interscience, Hoboken (1998).
- [152] J. Dugundji and A. Granas, *Fixed Point Theory*, Springer, New York (2003).
- [153] G. D. Birkhoff, *Proof of the Ergodic Theorem*, Proc. Natl. Acad. Sci. U.S.A. **17**, 656 (1931).
- [154] K. Kraus, *States, Effects, and Operations*, Springer, New York (1983).
- [155] M. Keyl, *Fundamentals of quantum information theory*, Phys. Rept. **369**, 431 (2002).
- [156] W. F. Stinespring, *Positive Functions on C^* -Algebras*, Proc. Am. Math. Soc. **6**, 211 (1955).
- [157] K. M. R. Audenaert and J. Eisert, *Continuity bounds on the quantum relative entropy*, J. Math. Phys. **46**, 102104 (2005).
- [158] M. B. Ruskai, *Inequalities for quantum entropy: A review with conditions for equality*, J. Math. Phys. **43**, 4358 (2002).
- [159] M. B. Ruskai, *Erratum: Inequalities for quantum entropy: A review with conditions for equality [J. Math. Phys. 43, 4358 (2002)]*, J. Math. Phys. **46**, 019901 (E) (2005).
- [160] R. A. Horn and C. R. Johnson, *Matrix Analysis*, Cambridge University Press, Cambridge (1990).
- [161] R. Schrader, *Perron-Frobenius Theory for Positive Maps on Trace Ideals*, volume 30 of *Fields Inst. Commun.*, American Mathematical Society, Providence, math-ph/0007020 (2001).

- [162] P. Hayden, D. Leung, P. W. Shor, and A. Winter, *Randomizing Quantum States: Constructions and Applications*, Commun. Math. Phys. **250**, 371 (2004).
- [163] T. Wellens, *Entanglement and control of quantum states*, Ph.D. thesis, Ludwigs-Maximilians-Universität München (2002).
- [164] S. Lloyd, A. J. Landahl, and J.-J. E. Slotine, *Universal quantum interfaces*, Phys. Rev. A **69**, 012305 (2004).
- [165] J. Cai, Z. Zhou, and G. Guo, *Decoherence effects on the quantum spin channels*, Phys. Rev. A **74**, 022328 (2006).
- [166] A. Bayat and V. Karimipour, *Thermal effects on quantum communication through spin chains*, Phys. Rev. A **71**, 042330 (2005).
- [167] L. Zhou, J. Lu, T. Shi, and C. P. Sun, *Decoherence problem in quantum state transfer via an engineered spin chain*, quant-ph/0608135 (2006).
- [168] H. Schmidt and G. Mahler, *Control of local relaxation behavior in closed bipartite quantum systems*, Phys. Rev. E **72**, 016117 (2005).
- [169] H.-P. Breuer, D. Burgarth, and F. Petruccione, *Non-Markovian dynamics in a spin star system: Exact solution and approximation techniques*, Phys. Rev. B **70**, 045323 (2004).
- [170] O. Mülken and A. Blumen, *Continuous-time quantum walks in phase space*, Phys. Rev. A **73**, 012105 (2006).
- [171] M. Koniorczyk, P. Rapčan, and V. Bužek, *Direct versus measurement-assisted bipartite entanglement in multiqubit systems and their dynamical generation in spin systems*, Phys. Rev. A **72**, 022321 (2005).
- [172] G. D. Chiara, R. Fazio, C. Macchiavello, S. Montangero, and G. M. Palma, *Cloning transformations in spin networks without external control*, Phys. Rev. A **72**, 012328 (2005).
- [173] A. Hutton and S. Bose, *Mediated entanglement and correlations in a star network of interacting spins*, Phys. Rev. A **69**, 042312 (2004).
- [174] A. Olaya-Castro, N. F. Johnson, and L. Quiroga, *Robust One-Step Catalytic Machine for High Fidelity Anticloneing and W-State Generation in a Multiqubit System*, Phys. Rev. Lett. **94**, 110502 (2005).

- [175] A. Olaya-Castro, C. F. Lee, and N. F. Johnson, *Exact simulation of multi-qubit dynamics with only three qubits*, Europhys. Lett. **74**, 208 (2006).
- [176] A. Khaetskii, D. Loss, and L. Glazman, *Electron spin evolution induced by interaction with nuclei in a quantum dot*, Phys. Rev. B **67**, 195329 (2003).
- [177] D. D. B. Rao, V. Ravishankar, and V. Subrahmanyam, *Spin decoherence from Hamiltonian dynamics in quantum dots*, Phys. Rev. A **74**, 022301 (2006).

Index

- amplitude damping, 41
- amplitude delaying channel, 33
- Anderson localisation, 43
- arbitrary and unknown qubit, 11
- asymptotic deformation, 81

- black box, 12, 49, 53

- chocolate, 11
- classical averaged fidelity, 27
- coding transformation, 96
- conclusively perfect state transfer., 33
- cooling protocol, 17
- coupled chains, 53
- CPT, 83
- criteria for quantum state transfer, 31

- decoherence-free subspace, 41
- destabilisation, 116
- dispersion, 21
- distillation, 27
- dual rail, 35

- efficiency, 58
- engineered couplings, 29
- entanglement distillation, 37
- entanglement of distillation, 27, 63
- entanglement of formation, 27
- entanglement transfer, 27
- ergodic, 76
- experiments, 15

- fidelity, 16
- fix-point, 76
- flux qubits, 15

- generalised Lyapunov function, 77

- Heisenberg Hamiltonian, 20
- homogenisation, 92

- Lindblad equation, 109

- maximal peak, 23
- minimal fidelity, 16, 20
- mixing, 76
- multi rail, 68

- non-expansive map, 80
- non-Markovian, 117

- peak width, 27
- peripheral eigenvalues, 86
- phase noise, 41
- pure fix-points, 87

- quantum capacity, 28
- quantum chain, 12
- quantum channel, 16, 83
- quantum computer, 10
- quantum erasure channel, 37
- quantum gates, 11
- quantum memory, 93
- quantum relative entropy, 84

quantum-jump approach, 41
qutrits, 55

reading and writing fidelities, 100

scalability, 12
Schrödinger equation, 109
Shor's algorithm, 10
spectral radius, 67
spin chain, 12
strict contraction, 80
swap gates, 26

time-scale, 38
tomography, 49
topological space, 74
transfer functions, 18

valve, 103

weak contraction, 80